CHARACTERIZING MULTI-SCALED IMPACTS OF HYDRO-DAMS ON ECOSYSTEMS AND SOCIETY UNDER CLIMATE CHANGES IN SOUTHEAST ASIA

By

Myung Sik Cho

A DISSERTATION

Submitted to
Michigan State University
in partial fulfillment of requirements
for the degree of

Geography – Doctor of Philosophy

2022

ABSTRACT

CHARACTERIZING MULTI-SCALED IMPACTS OF HYDRO-DAMS ON ECOSYSTEMS AND SOCIETY UNDER CLIMATE CHANGES IN SOUTHEAST ASIA

By

Myung Sik Cho

Hydro-dams provide many benefits, but can also adversely affect ecosystems and society. Given that dams have influences at large scales, the impacts of dams are so complicated that it is difficult to make accurate estimates of results from dams. Three basins in Southeast Asia, the Mekong, Salween, and Irrawaddy Basins, have recently constructed hydro-dams, but their impacts on ecosystems and society remain poorly characterized due to insufficient monitoring systems, poor economic status, and complicated international relationships of the region. The spatial impacts of dams can represent the dam-related events on ecosystems and society. Given the heterogeneity of the spatial impacts of dams, understanding the impacts of dams at multiple scales can make a better estimate for better policies for Southeast Asia. In this dissertation, I employed novel remote sensing approaches to quantify the spatial impacts of dams on ecosystems and society using a multi-scale perspective. The specific objectives were: (1) to quantify the site-based spatial impacts of dams on land systems, (2) to characterize the watershed-scale spatial impacts of dams on wetlands, and (3) to determine the distant impacts of dams on watersheds.

The results in this dissertation quantified the spatial heterogeneity of dam impacts on ecosystems and society according to the spatial scales, locations, and distances. Specifically, analyses in this dissertation led to three major findings. First, the spatial impacts of dams in the on-site based scale were quantified, and the different spatiotemporal impacts of dams on land systems according to dam stages were found. Second, the spatial impacts of dams on wetlands in

watershed-scale were characterized by distinguishing the influences from local human activities and climate variability on wetland inundations. This showed how dams affect wetlands differently according to the location (upstream / downstream) and distance (close / far) in watersheds. Third, the distance and areas of the spatial impacts of dams on watersheds were determined. This found the anisotropic spatial patterns of the distant effects of dams on upstream and downstream watersheds. Therefore, this dissertation highlights the benefits of geographical perspectives and spatial information in understanding the consequences of dams which are complicated interactions between humans and the environment.

ACKNOWLEDGEMENTS

I would like to thank Dr. Jiaquo Qi, my advisor, for his guidance, support, and encouragement during my graduate study. He enabled me to derive scientific questions from the problems and answer the questions based on geographical perspectives. Also, I would like to express my appreciation to my committee members, Dr. Julie A. Winkler, Dr. Peilei Fan, and Dr. Yadu Pokhrel for their support, advice, comments, and contributions to my doctoral program. Without their academic guidance, I would not be able to complete this dissertation and accomplish my academic career.

I do appreciate all the faculty and staff members in the Department of Geography, Environment, and Spatial Sciences and Center for Global Change and Earth Observations at Michigan State University. Special thanks to Sharon Ruggles, Joni Burns, Jean Lepard, Kathleen Mills, and Cameron Williams for their support in administrative works and IT. Also, I would like to thank Dr. David P. Roy for his support and advice to me.

I was so lucky that I have met good friends and fellows during my graduate study in Michigan State University and Kyung Hee University. They enabled me to accomplish my doctoral program through their help, emotional support, and advice. I am happy that we are on the same path together.

Finally, my deepest thanks to my wife Doyun Kook who gave me endless support and love throughout my graduate study. Thanks to my father, mother, sister, grandmother, and family in-law in South Korea for giving me the confidence and support to pursue my goal as a scientist.

TABLE OF CONTENTS

LIST OF TABLES

LIST OF FIGURES

Chapter 1. Introduction

1.1. Research Problems

Hydro-dams (Hydroelectric dams) have been constructed globally as an east way of gaining water, food, and energy. Under global climate change, hydro-dams are considered to facilitate stable water resources and produce green energy (Arias et al., 2020; Faria et al., 2017). However, the dams bring numerous unintended negative consequences to ecosystems and society, such as land degradation (Chen et al., 2015), hydrological alteration (Pekel et al., 2016), water pollution (Gauthier et al., 2019), ecosystem disturbance (Barbarossa et al., 2020), sediments blockage (Baird et al., 2021), dislocation of people (Scudder, 2005), and lifestyle changes (Wang et al., 2013). Given that the dam impacts on ecosystems and society are temporally lagged (Castro et al., 2016), spatially lagged (Baird et al., 2021), cumulative (Timpe and Kaplan, 2017), and indirect (Rufin et al., 2019), it is difficult to accurately estimate the dam consequences (Tullos, 2009). For example, a global analysis of 245 large dams found that actual costs averaged ninety-six percent higher than expected (Ansar et al., 2014; Latrubesse et al., 2017). Since human activities cause changes in Earth's surface, a spatial quantification of the human activities provide the baseline information in understanding and unraveling the complicated results (Baird et al., 2021; Matthews and McCartney, 2018; Tullos, 2009). Thus, characterizing the spatial consequences of dams on ecosystems and society will improve our understanding of how dams affect ecosystems and society.

Because of the complicated spatial impacts of dams, taking a specific scale has been considered in estimating the impacts, rather than multi-scales (Chen et al., 2015; Winemiller et al., 2016). However, this has been notably insufficient for understanding the full scope of the spatial impacts of dams (Dang et al., 2021; Turner et al., 2016). For example, some studies focused on the scale of dam-sites, but they failed to consider the impacts of the dams beyond the dam sites (Chen et al., 2015; Jiang et al., 2018). Also, other studies examined the dam impacts in the scale of watersheds, but they failed to address the dam impacts outside of the watersheds (e.g., transfer of water and energy to other regions) (Wyatt and Baird, 2007). These limited considerations of scales have caused inaccurate estimations of results from dams on ecosystems and society (Tullos, 2009; Winemiller et al., 2016). Thus, the spatial heterogeneity of the dam impacts should be considered at multi-scales. Characterizing the spatial impacts at multi-scales will improve our understanding of the spatial boundaries of the consequences and spatial patterns of the impacts of dams. Furthermore, this can provide the basis for the accurate estimation and the clarification of the complicated effects of dams.

Remote sensing can help quantify dam-related information across various scales in space and time. Recently developed geospatial cloud platforms, time-series image analyses, and the integration of multiple sensors enable estimates of the consequences of the dams which had not been studied before (Ablat et al., 2019; Gorelick et al., 2017). The development of geospatial cloud platforms (e.g., Google Earth Engine) has reduced computational time and resources that enable the processing of huge amounts of data over relevant regions (Kang et al., 2020; Pekel et al., 2016). Time-series image analysis enables the detection of the dam-related events on the surface by measuring across various scales in space and time (Nguyen et al., 2018; Wang et al., 2014). Multi-sensor approaches offer rich information for characterizing the dam impacts by reducing issues related to cloud cover and improving spatial and temporal resolution of earth observations (Ashraf et al., 2012; Hilker et al., 2009; Wilson et al., 2022).

Southeast Asia is a region that requires the quantification of the multi-scale impacts of dams using remote sensing. Many hydro-dams have been recently built in the mainland of Southeast Asia (Hennig et al., 2013), and the region does not have sufficient monitoring stations (Bonnema and Hossain, 2019; Kuenzer et al., 2014). Along with their complex political issues (Hirsch, 2016; Soukhaphon et al., 2021), economic status (Arias et al., 2019; Wild et al., 2019), and climatic characteristics (Han et al., 2019; Yang et al., 2019), the results of the dam impacts on ecosystems and society are very complicated and insufficiently estimated. Given that accurate estimates would reduce irreversible damages from dams to their ecosystems and society (Pearse-Smith, 2012; Yoshida et al., 2020), this dissertation attempted to fill current gaps in knowledge about the spatial impacts of dams by quantifying the multi-scaled impacts using a remote sensing approach.

1.2. Research Objectives

This dissertation aims to characterize the multi-scaled spatial impacts of hydro-dams on ecosystems and societies under climate change in Southeast Asia. Remote sensing methods are developed to address the multi-scaled spatial impacts. The following three objectives are pursued in this dissertation:

(1) to quantify the site-based spatial impacts of dams on land systems

(2) to characterize the watershed-scale spatial impacts of dams on hydrology

(3) to determine the distance and areas of distant impacts of dams on watersheds.

The first objective is investigated by detecting human activities and vegetation disturbance around the dam sites. The second objective is fulfilled by quantifying the changes in inundation characteristics of wetlands. The third objective is examined by characterizing the different inundation characteristics of wetlands with linkage with dams from those of wetlands without the linkage.

1.3. Conceptual Framework

This dissertation is comprised of seven chapters as follows.

Chapter 2 reviews the related literature in methodology of quantifying the spatial impacts and multi-scaled spatial impacts of dams.

Chapter 3 presents the study area, which is the Mekong, Salween, and Irrawaddy Basins, focusing on climate, physical geography, and human geography of the region.

Chapter 4 proposes a spatial methodology to quantify the spatial impacts near the dam-site. The generalized spatial boundaries representing the dam impacts are presented to be applicable to other regions. Also, different dam stages are considered to quantify the spatiotemporal impacts of the hydro-dams on dam-sites using land use/land cover changes (LULCC)

Chapter 5 characterizes the spatial impacts of dams on wetlands to examine the dams' effects on watersheds focusing on wetlands. A multi-sensor approach is developed to extract inundation areas of natural wetlands in weekly scale across the region. Along with considering human activity around the wetlands and climate variability, the hydrological alterations on wetlands caused by dams are quantified.

Chapter 6 delineates how distantly dams hydrologically affect wetlands in watersheds and addresses the distance and areas of dams on watersheds. A geospatial approach is proposed to consider the relationship of watersheds with dams and determine the distant impacts of dams on upstream and downstream watersheds.

Last, Chapter 7 draws the conclusions and discussion of the dissertation. I discuss the contributions and implications of my dissertation in quantifying dam impacts on ecosystems and society. Then, limitations and future research directions are addressed.

Chapter 2. Literature Reviews

2.1. Multi-scaled Spatial Impacts of Hydro-dams on Ecosystems and Society

This dissertation defines three spatial scales in measuring the impacts of dams on ecosystems and society. First, the site-based scale refers to the spatial impacts of dams on the dam sites. Second, the watershed scale refers to the impacts of the hydrological alteration of dams on watersheds. This scale can cover the distant impacts of dams on watersheds, such as transboundary influences of dams. Spatial impacts of dams were measured in distance based on study sites of previous studies.

2.1.1. On site-based scale

At dam sites, dam activities, such as dam construction and dam operation, have different spatial impacts. The dam construction changes the land cover and land uses and impounds the water, and the dam operation results in additional human activity within the land it occupies, including land use and land cover changes (LULCC) due to gains of water and energy from the dams. Previous research studied the site-based scaled spatial impacts of dams mainly on societal changes and LULCC (Chen et al., 2015; Faria et al., 2017; Gauthier et al., 2019; Jiang et al., 2018; Ouyang et al., 2013; Wang et al., 2013; Zhao et al., 2010).

As for societal consequences, economic activities and lifestyle changes occurred within 52km around the dam sites. Faria et al. (2017) found that economic benefits (GDP increases) to local livelihoods within counties with dams lasted for only the first 15 years. Similarly, Wang et al. (2013) quantified that the economic benefit was larger for the distantly-located societies, but economic losses were larger for the closely-located societies within 30km due to different environmental changes between different locations. The closer one gets to dams, water quality and water impoundment significantly changes. As a results, many people have suffered from the necessity of new embodied skills, such as their agricultural skills, in the altered environment. This requires these people to change their jobs, and it has led to economic losses and lifestyle changes among people living in areas where dams have been constructed (Wang et al., 2013). Also, Gauthier et al. (2019) quantified the contamination of the groundwater in a 52km upstream located city, named Altamira, from the Belo Monte dam in Brazil due to the population growth and increases of groundwater level.

With regards to LULCC, forest, water, agricultural lands, and bare lands were changed within 80km around the dam sites (Chen et al., 2015; Jiang et al., 2018; Ouyang et al., 2013; Zhao et al., 2010). Deforestation was a major LULCC due to the construction of infrastructure (e.g., dams and roads) and agricultural expansion within 2km along river around the Belo Monte dam in Brazil (Jiang et al., 2018), 10km buffered areas around the Manwan dam in China (Zhao et al., 2010), 30km around the dams in the Upper Mekong Basin (Wang et al., 2013), and 80km around the Belo Monte dam in Brazil (Chen et al., 2015). Water impoundment increased the water inundation areas around the dam sites, but Ouyang et al. (2013) found that water had increased at first, but decreased after 30 years of dam construction (Qingtongxia dam in China) within 5.5km, possibly due to increase of agricultural development. Because of additional water, energy, and access, the agricultural lands were expanded within 2km and 5.5km along the river (Jiang et al., 2018; Ouyang et al., 2013), and 10km buffered areas (Zhao et al., 2010). Lastly, human-made and naturally-occurring bare lands were increased along the river with 2km distance due to the hydrological changes and deforestation (Jiang et al., 2018).

2.1.2. Watershed scale

In watershed scale, the trapping of water and sediment have caused most of the spatial impacts. The most significant spatial impacts are changing hydrology, sediment transport, ecosystems, and local livelihoods. Previous studies can be divided into two groups in terms of study sites. First, some research studied the changes in selected watersheds and linked them with the dams. Second, others studied a single or several study sites (e.g., selection of downstream wetlands from dams) and connected the changes with the dams.

2.1.2.1. Hydrology

The hydrological impacts of dams on watersheds are the changes to the characteristics of inundation areas of wetlands, (Arias et al., 2012; Feng et al., 2016; Han et al., 2018; Ji et al., 2018; Pal and Saha, 2018; Wang et al., 2014; Zheng et al., 2019), river connectivity (Grill et al., 2014; Pal and Saha, 2018), and the hydrological regime of streamflow within 1,000km. Downstream wetlands show a decline in inundation areas within the distances of 90-250km (Pal and Saha, 2018), 150km (Zheng et al., 2019), 200-1000km (Feng et al., 2016; Han et al., 2018; Wang et al., 2014), and the entire basin (Ji et al., 2018). The seasonal inundation areas decreased and were converted to permanent inundation areas from dams in upstream watersheds (Arias et al., 2012). Also, dams reduce connectivity of wetlands within 90-250km of the upstream dam (Pal and Saha, 2018) and river connectivity in watersheds (Grill et al., 2014).

The water levels of Poyang Lake (PL) in the Yangtze River Basin (YRB) decreased due to the Three Gorges Dams (TGD) which is located 1,000 km upstream (Mei et al., 2015; Zhang et al., 2012), and Zhang et al. (2022) pointed out the decrease in the amplitude (i.e., differences between the maximum and minimum peak) of water levels. The water levels of Tonle Sap Lake

(TSL) in the Mekong River Basin (MRB) also decreased due to dams in upstream watersheds (Cochrane et al., 2014), especially at the peak of wet seasons (Kummu and Sarkkula, 2008).

Dams can significantly alter the flow regimes of streamflow in entire basins both upstream and downstream of dams (Bonnema and Hossain, 2017; Timpe and Kaplan, 2017). Within the distance of 1,000km downstream, it has been shown that there are impacts of dams on streamflow. However, Xue et al. (2011) showed that upstream dams in the MRB do not have significant influence on the streamflow of 1,600km downstream. The streamflow discharge of the dry season was increased at the distance of 700km (Lauri et al., 2012; Maingi and Marsh, 2002), but that of the wet season decreased at 10km (Graf, 2006), 150km (Zheng et al., 2019), 700km (Zhao et al., 2012), and 1,000km (Zhang et al., 2012). Also, the streamflow peak was reduced (Chaudhari and Pokhrel, 2022; Graf, 2006; Maingi and Marsh, 2002), especially for wet season (Kummu and Sarkkula, 2008; Zhao et al., 2012; Zheng et al., 2019), and the period of wet seasons were decreased (Maingi and Marsh, 2002; Zheng et al., 2019). Additionally, streamflow became more variable (Cochrane et al., 2014; Graf, 2006), and the amplitude of the streamflow became smaller (Graf, 2006; Poff et al., 2007; Zhang et al., 2022).

2.1.2.2. Sediment Transport

The hydrological alteration caused by dams affects the sediment transport downstream within 2,000km. The suspended sediment was decreased within 1,000km (Humbord et al., 1997) and 500-2,000km (Bussi et al., 2021). However, Xue et al. (2011) refused the impacts of dams on sediment in the MRB, which conflicted with Bussi et al. (2021)'s study on MRB that the impacts on suspended sediment reached 2,000km. This can be addressed by the following: (1) there are different characteristics of sediment load with suspended sediment, (2) Bussi et al. (2021)'s method was based on simulation based on the water stations, but Xue et al. (2011)'s was based on the measurement from water stations, and (3) Xue et al. (2011) considered a few upstream dams.

The downstream terrain was altered by decreasing the (suspended) sediment and streamflow within 111km (Ezcurra et al., 2019; Graf, 2006; Mohammed-Ali et al., 2020). Graf et al. (2006) found that the changes in streamflow led to larger low flow channels, smaller high flow channers, and less active floodplain areas for the distance 5-10km. The riverbank stability was affected by controlling streamflow within 111km due to sudden flow drawdown and shorter time of low flow (Mohammed-Ali et al., 2020). Also, the decreased sediment caused the coastal recession at 100km (Ezcurra et al., 2019).

2.1.2.3. Ecosystems

The spatial impacts of dams in watershed scale on ecosystems are alterations in ecosystem structure and composition within 1,000km. For ecosystem structures, there are significant changes in land cover, habitats, connectivity, and fragmentations (Arias et al., 2012; Ezcurra et al., 2019; Feng et al., 2016; Han et al., 2018; Kummu and Sarkkula, 2008; Yang et al., 2014; Zhao et al., 2012). The reduction of habitat was caused by coastal recession due to trapping the sediments in 40-100km upstream dams (Ezcurra et al., 2019). Also, upstream dams in watersheds destroyed the flood pulses in TSL of MRB, so they caused conversions in seasonal flooding habitats, which are vital ecosystems in the region, to open water (Arias et al., 2012; Kummu and Sarkkula, 2008). Unlike TSL, PL of YRB showed increasing vegetation led by the decline in discharge due to the TGD, which is 1,000km upstream dams (Feng et al., 2016; Han et al., 2018). They found that open water was replaced by vegetation, such as Phragmites. A basin-wide fragmentation of river connection was explained by hydrological alteration (Yang et al., 2014) and additional human activity (Zhao et al., 2012) due to dams. They quantified that dams increased the landscape fragmentation by losing the river connectivity, the complexity of the landscape shape, and deforestation.

The dams adversely alter ecosystem composition, in terms of biodiversity (Barbarossa et al., 2020; Ezcurra et al., 2019; Maingi and Marsh, 2002). Dams fragment the connectivity of the river networks so the basin-wide occurrence of lotic fish species is reduced, especially non-diadromous fish species (Barbarossa et al., 2020). For estuaries, the fish population was decreased due the impacts of 40-100km upstream dams on coastal recessions (Ezcurra et al., 2019). Also, the altered water level pattern of river caused by 500-700km upstream dams decreased the unique forest system in Kenya (Maingi and Marsh, 2002).

2.1.2.4. Society

The spatial impacts of dams on society in watershed scale are changes to economic activity and lifestyle among those living within 600km of them (Baird et al., 2021; Ezcurra et al., 2019; Kura et al., 2017). Baird et al. (2021) found that downstream societies in MRB, Amazon River Basin, and Peace-Athabasca River in Canada that were located 100km, 200km, 600km away from dams, respectively, were affected in terms of hydrological changes and fisheries. Ezcurra et al. (2019) confirmed the amount of fish caught decreased 40-100km away from the upstream dams due to coastal recession and habitat loss. Upstream communities also suffered from the dam's construction. The four resettlement villages (two were from downstream, but two were from upstream), located 30km upstream of the dam in the MRB, represented changes of human, natural, social, and financial capital (Kura et al., 2017).

2.2. Remote Sensing Methodology for Quantifying Spatial Impacts

Many studies use various remote sensing methods to quantify the multi-scaled spatial impacts of dams on the environment and ecosystems. The ability to distinguish dam-related surface changes over extensive space and time enables to fill the gaps in methodology using field data (e.g., discharge), simulation, models, and interviews.

2.2.1. Time-series analyses

For the impacts of dams on vegetation changes, Chen et al. (2015) determined the deforestation and degradation from Landsat using spectral mixture analysis (SMA). Statistical analyses (Friedman test, Wilcoxon signed-rank test, and Chi-square test) were applied to link deforestation and degradation with dam construction using multiple buffer areas surrounding dams. Han et al. (2018) classified water, mudflats, and five major vegetation communities in the PL (Poyang Lake) using decision tree classifiers (DTC) with normalized differences vegetation index (NDVI) to investigate how TGD (i.e. Three Gorges Dam located 1,000km upstream) altered the PL's systems.

For the impacts of dams on wetland inundations, Wang et al. (2014) monitored 80 lake inundations for 10 years using image segmentation and support vector machines (SVM) on MOIDS. The trend analysis was conducted to examine how TGD affected the lake systems in YRB (Yangtze River Basin). Zheng et al. (2019) used time-series water distribution data to relate streamflow discharge changes for quantifying the impacts of dams on downstream wetlands. Ji et al. (2018) examined how upstream dams affect the runoff of TSL (Tonle Sap Lake) using trend analysis on inundation areas with the modified normalized differences water index (MNDWI) from MODIS.

2.2.2. Change Detection

The change detection method was conducted by comparing two periods (e.g., before and after dams). LULCC around the dams were linked with the site-based scaled impacts of dams on ecosystems and society using transition matrix. The maximum likelihood classifier was used to quantify LULCC, and change detection was applied to buffer areas surrounding the dam sites (Jiang et al., 2018; Zhao et al., 2010). Cochrane et al. (2017) classified water and forest using SMA and DTC and conducted change detection on buffer areas surrounding the river flow. Also, Feng et al. (2016) did change detection analysis on LULCC of the PL which was derived from the SVM and NDVI on MODIS.

Along with the transition matrix, which shows how LULC was changed from the earlier period to the latter period, the spatial comparison of scenes was facilitated to quantify the changes related to the dams. Pal and Saha (2018) delineated the inundated areas of wetlands using the normalized differences water index (NDWI) on Landsat and linked the fragmentation and the decline of the wetlands with the upstream dams. Ezcurra et al. (2019) manually digitized the coastal terrain and found the coastal recessions due to dams. Similarly, Graf (2006) manually delineated the flow channels and floodplain on aerial photos and linked the changes with the hydrological alterations of upstream dams.

2.2.3. Uses for further analysis

The remote sensing method was used to process the remote sensing data for further analysis. The landscape ecology used remote sensing product to determine the structure and composition of ecosystems at the macro-scale. The fragmentation, shape, and size of the patches were calculated from LULC products to quantify the impacts of dams on watersheds (Yang et al., 2014; Zhao et al., 2012). Bonnema et al. (2017) estimated the water storage of dam reservoirs using the area-elevation curve with water inundation derived from NDWI of Landsat. The estimated water storage was used to quantify the impacts of dams on flow alteration. Arias et al. (2012) used water inundation areas from MODIS to validate the estimation of flooded areas from the water level measurements. The estimated flooding areas were used to simulate how future dams will affect the downstream wetland systems.

Chapter 3. Study Area

3.1. Overview

The Mekong, Salween, and Irrawaddy Basins in the mainland of Southeast Asia were selected as study areas because many dams have been constructed recently and have imposed strong impacts on the local community and ecosystems (Figure 3.1). The three basins are the largest in the region and cover seven countries: Vietnam, Thailand, Laos, Cambodia, Myanmar, China, and India. By 2017, 186 hydro-dams were already commissioned, 45 were under construction, and 110 were proposed and planned (WLE, 2017). Additionally, the basins share similar climate, topography, and society characteristics, so considering the three basins helps determine the multi-scaled impacts of dams on society and ecosystems.

The Mekong River starts from the Tibetan Plateau at 4,500 m and flows out to the South China Seas through China, Myanmar, Thailand, Laos, Cambodia, and Vietnam (MRC, 2005). It is the 10^{th} largest river in the mean annual flow with 4,800km length (Ziv et al., 2012). The catchment area of Mekong River Basin (MRB) is 795,000 km^2 and sustains more than 72 million people (Kuenzer, 2014). Its mean annual discharge is 14,500 m^3/s (Wang et al., 2017). Due to its rich water resources and topographical characteristics, the Mekong can generate over 30,000 MW of electricity (Yoshida et al., 2020).

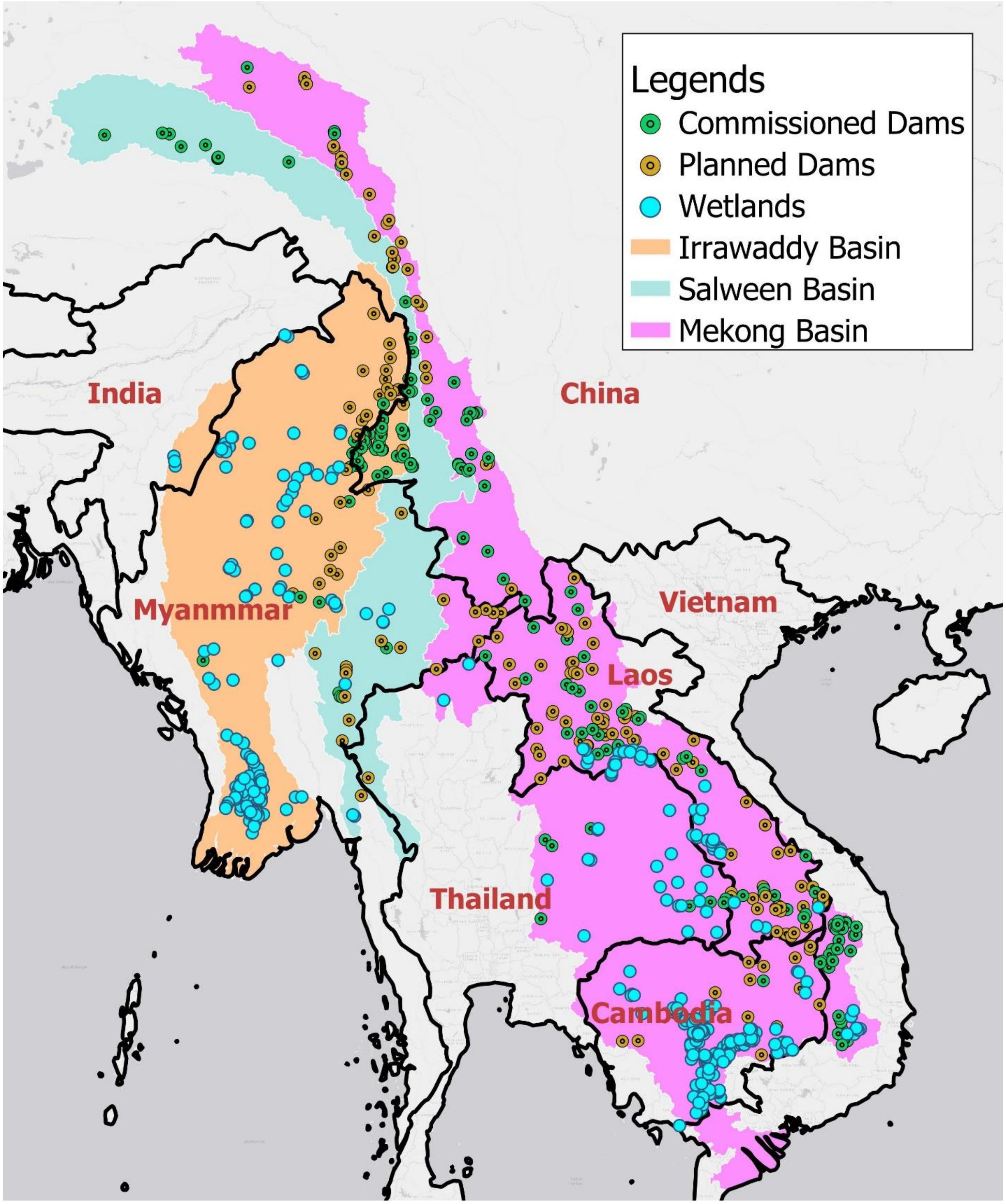

Figure 3.1. Study area of this dissertation. Wetlands and dams in Mekong, Salween, and Irrawaddy River Basins.

The Irrawaddy River rises from the Himalayan Mountains and flows out to the Andaman Sea through China, India, and Myanmar, and is approximately 2,170 km long (Shamsudduha and Panda, 2019). The Irrawaddy River Basin (IRB) has a catchment of 413,000 km^2 (Robinson et al., 2007) and supports of 39.5 million local livelihoods (Bridgestock et al., 2022). Its average annual discharge is 13,000 m^3/s and its suspended load is 364 ± 60 MT, which is the fourth highest total dissolved load of the world's rivers (Robinson et al., 2007). No dams have been built in the mainstream so far (WLE, 2017).

The Salween River is 3,200 km long and originates at the Tibetan Plateau, and flowing out to the Gulf of Martaban through China, Thailand, and Myanmar with 3,200 km long (Chapman et al., 2015). The Salween River Basin (SRB) has a catchment of 283,500 km^2, with a population of over 10 million people (Bridgestock et al., 2022). Its average annual discharge is 210 km^3/yr, ranking 26th globally (Salmivaara et al., 2013). No dams have been built in the mainstream so far (WLE, 2017).

3.2. Climate

The climate of the three basins is dominated by a Monsoon climate system, which creates dry and wet seasons (MRC, 2005), and the El Niño-Southern Oscillation (ENSO), which causes flooding and drought events (Räsänen and Kummu, 2013). Given that climate patterns play a significant role in water resources (e.g., streamflow and seasonality) (Pokhrel et al., 2018), the climate of the basins have a major influence on ecosystems and society (Cochrane et al., 2014). The Mekong, Salween, and Irrawaddy Basins share similar climate patterns in upper and lower basins. The upper basin, which consists of mountainous areas, has less precipitation (500 to 900 mm/yr) and lower temperatures (winter: -4 ~ 8°C; summer: 13 ~ 20°C) (MRC, 2005; Sirisena et al., 2021). The lower basin, made up of flat areas, has more precipitation (1,730 to 3,700 mm/yr) and higher temperatures (winter: 11 ~ 27°C; summer: 26 ~ 34°C) (MRC, 2005; Sirisena et al., 2021). For water resources, the upper basin is mainly controlled by snowmelt, while the lower basin is related to the intense rainfall during the monsoon season (Delgado et al., 2010; Pokhrel et al., 2018).

The climate of the three basins is controlled by the Southwest Asian Monsoon and Northeast Asian Monsoon (MRC, 2005; Salmivaara et al., 2013). The Southwest Asian Monsoon makes wet seasons from May until early October and the Northeast Asian Monsoon generates dry seasons with lower temperature from late October to April (Delgado et al., 2012; Sirisena et al., 2021). The large seasonal variation of climate constructs the seasonal patterns of hydrology which make the basin as the second most biodiverse ecosystem, providing fruitful resources to society (Arias et al., 2012; Cochrane et al., 2014). Also, ENSO strongly influences the climate variability and the water resources (Frappart et al., 2018). El Niño leads to drought events by reducing the rainfall, discharge and annual flood period, while La Niña is responsible for flooding events by elevating rainfall, discharge, and annual flood period (Räsänen and Kummu, 2013). For instance, the MRB during the El Niño years (period 1993-1995, 1997-1998 and 2014-2016) had suffered from severe drought events, especially lower basin (Tran et al., 2019; Ward et al., 2010).

The global climate changes have affected the climate patterns of the region. The precipitation in the upper basin was found to have increased, while the lower basin did have insignificant changes over the past 50 years (Delgado et al., 2012; Pokhrel et al., 2018; Ward et al., 2010). Furthermore, future climate changes are estimated. The upper basin will be more sensitive to climate change due to snowmelt and changes in precipitation (Han et al., 2019).

Early snowmelt will shift the flood peak earlier in the basin (MRC, 2005). For the lower basin, the precipitation, higher temperatures, and extreme rainfall events frequently occur because of the influence of higher temperature on the moisture supply (Wang et al., 2017). Also, the drought events have been frequent and severe (Guo et al., 2017).

3.3. Topography

MRB, IRR, and SAL share similar topographical characteristics in that the upper basin has rough mountains with steep valleys (Himalaya Mountains and Tibetan Plateau) and the lower basin has relatively flat terrain with floodplains and deltas in estuaries. The upper part of the Mekong River (Lancang River in Chinese) runs through deep, narrow and steep terrains for over 2200 km across China (16% of the basin) and Myanmar (2%), and it enters the lower basin at the boarder with Thailand, the so called the Golden Triangle (Pokhrel et al., 2018). The river flows to Laos (35%) and Thailand (18%), which are less mountainous areas with sub-tropical forests and savannah, and large agricultural lands over the Korat Plateau (Frey and Kuenzer, 2014; MRC, 2005). In Cambodia (18%), the river widens in the alluvial lowlands and floodplains, and it has large floodplain lake systems with the flow reversal, the so called Tonle Sap Lake systems (MRC, 2005). Due to water elevation differences, water from the Tonle Sap Lakes (TSL) flows into the Tonle Sap River, which is a tributary of the Mekong River during dry season, while the streamflow of the Mekong River flows back to the TSL during the wet season (Kummu and Sarkkula, 2008). In Vietnam (18%), the river passes through floodplains and reaches the Mekong Delta (MRC, 2005).

The Irrawaddy River (locally known as the Ayeyarwady River) has two main tributaries, the Nmai and Mali Rivers, which arise from the Himalayan glaciers (Shamsudduha and Panda, 2019). The Mali River, which is on the western side, has a relatively gentle topographic gradient and the Nmai River, which is on the eastern side, has a greater volume of discharge and a steep gradient (Shamsudduha and Panda, 2019). The river passes through a low-lying central valley with margins of pristine forest covered mountainous areas in the Indo-Myanmar ranges and Shan plateau (Bridgestock et al., 2022). Then it reaches the Irrawaddy Delta with many sediments (Chapman et al., 2015).

The upper basin of the Salween River, which is called the Nu River in Chinese, flows through steep and narrow mountainous areas (Chapman et al., 2015). It flows from China (48%) and Thailand (7%) and enters to Myanmar (44%) (Bridgestock et al., 2022). Even after entering the lower basin, the basin rarely has floodplains and flat topography except for the floodplains at the mouth because 75% of the Salween Basin is mountainous areas (Bridgestock et al., 2022; Salmivaara et al., 2013).

3.4. Freshwater Ecosystems and Society

Southeast Asia is the fourth global biodiversity hotspot, comprised of 36 site, according to the Conservation International (Myers et al., 2000), and the Mekong River is the second most biodiverse river (Ziv et al., 2012). Especially, the climate and topography in the region make its unique hydrological systems which richen freshwater ecosystems. The MRB has 1,300 fish species (Kuenzer, 2014), and the IRB has approximately 500 fish species, half of which are endemic (Li et al., 2021). These affluent freshwater ecosystems provide food, economic activities, and other ecosystem services to local livelihoods (Dang et al., 2021). In the MRB, the estimated annual harvest of wild fish is 2.2 million tons, worth 4.3 – 7.8 billion US dollars (Hortle, 2009). Fish consumption in the region is the major source of protein intake for the local population, comprising of 49 – 82% of the annual protein consumption (e.g., Cambodia - 53.6 kg/person*year; Laos – 36.2 kg/person*year) (Hortle, 2009; Intralawan et al., 2018; Millar et al., 2019). Additionally, 65% of Cambodians living in TSL (Tonle Sap Lake, which is the largest wetland system in Southeast Asia) have jobs related to fishing, aquaculture, and agriculture (NG and Park, 2021).

Given that the freshwater ecosystems are vulnerable to hydrological alterations and that the society highly depends on the ecosystems, the dams have seriously affected both ecosystems and society. Many fish in the region have long migration distances of over 1,500km, so the fragmentation of the river network destroys their migratory patterns (Vaidyanathan, 2011). Also, changes in hydrological patterns (e.g., seasonal variability and amplitude) ruin the connectivity of abiotic and biotic components (Kingsford, 2000; Leibowitz et al., 2018), so they negatively affect ecosystems and society (Ellis and Jones, 2013; Poff et al., 2007). Furthermore, decreases in food supply and economic benefits in ecosystems and society after dams cause the local livelihoods to expand their agriculture and aquaculture through deforestation and water extraction from wetlands (Millar et al., 2019). Thus, the spatial impacts of hydro-dams on ecosystems and society should be studied.

Chapter 4. Spatial Impacts of Dams in On-site Based Scale on Land Systems[1]

4.1. Introduction

Determining environmental consequences of human activities needs to be put in a spatial context (Connors et al., 2012). This is particularly true when one attempts to quantify consequences from mega-projects such as hydro-dams, because of their complex environmental and societal impacts (Kirchherr et al., 2016; Lin and Qi, 2019; Maingi and Marsh, 2002; Matthews and McCartney, 2018; Tullos, 2009; Vaidyanathan, 2011; Winemiller et al., 2016).

Hydro-dams have been constructed for meeting human needs such as water, food and energy (Fearnside, 2016; Kornijów, 2009; Lin and Qi, 2017; Pueppke et al., 2018), but they have also brought various unintended consequences for the environment and society, including land loss (Zhao et al., 2010), land degradation (Chen et al., 2015; Qi et al., 2012), water pollution (Gauthier et al., 2019), ecosystem disturbance (Han et al., 2018; Wu et al., 2013), sediments blockage (Bonnema and Hossain, 2017), dislocation (Fearnside, 2016; Scudder, 2005), and lifestyle changes (Pueppke et al., 2018; Wang et al., 2013). The unintended consequences are spatially heterogeneous and thus are difficult to quantify (Kirchherr et al., 2016; Moran et al., 2018; Tullos, 2009; Winemiller et al., 2016). For example, a global analysis of 245 large dams found that actual costs averaged 96% higher than expected (Ansar et al., 2014; Latrubesse et al., 2017). A major reason for the uncertainty is insufficient information on spatial extents of dam impacts on the environment and society (Chen et al., 2015; Holdman, 2011; Kirchherr et al., 2016; Lin and Qi, 2019; Vaidyanathan, 2011). For instance, Environmental Impact Assessments

[1] This chapter updated and reused the publication of CHO, M., QI, J. (2021). Quantifying Spatiotemporal Impacts of Hydro-dams on Land Use Land Cover Changes in the Lower Mekong Basin. Applied Geography, 136. under permission.

(EIAs), a fundamental requirement for the planning process for large dams (IAIA, 1999; Tullos, 2009), have been criticized for their inaccuracy because EIAs have downplayed the spatial boundaries of dam impacts (Jiang et al., 2018; Tullos, 2009; Vaidyanathan, 2011; Winemiller et al., 2016). In order to better understand environmental and societal implications, spatial patterns and extents of dam impacts must be quantified.

Remote sensing helps us specify the spatial extents of environmental consequences of human activities in details (Cochrane et al., 2017; Feng et al., 2012; Han et al., 2018; Kashaigili et al., 2006; Liu et al., 2014; Pal and Saha, 2018), and some studies have quantified spatial boundaries of dam impacts on the environment and society using remotely sensed imagery (Chen et al., 2015; Jiang et al., 2018; Lin and Qi, 2019; Ouyang et al., 2013; Zhao et al., 2010). However, these studies have limitations in defining spatial patterns and the extent of the dam impacts. First, their research confined the spatial pattern to a circular shape. The spatial pattern refers to a shape that can represent the two-dimensional extent of a geographical feature (Li et al., 2013; Maceachren, 1985; Zick and Matyas, 2016), and it plays a significant role in representing impacts in spatial pattern, dimension, and size (Miller and Wentz, 2003; Wentz, 2000). Since the consequences of dams tend to occur along the river (Jiang et al., 2018; Ouyang et al., 2013; Scudder, 2005), the circular shape might omit some spatial patterns of dam impacts. Some previous studies assumed the spatial pattern to be a circular area centered on the dam and assessed the variability of the Normalized Difference Vegetation Index (NDVI) (Lin and Qi, 2019), deforestation (Chen et al., 2015) and Land Use/Land Cover Changes (LULCC) (Zhao et al., 2010). Others considered the pattern of dam impacts be represented along the river corridor, but these studies only considered the extents along the river through distance-based buffers (Jiang et al., 2018; Ouyang et al., 2013). These studies are likely to omit dam impacts in the areas perpendicular to the rivers, since significant changes caused by dams tend to be strongly asymmetric around the dam sites (Chen et al., 2015; Lin and Qi, 2019; Vaidyanathan, 2011; Zhao et al., 2010).

Second, it is also challenging to determine the spatial extents of dam impacts, although some studies suggested 5 – 5.5km as the influential distances of dams. Some studies used a single dam in analyzing the spatial extent (Jiang et al., 2018; Ouyang et al., 2013; Zhao et al., 2010), and conclusions drawn from one single dam analysis may not be generalized to other dams. Finally, some ways to determine spatial extents may not be realistic (Chen et al., 2015; Jiang et al., 2018; Lin and Qi, 2019; Ouyang et al., 2013; Zhao et al., 2010). More realistic ways to quantify the spatial extents should include the selection of extents from all distances and all time periods. For example, Zhao et al. (2010) suggested 5km as the spatial extent within the radius of 1, 5, and 10km, Ouyang et al. (2013) selected 5.5km as the spatial extent among the radius of 5.5km and 10km, and they did not consider all time periods in that they just compared the LULCC of the snapshots before and after a dam construction. Jiang et al. (2018) assumed 2km distance along the river as the spatial extent without any supported reasoning. Lin and Qi (2019) and Chen et al. (2015) quantified the spatial extents of dam impacts by considering all distances and time periods, but their time periods are so long that some unrelated impacts might have been included. For instance, converting forests into agricultural lands more than 10 years before the beginning of the dam construction are irrelevant to the dam impacts, but their analyses included this change as spatial extents of dam impacts since they analyzed spatial differences for 30 years.

This chapter developed an innovative spatial extent model of dam impacts to better quantify the spatial extents and the environmental consequences of dams. Two research questions will be answered in this study: 1) what spatial pattern is more realistic in characterizing dam impacts on the environment and society? 2) what is the spatial extent of dam impacts?

This study defines the spatial impacts as significant changes in surface reflectance caused by dams surrounding dam-sites. It is noted that impacts of dams extend beyond the dam-sites (Maingi and Marsh, 2002; Winemiller et al., 2016), but this chapter focuses on impacts on surrounding areas, as they are the primary concerns of policy-makers and researchers (Tullos, 2009; Vaidyanathan, 2011). This research fulfills the aforementioned gaps in understanding the spatiotemporal effects of dams, especially that gaps resulting from a single dam analysis, discrete spatial boundary and discontinuous temporal period, using recently developed CyberGIS infrastructure (Kang et al. 2020), which can reduce computational burdens.

4.2. Material and methods

4.2.1. Study area

The entire Lower Mekong River Basin (LMRB) was selected as our study area because many dams have been constructed recently to impose strong impacts on the local community and ecosystems (Figure 4.1). The LMRB consists of five countries in Southeast Asia: Laos, Thailand, Vietnam, Cambodia, and Myanmar. Monsoon climates affect the seasonality of the basin (Suepa et al., 2016) and have made the Mekong the second most biodiverse river in the world with 877 fish species (Ziv et al., 2012). However, many dams in the basin have altered the seasonality (Kummu and Sarkkula 2008; Lin and Qi, 2017), which is the most important factor for sustaining ecosystem (Barbarossa et al. 2020) and local livelihoods (MacAlister and Mahaxay, 2009; MRC, 2005) in this region. By 2017, 363 dams have been constructed and planned, including 177 hydro-dams (WLE, 2017). Among the hydro-dams, 75 are already commissioned, 30 are under construction, 60 are planned, and 11 are proposed (WLE, 2017). The primary reasons for the existence of so many dams in the LMRB are due to their hydropower potential (Sivongxay et al., 2017), economic development (Grumbine and Xu, 2011) and political characteristics (Hennig et al., 2013; Hirsch, 2016; Zeitoun and Warner, 2006).

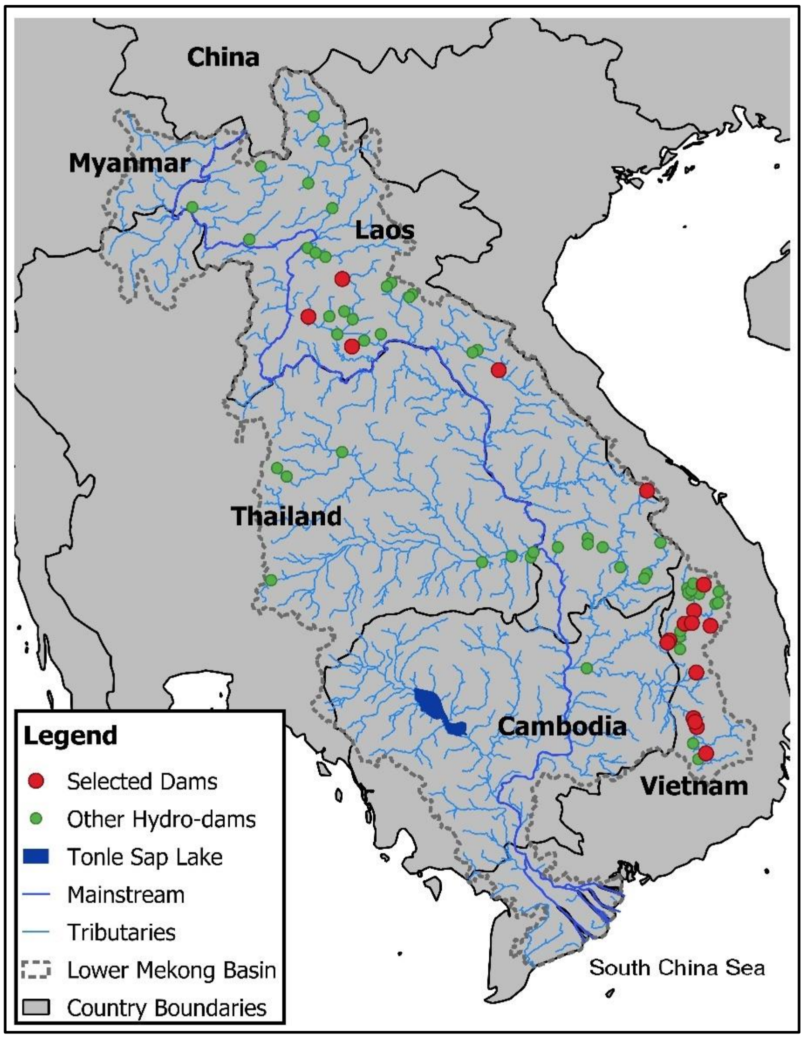

Figure 4.1. The Lower Mekong River Basin, and locations of dams. We selected 16 dams as our study dam sites (red circles).

However, urgent issues in the LMRB are that many hydro-dams have been planned and the accurate assessment on the effects were not established well. In the LMRB, there is no dam so far, but Laos proposed 11 new dams in the mainstream (Grumbine and Xu, 2011). Given that even dams on the tributaries and the Upper Mekong River Basin (UMRB) reduced the sediments up to 75%, and 2.1 million people suffer the losses (Grumbine and Xu, 2011), new dams in the mainstream would cause more serious issues in the LMRB. Although dams in the LMRB are criticized as projects without strategic estimation on their cumulative impacts on river (Schmitt et al. 2018), it is difficult to say that Laos' planned dams will be denied by other surrounding countries due to their reliance of electricity on Laos (Stone 2011). Currently, two of the 11 planned dams in the mainstream are in construction; Xayaburi dam is almost completed, Don Sahong dam is in the beginning stages of construction (Fox and Sneddon 2019). In order to make plans for new dams in a more sustainable way, accurate estimation on the effects of current dams is required in the LMRB.

4.2.2. Data

The time-series Nighttime Light Images (NLI) and Enhanced Vegetation Index (EVI) were used to extract the influential boundaries of dam effects, and LULCC were used to quantify the effects within the boundaries (Table 4.1). NLI have been widely used as an indicator of human activities (Amaral et al., 2005; Elvidge et al., 1999; Kim and Choi, 2015; Liu et al., 2012; Shao et al., 2014). In this paper, human activities related to dams, such as construction of dams and expansion of human settlement, were traced by time-series NLI. The Defense Meteorological Satellite Program – Operational Linescan System (DMSP-OLS) provides annual NLI from 1992 to 2013 with 1km spatial resolution, and it was selected as NLI in this study. Since six satellites (F10, F12, F14, F15, F16, and F18) were operated for DMSP-OLS mission, the inter-calibration method was applied to reduce inconsistent issues from different satellites (Elvidge et al., 2014).

Table 4.1. Remotely-sensed products used in this research.

Product	Date Availability	Temporal Resolution	Spatial Resolution	Data Provider
DMSP-OLS	1992-2013	Annual	1km	NOAA
MODIS-EVI (MOD13Q1)	2000-current	16-Day	250m	NASA
LMRB's RLCMS LCLUC	1987-2018	Annual	30m	NASA SERVIR Mekong

The EVI was used as an indicator of vegetation status, and it provides information related to the consequences of dams on changes in vegetative cover, as a proxy for changes in local characteristics, such as deforestation, land degradation and moisture patterns (Dahlin et al., 2014; Lausch et al. 2013; Lin and Qi, 2019). The EVI was selected among various vegetation indices due to its high sensitivity to areas with high biomass (Ustin, 2004) and low sensitivity to cloud effects (Suepa et al., 2016). The EVI product from the Moderate Resolution Imaging Spectroradiometer – Vegetation Indices (MOD13Q1- Version 6) was selected for this study. The product provides 16-day interval with 250m spatial resolution from year 2000, and this paper aggregated the products from 16-day interval to annual scale, which is the temporal resolution of DMSP-OLS, with average values.

The LULCC were used for quantifying the spatial impacts of dams on land use and cover disturbances (Jiang et al., 2018; Liu et al., 2007; Zhao et al., 2010), and LULCC from the

LMRB's Regional Land Cover Monitoring System (RLCMS) (https://landcovermapping.org/en/landcover/) was used. The LULCC product was derived from Landsat 4-7 and had a 30m resolution with considering phenology of surface which can improve the quality of classification. In this paper, the product was reclassified into five new classes ('water', 'forest', 'agricultural lands', 'shrubland-grassland', and 'urban-barren areas') from the 11 original classes ('water', 'forest orchard or plantation forest', 'evergreen broadleaf', 'mixed forest', 'urban and built up', 'cropland', 'barren', 'wetlands', 'grassland', and 'shrubland'), which were distributed in the study area. The original class 'water' and wetlands were reclassified to 'water', the original class 'forest orchard or plantation forest', 'evergreen broadleaf', 'mixed forest' were reclassified to 'forest', the original class 'urban and built up' and 'barren' were reclassified to 'urban-barren areas', the original class 'grassland' and 'shrubland' were reclassified to 'shrubland-grassland', and original class 'cropland' was re-labeled as 'agricultural lands.'

Dam data were from the '2017 Dataset on the Dams of the Irrawaddy, Mekong, Red and Salween River Basins' provided by the Greater Mekong Consultative Group on International Agricultural Research (CGIAR) Research Program on Water, Land and Ecosystems (WLE, 2017). For the dam selection, no information on dam commissioned year was removed. Based on the data availability of NLI and EVI, which are from 2000 to 2013, we selected 16 of the 75 commissioned hydro-dams, whose dam commissioned year is within the period from 2000 to 2013 (Figure 4.1 and Table 4.2).

Table 4.2. Selected dams and year of the temporal stages. T1 indicates “construction starting year”, T2 indicates “dam commissioned year”, and T3 indicates “stabilized year” (VN = Vietnam, LA = Laos, and CA = Cambodia).

Dam	Country	Capacity (MW)	T1	T2	T3
Plei Krong	VN	100	2003	2008	2011
Dak Doa	VN	14	2008	2010	2013
Nam Mang 3	LA	40	2002	2004	2007
Yali	VN	720	1993	2000	2003
Sesan 3	VN	260	2002	2006	2009
Dray Hinh 2	VN	16	2003	2007	2010
Sesan 4A	VN	63	2005	2008	2011
Sesan 4	VN	360	2004	2008	2011
Sre Pok 3	CA	220	2005	2009	2012
Sre Pok 4	VN	600	2008	2009	2012
Buon Tua Srah	VN	86	2004	2009	2012
Dak Psi 3	VN	45	2008	2010	2013
Nam Theun 2	LA	1075	2005	2009	2012
Nam Lik 1-2	LA	100	2007	2010	2013
Nam Ngum 5	LA	120	2008	2012	2015
A Luoi	VN	170	2007	2012	2015

4.2.3. Modeling temporal stages of dam constructions

Two spatial extents of consequences of dams were delineated based on two temporal stages of dams (Figure 4.2). Given that the consequences of dams are different depending on the time period of dam construction and completion (Chen et al., 2015; Jiang et al., 2018; Kirchherr et al., 2016), quantifying different patterns and extents according to different time periods will improve our understanding of the dam impacts. This study divided the temporal stages into the duration of the dam construction (P1) and after dam operation (P2). The spatial extent of the consequences during the P1 (P1-extent) can represent the spatial boundary of physical changes related to dams from the construction starting year (T1) to the commissioned year (T2), and those during the P2 (P2-extent) can represent the spatial delineation of physical changes related to dams from the T2 to the stabilized year (T3), which refers to the year of abrupt reduction of dam impacts. The P1 and the P2 of each dam were individually derived from T1, T2, and T3, which were defined by using official records, visual inspection, and changes of EVI because information on T1 and T3 is insufficient in the official records.

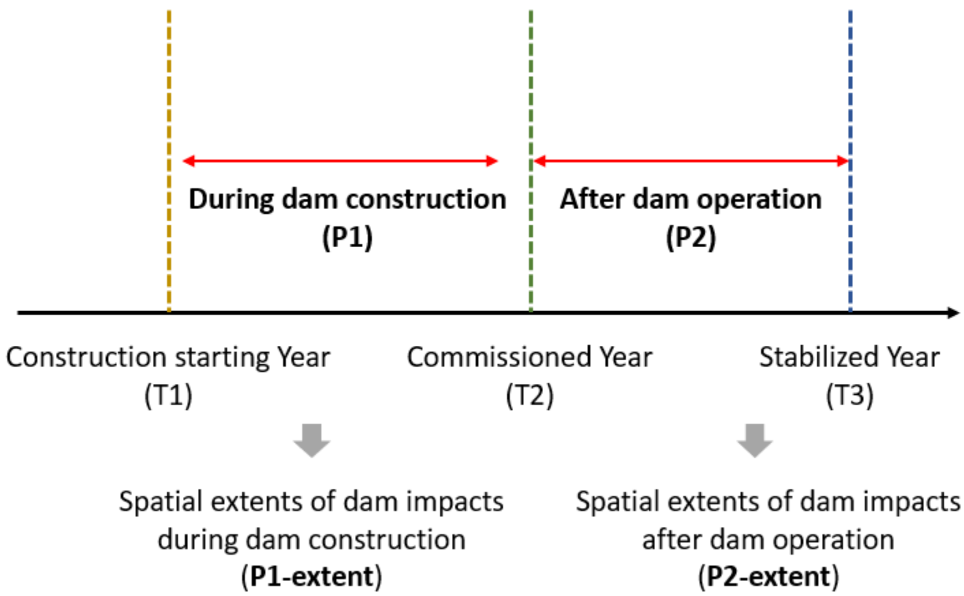

Figure 4.2. Temporal stages of the dam impacts on the environment and society. In this study, the P1-extent and the P2-extent were created from the P1 and the P2, respectively. Their different spatial pattern and extents can show that our model is appropriate for quantifying the consequences of dams.

The T1 was decided by visual-inspection of the time-series Landsat imageries when images of construction activities such as, logging and digging, were captured. The official information of the commissioned year was used for the T2. The T3 was selected three years after the T2 because it showed a significant stabilizing trend in EVI and NLI, which can intuitively show surface disturbance.

4.2.4. Modeling and quantifying spatial patterns of dam impacts

A standard deviational ellipse model (hereafter, referred to as the 'ellipse model') was developed to represent the shape of the spatial pattern of dams' impacts. Three parameters: major axis, minor axis, and orientation difference between the ellipse model and river were determined to represent the spatial pattern. The ellipse model is an effective shape to articulate the distribution and direction of spatial impacts (Gong, 2002; Kent and Leitner, 2007; Newsome et al., 1998; Yuill, 1971). The ellipse model was estimated as a more realistic spatial pattern to describe the individual travel activities in urban areas (Newsome et al., 1998) and the crimes (Kent and Leitner, 2007), but it has not been used in environmental studies yet. Kent and Leitner (2007) proved that the ellipse model had superior explanation on spatial distribution of crime than the circular-shape model (hereafter, referred it to as the 'circular model'). Since the consequences of dam impacts tend to occur along the river (Jiang et al., 2018; Ouyang et al., 2013; Scudder, 2005) and appear to be strongly a symmetric around the dam sites (Chen et al., 2015; Lin and Qi, 2019; Vaidyanathan, 2011; Zhao et al., 2010), the ellipse model was selected to fit the spatial patterns of dam impacts.

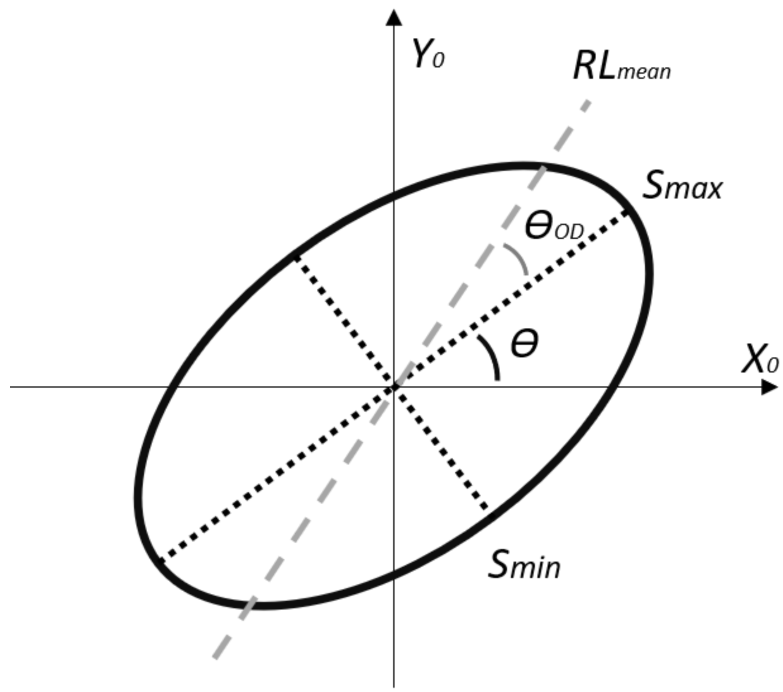

Figure 4.3. The conceptual ellipse model. The model is composed of the major axis (S_{max}), the minor axis (S_{min}) and the orientation difference (θ_{OD}), which is deviation between the orientation of the ellipse model (θ) and the mean orientation of river-lines.

The mathematical ellipse model was first developed by Lefever (1926), but it was criticized due to its unclear shape (Furfey, 1927; Gong, 2002; Yuill, 1971). Yuill (1971) modified this issue and suggested the mathematical expressions of axes and orientation for generating the ellipse model. Additionally, this paper devised new term 'Orientation of Differences (OD)' to suggest the orientation differences between the river-line and the orientation of the ellipse model (Figure 4.3). The OD can provide a more realistic model to estimate the spatial pattern of dam impacts. The mathematical expression for the OD is:

$$\theta_{RL}\ (mean\ orientation\ of\ river\ lines) = \frac{\sum \theta_i \cdot d_i}{d_{total}} \qquad (1)$$

$$\theta_{OD}\ (orientation\ difference) = |\theta - \theta_{RL}| \qquad (2)$$

where d_{total} refers to total distances of river-lines in the ellipse model, d_i refers to distances of ith segment of river-lines, θ refers to the orientation of the ellipse model and θ_i refers to orientation of ith segment of river-lines. The river-lines are segmented to each river-line (i.e., segment) at each curving point.

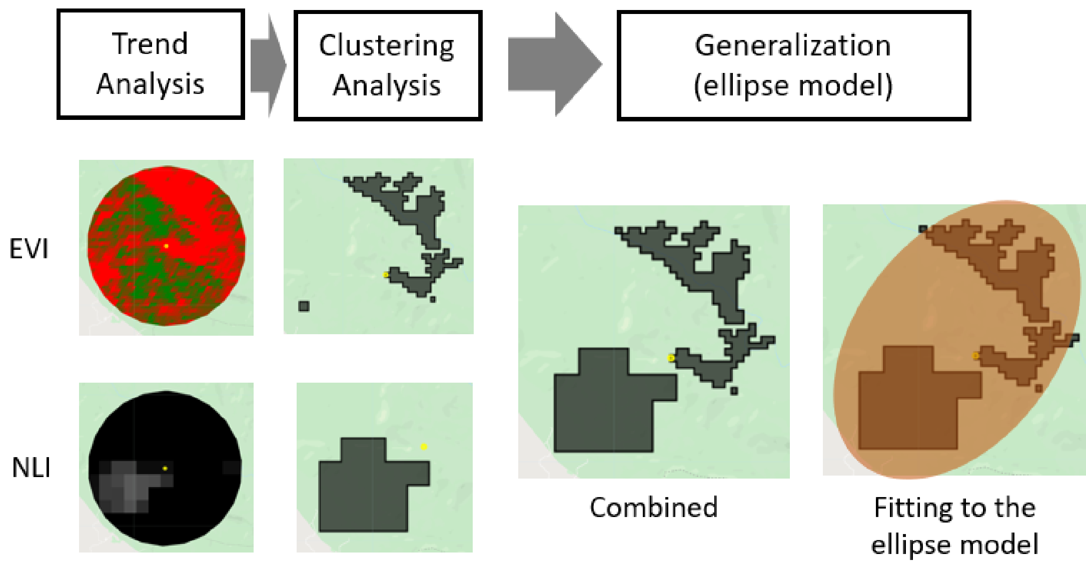

Figure 4.4. The workflow of deriving the spatial extents of consequences of dams for fitting it to the ellipse model.

The spatial patterns were obtained from time-series NLI and EVI through conducting proximity analysis, trend analysis, clustering analysis, and fitting to the ellipse model (Figure 4.4 & 5). The idea here is that areas with the effects of dams have distinguished temporal patterns within the buffered areas around dam-sites and grouping the distinct pixels can represent the influential areas of the effects. First, we conducted the proximity analysis on dam sites from 1km to 50km with 1km increments. The summation values of both EVI and NLI within buffers were checked for individual dams, and the radius with significant changes in the values was determined for individual dams. Second, the trend analysis was conducted for quantifying temporal trajectories of changes in time-series NLI and EVI within the selected radius. The Sen's slope analysis was selected because it can provide a significant trend, which is less sensitive to inconsistent changes among different images, by reducing the effects of outliers in trajectories using the median of the slopes of all lines through pairs of points in fitting (Sen, 1968; Suepa et al., 2016). Third, the clustering analysis was conducted to extract meaningful trends related to the consequences of dams. The k-mean clustering was selected because it is an effective method to make clusters without any prior knowledge (Perdinan and Winkler, 2015). Fourth, each cluster from NLI and EVI was combined, and its spatial distribution was fitted to the ellipse model with 95% confidence level.

4.2.5. Assessing the spatial patterns of dam impacts

4.2.5.1. Comparing the ellipse model to the circular model

The compactness index (eq. 3 below) and the omission index (eq. 4 below) were used to compare the performance in representing the dam impacts between the ellipse and circular models. The compactness index has been widely used to quantify the characteristics of the shape, such as intensification and dispersion (Maceachren, 1985; Zick and Matyas, 2016). We adopted the Lee-Sallee index (Lee and Sallee, 1970) in measuring the compactness because it is useful to compare the shapes in terms of the error of omission and that of commission. The Compactness Index (CI) is defined as:

$$CI\ (compactness\ index) = \frac{A_{intersection}}{A_{union}} \qquad (3)$$

where $A_{intersection}$ refers to the intersected areas between the combined extents (i.e., combined areas of extraction from NLI and EVI, see Figure 4.4) and the shape (i.e., the ellipse shape or the circular shape). A_{union} refers to the merged areas of the combined extents and the shape. The compactness index has a range from 0 to 1, where 1 indicates that the shape covers all the extracted areas, while 0 indicates the shape does not cover the extracted areas.

We also calculated the Omission Index (OI) to examine the error of omission because it is important not to miss the dam impacts:

$$OI\ (omission\ index) = \frac{A_{intersection}}{A_{combined\ extents}} \qquad (4)$$

where $A_{combined\ extents}$ refers to the extents of the combined areas of extraction from NLI and EVI. The omission index has a range from 0 to 1; the closer to 0, the more dam impacts are missing. We will compare the compactness index and omission index of the ellipse model and the circular model and determine the better model. The circular model was driven by the same areas as the ellipse model.

4.2.5.2. Measuring the spatial pattern of dam impacts

The ellipse index (eq. 5 below) was used to determine the different spatial pattern of dam impact while the deviations (eq. 6 below) of Land Cover and Land Use (LCLU) were used to quantify the spatial impacts as well as the different temporal stages of dams (Figure 4.2). The ellipse index refers to the index that represents the distribution of the pattern, so it has been widely adopted to articulate the shapes (Kent and Leitner, 2007; Yuill, 1971). The Ellipse Index (EI) is defined as:

$$EI\ (ellipse\ index) = 1 - \frac{S_{min}}{S_{max}} \qquad (5)$$

The range of the ellipse index is from 0 to 1; 0 is a circle and 1 is a line. A value close to 0 indicates that the shape is like the circle, and one close to 1 indicates that the pattern is like the elongated ellipse model. It can show how spatial patterns of dams were changed during the different stages of dams.

The deviations of LCLU were analyzed to quantify different dam impacts according to the different spatial extents in the different stages. The deviations of LCLU (Dev) were defined as:

$$Dev\ (deviations\ of\ LCLU) = LCLU_{time2} - LCLU_{time1} \qquad (6)$$

where $LCLU_{time1}$ refers to the LCLU in the earlier time and $LCLU_{time2}$ refers to the LCLU in the latter time. In other words, Dev_{P1} (the deviations of LCLU during the P1) is the deviations from $LCLU_{T1}$ to $LCLU_{T2}$ based on the P1-extent, and Dev_{P2} (the deviations of LCLU during the P2) is the deviations from $LCLU_{T2}$ to $LCLU_{T3}$ based on the P2-extent.

4.3. Results

4.3.1. Quantifying the spatial pattern of dam impacts

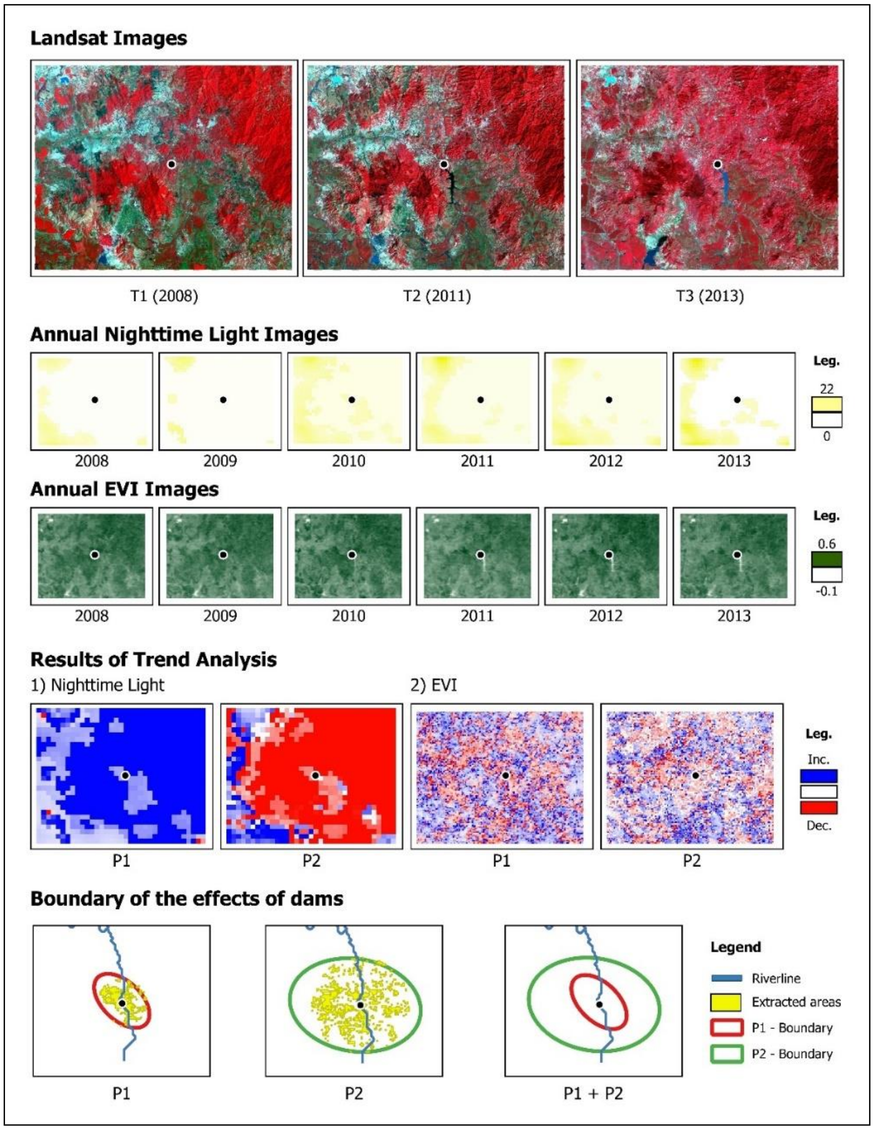

Figure 4.5. Delineation of the boundary of the effects of dams: Dak Doa dam (black point). Landsat Images showing the snapshot of T1 (construction starting year – 2008), T2 (commissioned year – 2011), and T3 (stabilized year – 2013) in false color. Annual Nighttime Light Images and EVI Images show the annual snapshot around the dam site. Results of Trend Analysis map show increasing (blue) or decreasing (red) trends of the NLI and EVI. From the slope values of the trend analysis, the dam-influential areas were extracted (yellow areas in bottom row) using the clustering analysis and they were fitted to the ellipse model (red edge – P1 and blue edge – P2).

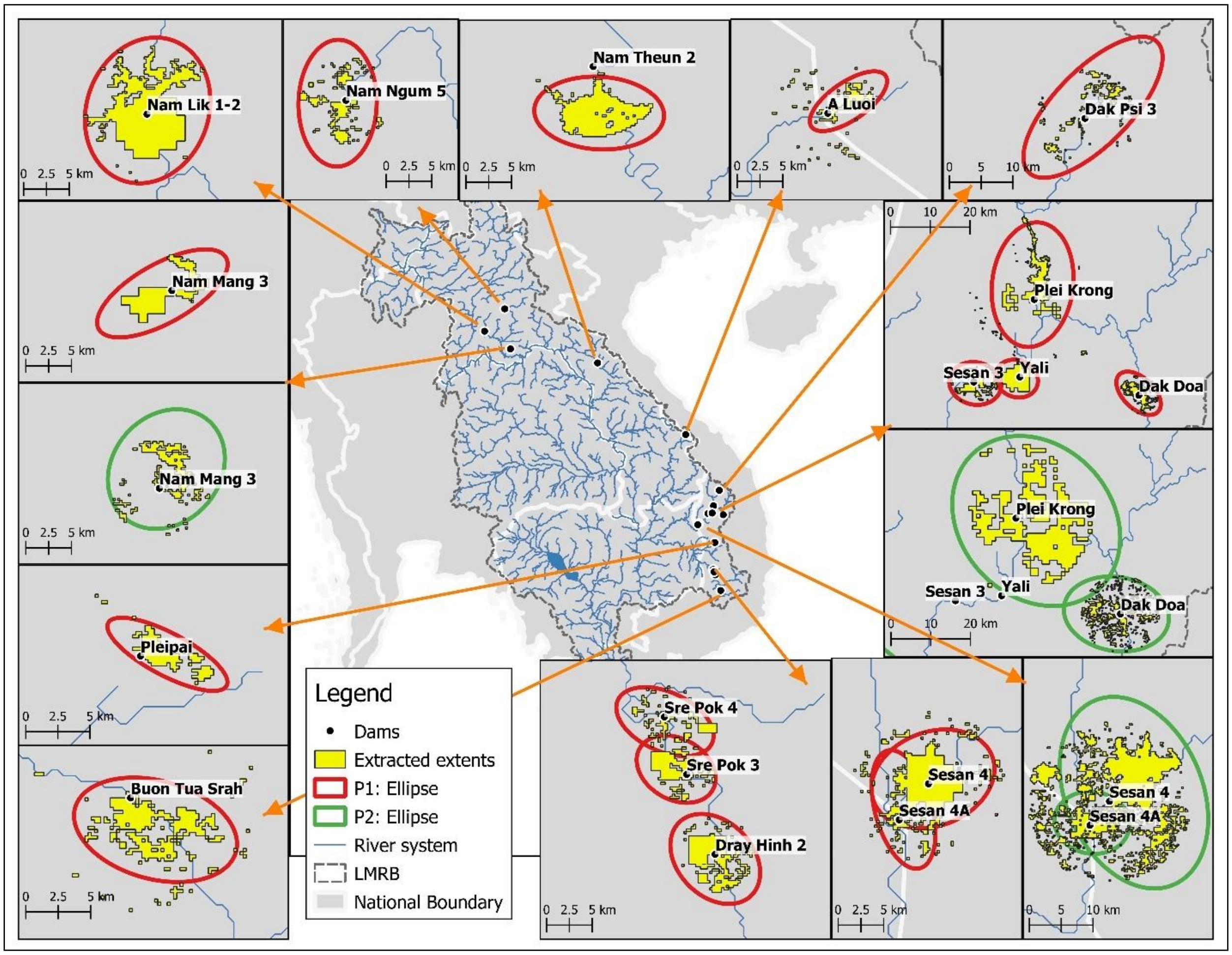

Figure 4.6. Spatial extents for the P1 and P2. The filled areas are integrated extents from time-series NLI and EVI. The non-filled areas are the ellipse-fitted extents from the integrated extents (see Figure 4.4).

The P1 extents of 16 dams and P2 extents of 7 dams (due to data availability, we only extracted 7 dams) were extracted, and they were fitted to ellipse models (Figure 4.5 & 6). Three components, the major axis (S_{max}), minor axis (S_{min}), mean orientation difference (θ_{OD}) were derived (Figure 4.7 & S1). The average of these components for P1 is 15.0km, 9.1km, and 28.5º and for the P2 is 21.3km, 16.3km, and 47.1º. Larger areas and orientation difference in the P2 showed that the spatial impacts during the P2 are likely to occur extensively and obviate from the river line.

4.3.2. Assessing the spatial extents of dam impacts

The compactness index (*CI*) and omission index (*OI*) were used to compare the performance of the ellipse model to the circular model (Figure 4.6 and 7) For the CI, the averaged CI of the ellipse model is 0.25 and 0.26 in the P1 and P2, respectively, while that of the circular model is 0.22 and 0.24. For the OI, the averaged OI of the ellipse model is 0.93 and 0.97 in the P1 and P2, respectively, while that of the circular model is 0.86 and 0.74. It showed that the ellipse model can make better representations for the spatial impacts of the dams. The CI is slightly better in the ellipse model, but the OI is much better in the ellipse model. This indicates that the ellipse model is generally better than the circular model, as it has a few omissions in quantifying the dam impacts. The ellipse index (*EI*) and deviations of LCLU (*Dev)* were used to examine the usefulness of the ellipse model in determining the different spatial patterns of the impacts in the different stages of dams (Figure 4.7). The averaged EI in the P1 is 0.38 and the P2 is 0.2, and it showed that the spatial extents of dam impacts are likely to be more elliptical shape during the P1 than the P2. In other words, there are more consequences of dams along the river during the P1 than the P2. The averaged deviation (*Dev*) in the P1 is 1.16km (water), -2.31km (forest), 0.93km (agricultural lands), 0.1km (grass-shrublands) and 0.08km (urban-barren areas), and the P2 is 0.12km, -1.55km, 1.32km, 0.08km and 0.03km. There are more areas of water inundation during the P1, expansions of agricultural lands during the P2, and deforestation during both periods.

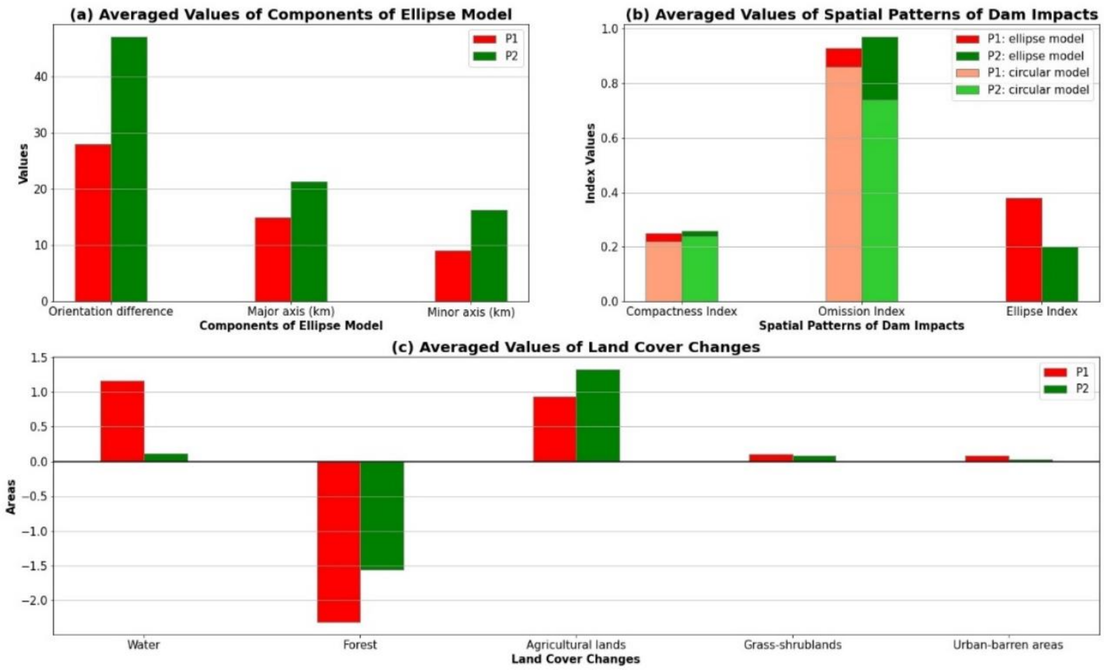

Figure 4.7. Comparison of P1 and P2 in components of ellipse model (a), spatial patterns of dam impacts (b), and land cover changes (c). The values were averaged from the dams in P1 and P2, and detail information is in S.1. In (a), the orientation difference (θ_{OD}), the major axis (S_{max}) and the minor axis (S_{min}) of P1 and P2 were compared. In (b), CI and OI of circular model (bright red – P1 and bright green –P2) and those of ellipse model (red – P1 and green – P2) were compared for examining the performance of the ellipse model. Then, CI, OI, and EI of P1 and P2 were compared. In (c), land cover changes of P1 and P2 were compared.

4.4. Discussion

4.4.1. The ellipse model for dam impact assessments

The ellipse model allows us to better quantify the consequences of dams than does the circular model. The ellipse model has 0.03 in the P1 and 0.02 in the P2 higher values in the compactness index and 0.07 in the P1 and 0.23 in the P2 in the omission index. The results showed the ellipse model has markedly better performance in capturing the spatial impacts of dams, while it might include additional areas of commission (irrelevant areas with dams). It is important not to omit the spatial impacts of dams because most dams have been underestimated in their extents (Jiang et al., 2018; Kirchherr et al., 2016; Tullos, 2009; Vaidyanathan, 2011; Winemiller et al., 2016). Underestimation of the extents led to misinform the economic benefits from the dams (Ansar et al., 2014; Fearnside, 2016; Latrubesse et al., 2017; Tullos, 2009; Winemiller et al., 2016) and make inappropriate compensations to local communities (Kirchherr et al., 2016; Scudder, 2005; Tullos, 2009; Vaidyanathan, 2011; Wang et al., 2013).

The main reason for the better performance of the ellipse model is that it can show the direction (Gong, 2002; Kent and Leitner, 2007; Newsome et al., 1998; Yuill, 1971), and this study found that the directional tendency of the ellipse model is useful in quantifying the dam impacts. The consequences of dam impacts are likely to occur along the river, such as water inundation (Ouyang et al., 2013), deforestation (Jiang et al., 2018) and dislocation (Scudder, 2005). The graphic representation of the ellipse model can summarize the direction of the distribution (Yuill, 1971), so it is effective to assess dam impacts. Distance, connectivity, and direction are three fundamental relationships for the spatial analysis on the space (Miller and Wentz, 2003; Nystuen and Marble, 1963), and the ellipse model can suggest these three things, while the circular model can only represent distance and connectivity.

The direction is useful in making quantitative and qualitative procedures of the spatial phenomenon (Miller and Wentz, 2003), so the ellipse model can allow us to make a better explanation on the spatial impacts of dams. Results of the EI (ellipse index) showed the advantages of the ellipse model. The averaged ellipse index during the P1 is 0.38 and the P2 is 0.2. It indicates that the spatial impacts of dams during the P1 are more likely to occur along the river and the P2 tends to obviate from the river. The results fit with different actual activities from dam stages. There are many activities along the river, such as dam construction during the P1 (Chen et al., 2015; Scudder, 2005), but comparatively fewer activities along the river, such as cultivation and urbanization, during the P2 (Jiang et al., 2018; Scudder, 2005). Differences in the ellipse index for the different stages showed the usefulness of the directional explanation of the ellipse model and capture the human activities.

4.4.2. Different spatial extents of dam impacts in different stages of dams

According to the dam stages, the spatial extents are different due to different activities. This paper is the first research on determining the different spatial extents according to the different stages of dam construction by applying the ellipse model. The axes and the orientation differences from the river of the ellipse model during the P2 are larger than during the P1. It indicates that the spatial impacts of dams are more extensive than during the P1. Additionally, the consequences of dams during the P1 are more concentrated along the river, as the ellipse index of the model during the P1 is larger than during the P2. The results from additional correlation analysis of the components of the ellipse model with the terrain (elevation and slope) revealed the differences in the spatial extents between the P1 and P2. According to the Spearman's correlation, terrains have positive relationships with the axes during the P1, while there is no relationship during the P2. In other words, there are more influences from the geomorphology (i.e., the river and the terrain) during the P1, and there are fewer, but more extensive, influences during the P2.

Different spatial impacts were determined during the P1 and the P2 by the ellipse model. According to previous studies, road construction for transporting materials of dam construction (Scudder, 2005), deforestation and excavation for dam construction (Chen et al., 2015), canal construction for diverting water and water inundation (Jiang et al., 2018) begins during the P1. Deforestation for expanding the agricultural lands and expansion of urban areas due to better accessibility of water, road, and electricity are major activities during the P2 (Chen et al., 2015;

Jiang et al., 2018; Wang et al., 2013). The analysis on LCLUC (Figure 4.7 & S.1) is similar to Jiang et al., (2018)'s research which quantified decreases in forest and increases in water and bare land during the P1, and they quantified more increases in water and urban-barren areas and more decreases in the forest during the P1 than the P2. The analysis showed that there are many deforestations during both periods, but the major reason is different. The results from the additional Spearman's correlation analysis showed that there is a strong negative relationship between water and forest, and it can be inferred that the major reason for deforestation during the P1 is water inundation. In contrast, there is a strong negative relationship between forest and agricultural land, so it can be linked to the major reason for the deforestation during the P2, which is the expansion of agricultural land. In summary, there are increases in water and agricultural lands and decreases in the forest during the P1, and there are increases in agricultural lands and decreases in the forest during the P2.

4.5. Conclusions

This chapter developed an ellipse model as a spatial extent model in representing dam impacts on the surrounding environment and society and quantified the spatial patterns and extents of the impacts at different stages of dams. The ellipse model was shown to have better representations of dam impacts than the circular model by three criteria: the compactness index, omission index, and ellipse index. The direction of the ellipse model was useful in articulating the consequences and effects dams have along the river.

Furthermore, this chapter divided the period of dam impacts into two periods (i.e., constructing period (P1) and operating period (P2)) and quantified different deviations of LCLU in order to show the usefulness of the ellipse model by applying different spatial extents to derive the LCLU. Different spatial extents showed that there are more influences from river and terrain during the P1 and less but extensive influences during the P2. For LULCC, there are many instances of deforestation related to water inundation during the P1 and deforestation related to the expansion of agricultural lands during the P2.

This paper contributes to better estimation of the environmental consequences of the human activities by adopting the ellipse model in quantifying its spatial impacts. Like dams, other human-environmental interactions leave a trace on earth observatory imageries, so our method for extracting the influential extent and fitting it to the ellipse model is applicable to detect spatiotemporal extents of other human-environmental interactions. Additionally, this paper pointed out that there are different extents of the impacts according to dam construction stages by using the ellipse model. It can provide an improved understanding of dam impacts, and it can be basic information for establishing policies on dam constructions. Especially, given that the LMRB is one of the most newly built dam areas and poor estimation, our study can provide an easy and effective decision tool to estimate the effects of dams.

In this paper, this chapter developed the ellipse model for the purpose of better characterizing and assessing dam impacts on the environment and society. This method could not consider the intensity of human activities. As the impacts are strong or intense around the dam sites, the intensity might be different according to the distance from the dam sites. Additionally, this study only focused on the effects of dams on surrounding areas, but the effects of dams occur beyond the sites. Therefore, future research may consider the intensity of dam impacts in addition to the spatial patterns and quantify the effects beyond the sites to make better understanding of the dams.

Chapter 5. Spatial Impacts of Dams in Watershed Scale on Wetland Inundations

5.1. Introduction

The inundation characteristics of wetlands play a significant role in their ecosystem functions and surrounding livelihoods in Southeast Asia. Large seasonal variation, caused by the Asian monsoon climate systems, creates and sustains wetland ecosystems for a variety of flora and fauna (Myers et al., 2000; Ziv et al., 2012), which are critical provisional services of wetland ecosystems for local livelihoods (Millar et al., 2019; Sabo et al., 2017). Given that large-scale changes in wetlands have been observed and reported in Southeast Asia (Frappart et al., 2018; Zhao et al., 2022), monitoring the wetland dynamics is essential in unveiling their subsequential influences on its ecosystem services and societies.

Hydro-dams largely alter the inundation characteristics of wetlands. They control the natural flow regime (Anderson et al., 2018; Poff et al., 2007) and trap the sediment (Bussi et al., 2021; Schmitt et al., 2019) and thus affect distant areas with the hydrological linkage (Ezcurra et al., 2019; Winemiller et al., 2016). Furthermore, dams in upstream cumulatively aggravate their influences on downstream hydrology in nonlinearity (Grill et al., 2014; Kummu and Sarkkula, 2008; Timpe and Kaplan, 2017). Since wetlands are hydrologically linked with dams (Leibowitz et al., 2018; Piman et al., 2013), it is inevitably affected by large-scale constructions of hydro-dams (Townsend and Foster, 2002; Wang et al., 2014). Particularly, the hydrology of wetlands is very sensitive to external stresses (Brasil et al., 2021; Nielsen et al., 2020; Reis et al., 2019) and, therefore, dams incur irreversible influence on wetland ecosystems (Richter et al., 1996).

Concomitantly, climate variability and local human activity around wetlands complicate the inundation dynamics. Climate variability, such as precipitation, temperature, and evapotranspiration, seriously influences wetland inundated areas (Erwin, 2009; Middleton and Souter, 2016). Specifically, Southeast Asian wetlands will suffer from increased precipitation and temperature with frequent extreme rainfall and drought events due to future climate changes (Han et al., 2019; Wang et al., 2017). Also, increasing demand for water and food has caused the local community to alter wetlands by the water use (Brock et al., 1999; Middleton and Souter, 2016), the conversion to agriculture and aquaculture (Yoshida et al., 2020), sand mining (NG and Park, 2021), and surrounding land cover changes (Brasil et al., 2021). Multiple drivers compounded the impacts of dams on the dynamics of wetland inundations and resulted in complex characteristics of these wetland dynamics (Arias et al., 2012; Modaresi Rad et al., 2022; Nielsen et al., 2020). Driving forces of wetland changes have been identified qualitatively, but the quantitative consideration of multiple drivers together is still challenging (Fernanda et al., 2017; Zheng et al., 2019).

Here, this chapter quantified the spatial and temporal dynamics of wetland inundations and quantitatively identified driving forces, focusing on the characteristics of wetland inundation dynamics in the three large basins of Southeast Asia (Mekong, Salween, and Irrawaddy Basins). Given that wetlands have hydrological linkages with dams, this research characterized their spatial relationships. Also, the different influence of dams on wetlands in direction and distance was quantified for a better understanding of the inundation dynamic. Three research questions motivate this study. First, to what degree has wetlands inundation been altered by hydro-dams? Second, how have wetlands been affected by the geographical location of hydro-dams? Third, to what degree are the spatial and temporal wetland dynamics related to local human activities and climate variability?

5.2. Materials and Methods

5.2.1. Selection of wetlands

439 natural wetlands were manually selected from HydroLAKES. The HydroLAKES dataset was derived from 8 global water products, including MOD44W and Global Lakes and Wetlands Database (GLWD). It has 1,427,688 water bodies over 10 ha, so it is popularly used for various studies (Cooley et al., 2021; Lehner and Döll, 2004). HydroLAKES provides a variety of water types, but most information about the natural wetlands was omitted, so we manually selected the natural wetlands. Here, natural wetlands refer to the naturally occurring water bodies. Thus, this chapter found the evidence of dammed or artificially created structures using Google Earth images, and time-series Sentinel 2 and Landsat 5-8. We labeled 'natural wetlands' for the wetlands without any evidence of artificial creation. As a result, the 439 water masks were selected from 2651 HydroLAKES water masks.

5.2.2. Water mask

362 water masks were created from the 439 selected water masks and used in delineating water inundation (Figure 5.1). Since HydroLAKES provide the static water mask (that shows a water inundated area for a period), the water masks should be updated to capture the maximum water inundation (Khandelwal et al., 2017; Reis et al., 2019). The maximum inundation area from the historical water product of European Commission's Global Water Surface Layer was used (Pekel et al., 2016). Some wetlands sharing the same water inundation area during the wet season were grouped as individual wetlands. Also, I thought that some wetlands combined with rivers during the wet season are largely influenced by the streamflow; thus, this chapter separated wetlands from the river. As a result, 362 water masks for wetlands were grouped and updated from 439 selected water bodies.

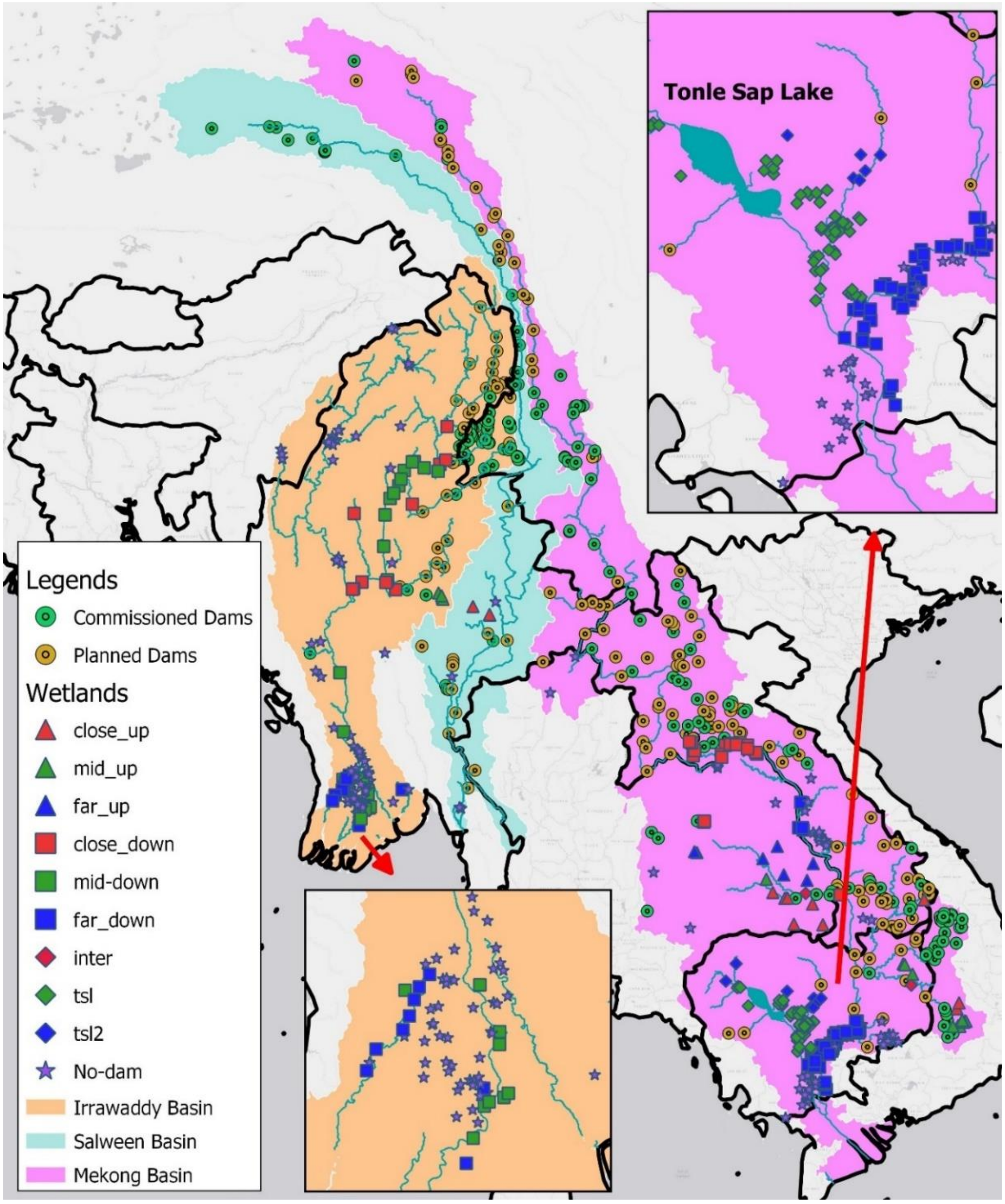

Figure 5.1. Study areas for Chapter 5. The distance was decided based on the watershed boundaries from HydroBASINS. No-dam is wetlands outside of the watersheds with dams.

5.2.3. Inundation delineation of wetlands in weekly scale

Using the newly generated 362 water masks, we extracted weekly inundated areas of wetlands from 2014 to 2021 using MODIS, Landsat 8, and Sentinel 1. For the optical sensors

(MODIS and Landsat 8), the water inundation areas were delineated using Automated Water Extraction Index (AWEI) for MODIS (MCD43A4.006) and Landsat 8 (Collection 1 - Surface Reflectance Tier 1) due to its high ability of the water detection for various environmental settings (Feyisa et al., 2014) (1-3):

$$AWEI_{nsh} = 4 * \left(\rho_{green} - \rho_{SWIR1}\right) - (0.25 * \rho_{NIR} + 2.75 * \rho_{SWIR2}) \quad (1)$$

$$AWEI_{sh} = \rho_{blue} + 2.5 * \rho_{green} - 1.5 * (\rho_{NIR} + \rho_{SWIR1}) - 0.25 * \rho_{SWIR2} \quad (2)$$

$$Water_{optical} = AWEI_{nsh} \cap AWEI_{ssh} \quad (3)$$

where ρ is the reflectance value of spectral bands, and $Water_{optical}$ is delineated water pixels from optical sensors, which are Landsat 8 and MODIS. The AWEI was originally developed based on Landsat 5, but it can be applied to various sensors (Tobón-Marín and Cañón Barriga, 2020; Yue et al., 2020). $AWEI_{nsh}$ is an index to eliminate nonwater pixels (e.g., dark built surfaces in areas with urban background), and *nsh* indicates non-shadow (Feyisa et al., 2014). $AWEI_{sh}$ is an index for removing shadow pixels for improving the accuracy of the water detection, and *sh* indicates shadow (Feyisa et al., 2014).

For SAR, thresholding methods were used on VV and VH polarization on Sentinel 1 (IW mode) (Chang et al., 2020) (4):

$$Water_{SAR} = \rho_{VV} \leq -14 \cap \rho_{VH} \leq -22 \quad (4)$$

where ρ is the polarization of VV or VH, and $Water_{SAR}$ is delineated water pixels from SAR, which is Sentinel 1. The thresholding values for VV and VH were determined by preliminary research on 362 water bodies in the region based on methods from Markert et al. (2020).

Each scene of MODIS, Landsat 8, and Sentinel 1 was processed to delineate the inundated areas (1-4), then the extracted areas were merged and aggregated to weekly scales. The results were evaluated by accuracy assessment on these binary classified results (i.e., water or not) based on visual inspections using Landsat 5-8 and Sentinel 2. 5% of the weekly observations were randomly selected (i.e., 18 validation points per week), so 9504 validation points (18 points*52 weeks*8 years) were randomly distributed over 362 water masks. All processes were conducted in Google Earth Engine, and the results were 92.1%, which showed good performance.

5.2.4. Location of wetlands in regard to dam placement

The locations of wetlands in regard to dam placement were decided based on the watershed boundaries from HydroBASINS and HydroRIVERS (Lehner and Grill, 2013) (Figure 5.1). The selected 362 wetlands were grouped to 10 categories as ‘upstream-close’, ‘upstream-mid’, ‘upstream-distant’, ‘downstream-close’, ‘downstream-mid’, ‘downstream-distant’, ‘INT’, ‘TSL1’, ‘TSL2’, and ‘no-dam.’ First, the wetlands with the existence of dam impacts were determined by the connection from HydroRIVERS using the visual inspection. Wetlands without the river connection or close location with the river of dams were labeled as ‘no-dam.’

Second, for wetlands in ‘yes-dam’, the location of upstream or downstream of dams were determined by the spatial location and river order information from HydroRIVERS. For instance, if the river order of a wetland is higher than that of a dam, then the wetland is located downstream of a dam. Two wetlands are located between upstream of dams and downstream of dams, and they were labeled as INT (inter-basin wetlands).

Third, the distance of wetlands in regard to dams in the watershed scale from HydroBASINS was labeled as ‘close’, ‘mid’, and ‘distant.’ A wetland, which is located the same watershed with a dam in HydroBASINS' level 6, 7, and 8, was labeled as 'close', 'mid', and 'distant,' respectively (There are 12 hierarchical levels in HydroBASINS, and the larger number has a smaller-sized watershed boundary). The Tonle Sap Lake system (TSL) is located in the lower Mekong (Figure 5.1), and it was labelled separately due to its unique system. Due to the water level changes with the mainstream, water is flowing to the mainstream during the wet season, but it is reverse flow from mainstream of Mekong during the dry season. This distinct flooding pulse system contributes to one of the most unique and biodiverse areas in the world (Arias et al., 2012; Hecht et al., 2019; Kummu et al., 2008). TSL is linked with the mainstream through the Tonle Sap River, and there are many wetlands on the floodplain. The wetlands here experience the flooding pulse system like TSL, and they were labelled as TSL1. The upstream tributaries flowing to TSL was labelled as TSL2, and they will have less influence from the mainstream.

Fourth, the distance of wetlands from the closest dams using the river network from HydroRIVERS.

5.2.5. Climate variability

The impacts of climate variability on the wetland inundations were considered to clarify the impacts of human activity on the hydrological alteration of the wetlands. This study considered the regional climate variability and local climate variability due to their influences on the inundated areas of wetlands. For the regional climate variability, El Nino-Southern Oscillation (ENSO), which is a recurring large-scale climate pattern every 2-7 year over Southeast Asia (Wang et al., 2021), was considered. For the ENSO, Niño 3.4 index, which is the averaged sea surface temperatures within the range of longitude 170-120W and latitude 5S-5N, was used (Fok et al., 2018; Wang et al., 2021). The index was obtained from NOAA (last accessed on July 20th, 2022; https://psl.noaa.gov/gcos_wgsp/Timeseries/), and they were recorded monthly. For local climate variability, Palmer Drought Severity Index (PDSI) was considered because this can summarize the complex results of precipitation, temperature, and evapotranspiration, which affect the surface water (Fok et al., 2018). PDSI was derived from TerraClimate, which are based on climate observations and climate reanalysis dataset (Abatzoglou et al., 2018). The size of grid is 4638m so the grids including each wetland were collected in monthly scale.

Since this research's weekly scaled water inundation dataset covered 8 years, the longer water inundation dataset was required to quantify the relationship between the climate and water inundation. In considering the relationship, the monthly scale is sufficient to examine the relationship between wetland inundations and climate variability in long-term, so the European Commission's Global Water Surface Layer was used (Pekel et al., 2016). This dataset can provide monthly inundation information over 30 years, but there are many omissions due to cloud covers. Thus, this study selected 56,460 observations with cloud cover less than 10% for 360 wetlands (2 wetlands were removed due to the cloud cover).

The Spearman's rank correlation was used to quantify the relationship between climate variability (i.e., EINO 3.4. and PDSI) and the wetland inundations. This chapter hypothesized the location of wetlands in regard to dam placement may have different relationships with the climate variability due to the dam impacts, we conducted the Spearman's rank correlation for each location group (i.e., 'upstream-close', 'upstream-mid', 'upstream-distant', 'downstream-close', 'downstream-mid', 'downstream-distant', 'INT', 'TSL1', 'TSL2', and 'no-dam'). Due to the data availability, years from 1987 to 2020 were considered. Also, standardization was conducted to compare variables with different units. The correlation analysis was conducted for each wetland and then averaged to 10 location groups.

5.2.6. Local human activities

Along with dams and climate, local human activities significantly affect the wetland inundations. In order to clarify impacts of dams on wetlands, local human activities were considered to distinguish their impacts on wetlands from dams. Using visual inspections on earth observations, this chapter labeled ‘human intervention (HI)’, ‘human intervention changes (HIC)’, ‘Land cover changes (LCC)’, and ‘water use (WU)’ as local human activities because they can be measured in earth observations. HI refers to the status of human intervention surrounding wetlands, such as agricultural lands, aquaculture, plantation, deforestation, and urbanization. HIC refers to the changes in human intervention (i.e., land surface changes from artificial surface to other human activities), such as converting agricultural lands to urban areas, and converting plantations to rice paddies. LCC refers to land surface changes from natural surface to artificial surface, such as converting forest to agricultural lands, and the expansion of aquaculture. WU refers to the status of direct water use on wetlands, such as canals, damming, and drainages. The four human activities were manually determined using time-series Sentinel 2, Landsat 5-7, and Google Earth images. When the evidence of mentioned surface changes was captured, the applicable human activities were labelled.

5.2.7. Hydrologic characteristics of wetlands

Dynamics of the inundations play a significant role in the wetland ecosystems and society (Kummu and Sarkkula, 2008) and this pattern is influenced by the climate variability and human activities (Han et al., 2019). The influences of the climate variability on inundated areas were considered by the correlation analysis (see the section ‘Climate variability’), and the influences of human activities were considered by four characteristics of wetland inundations. The four characteristics of wetland inundations were calculated from the weekly water inundation areas from 2014 to 2021.The cyclical inundation pattern, trend, inter-annual variability, and amplitude of inundated areas were calculated (Figure 5.2).

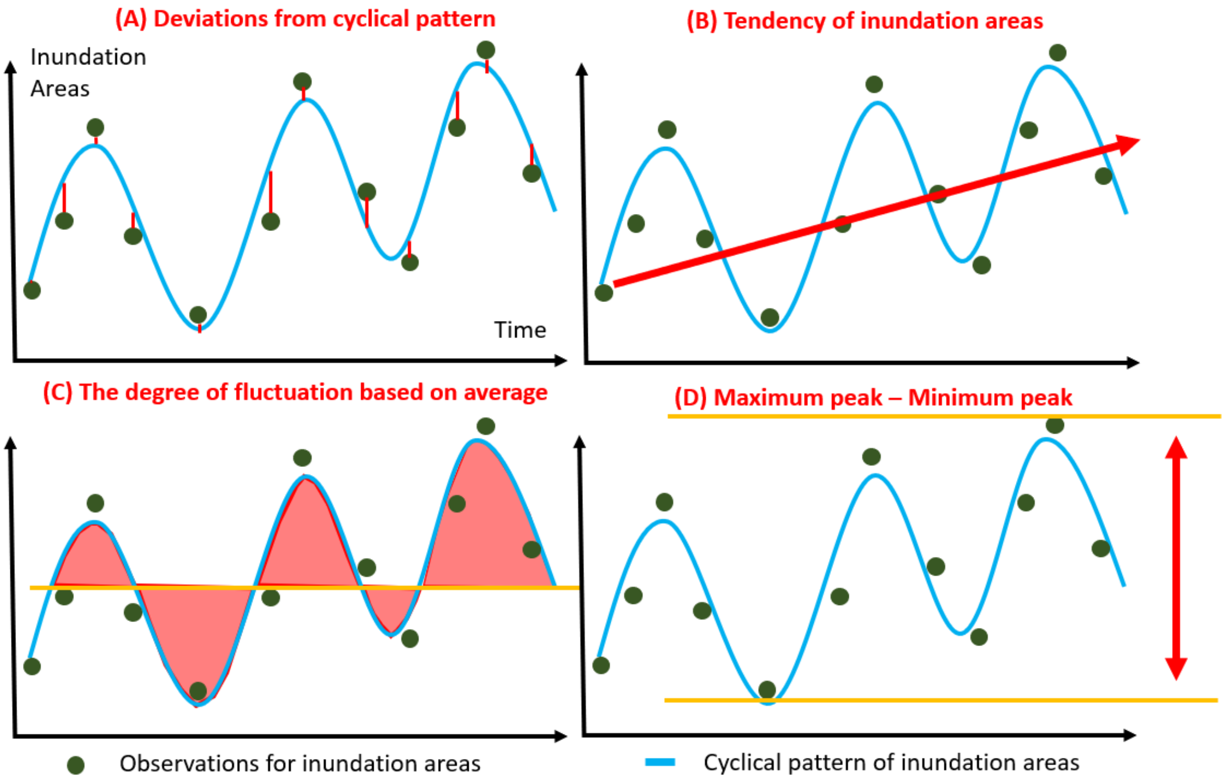

Figure 5.2. Hydrologic characteristics of wetlands. The natural pattern, trend, intra-annual variability, and amplitude of wetlands were considered. The inundation patterns of the wetlands show a seasonally cyclical pattern. The natural pattern was measured by the deviations from the cyclical pattern (A), trend was measured by the tendency of inundation changes (B), intra-annual variability was measured by the fluctuations in inundation patterns (C), and amplitude was measured by the difference between maximum and minimum peaks (D).

First, the cyclical inundation pattern is showing naturally controlled phenology of the inundations that are mainly caused by climate. Given that the cyclical pattern has the regularity, the pattern was measured by the degree deviating from the regularity. This can show how a wetland's inundation pattern is disturbed. This study assumed the sinusoidal model as representing the cyclical pattern of the wetlands in the region, because Southeast Asian wetlands have a sinusoidal shape of regular and cyclical hydrological patterns (Arias et al., 2012; Frappart et al., 2018; Kummu and Sarkkula, 2008) (Figure 5.2 and Figure 5.7). The deviations from the sinusoidal model were measured by the residuals from decomposing the weekly inundated areas of wetlands into the trend, cycle, and residuals. Weekly inundations of each wetland were fitted to the sinusoidal model (5):

$$Sin_i = C + \alpha * \sin(wx_i + \phi) + E_i \quad (5)$$

where i is i^{th} week, C is a constant value, which is the mean values of water inundated areas and α is an amplitude of the areas, which is the difference between maximum and minimum areas. ω is the frequency, here is 1/52 because there are 52 weeks a year. x_i is the inundation area of time i, Φ is the phase shift, and E is the error.

In order to examine whether the cyclical patterns of the inundation were disturbed or not, the n^{th} polynomial model was considered. By comparing the performance of fitting the inundations to the sinusoidal model with polynomial model, the model with higher performance (here, we used r^2) was selected for each wetland. If the polynomial model (sinusoidal model) was selected for a wetland, then this wetland is determined as having disturbance (less disturbance) (Figure 5.7). Each wetland was fitted to the n^{th} polynomial models (6):

$$Poly_{i,n} = a + bx_i + cx_i^{\,2} + \cdots + zx_i^{\,n} \quad (6)$$

where n is the order, a is a constant value, b, c …, z is coefficients. The n^{th} order was determined by having the maximum r-squared value

Second, the trend of inundation refers to the tendency of water inundation areas in weekly scale (Figure 5.2). It was calculated by the seasonal Kendall Trend test, which is a nonparametric test analyzing whether seasonal data are changed in monotonic trends (Hirsch et al., 1982) (7-10):

$$S_i = \sum_{k=1}^{n_i - 1} \sum_{j=k+1}^{n_i} sgn(x_{ij} - x_{ik}) \quad (7)$$

$$sgn\,(x_{ij} - x_{ik}) = \begin{cases} 1, & x_{ij} - x_{ik} > 0 \\ 0, & x_{ij} - x_{ik} = 0 \\ -1, & x_{ij} - x_{ik} < 0 \end{cases} \quad (8)$$

where x_{ij} is an observation (an inundated area) of year *j* in week *i*, and n_i is the observation of year *n* in week *i*. $sgn(x_{ij} - x_{ik})$ decides the value 1, 0, and -1 according to its sign. For example, x_{ij} is larger than the x_{ik}, then the value 1 is assigned. S_i shows whether positive value (negative value) shows inundated areas in week *i* in the later years tend to be larger (smaller) than those in week *i* in earlier years.

$$Var\,(S_i) = n_i(n_i - 1)(2n_i + 5) - \sum_{p=1}^{g_i} t_{ip}(t_{ip} - 1)(2t_{ip} + 5) \quad (9)$$

where g_i is the number of tied groups for the week *i*, and t_{ip} is the number of data in the group *p* for week *i*. Then, S' and $VAR(S')$ are calculated by summing all values of S_i and $Var\,(S_i)$, respectively, from week 1 to 52 (*i*).

$$Tr = \begin{cases} \dfrac{S' - 1}{(Var\,(S'))^{1/2}}, & S' > 0 \\ 0, & S' = 0 \\ \dfrac{S' + 1}{(Var\,(S'))^{1/2}}, & S' < 0 \end{cases} \quad (10)$$

where *Tr* is the result of the seasonal Kendall Trend test for a wetland over the observations, and a positive (negative) value indicates that the inundation areas trend to increase (decrease) over time. The trend of the inundated areas of wetlands (*Tr*) was used for the study, but the significance of level was not considered. The slope was converted to binary variables for the logistic regression model; 1 (positive) and 0 (negative).

Third, the intra-annual variability refers to the degree of fluctuations in weekly scaled inundation areas (Figure 5.2). The measure was based on the method suggested by Feng et al. (2013) that comparing distribution of weekly inundated areas for a year by the uniform distribution, which has same inundated areas for a year (11-14):

$$\bar{I}_k = \sum_{w=1}^{52} i_{k,w} \quad (11)$$

which is total inundated areas in weekly scale for a year *k*, and $i_{k,w}$ is an inundated area for week *w* in year *k*.

$$\bar{P}_{w,k} = \frac{i_{k,w}}{\bar{I}_k} \quad (12)$$

which is probability distribution of the total inundated areas for week *k* in year *y*.

$$\bar{D}_k = \sum_{w=1}^{52} \bar{P}_{w,k} \cdot \log_2(52 \cdot \bar{P}_{w,k}) \quad (13)$$

which measures the distance between the distribution of a observed weekly inundated area in for a year *k* and the uniform distribution of weekly inundated areas (i.e., 1/52).

$$IV_k = \bar{D}_k \cdot \frac{\bar{I}_k}{\bar{I}_{max}} \quad (14)$$

where $\bar{I}_{max}$ is the maximum inundated areas for the entire observations. IV_k measures the intra-annual variability for a year *k* by comparing the observed distribution with the uniform distribution. IV_k is 0 when the inundated areas are same for a year *k* and IV_k is maximized (at $\log_2 52$ = 5.7) when a wetland is inundated only for one week.

The intra-annual variability was calculated for each year, and the trend of the variability for 8 years was calculated using Sen's Slope Estimator for the robustness, which takes the median value of the slopes by all pairs of sample points (Hirsch et al., 1982). The slope was converted to binary variables for the logistic regression model; 1 (positive) and 0 (negative).

Fourth, the amplitude refers to differences between the maximum and minimum peaks (Figure 5.2). The measure was based on (15):

$$Amp_k = I_{k,max} - I_{k,min} \quad (15)$$

where the difference between a maximum inundated area ($I_{k,max}$) and a minimum inundation area ($I_{k,min}$) for a year *k* (see (11)). The amplitude was calculated for each year, and the trend of the amplitude for 8 years was calculated using Sen's Slope Estimator for the robustness. The slope was converted to binary variables for the logistic regression model; 1 (positive) and 0 (negative).

5.2.8. Logistic regression model

Logistic regression models were constructed to assess the contribution of dams and local human activities to the four hydrological characteristics. The logistic regression model has been widely used to evaluate the functional relationship between the dependent variable and potential drivers and identify the relative significance of each explanatory variable (Huang et al., 2009; Kominoski et al., 2018). This method is used to find the drivers of land cover changes (Huang et al., 2009) and identify dams as driving force on destroying fish extirpations (Kominoski et al., 2018). The logistic regression model is expressed as (15,16):

$$y = a + b_1x_1 + b_2x_2 + \cdots + b_mx_m \quad (15)$$

$$P_h = \frac{1}{1 + exp^{-y}} \quad (16)$$

where y is the dependent variable, x_n is explanatory variable, and b_n is the regression coefficients to be estimated. The function y is showing a linear relationship from a linear combination of the explanatory variables. P_h refers to the probability of occurrence of the hydrological alterations (h), and the range is from 0 to 1. The values close to 1 (0) indicates the hydrological alteration is more (less) likely to occur.

Four dependent variables, the cyclical pattern, trend, annual-variability, and amplitude of inundation were selected, and seven explanatory variables were considered for each dependent variable. For the explanatory variables, three are related to dams, which are the existence of dam (presence or not; a binary variable), location of wetlands in regard to dam placement (upstream or downstream; a binary variable), and distance of wetlands from the dams (a continuous variable). Other four binary variables are related to local human activities, which are HI, HIC, LCC, and WU. For each variable, five regression models were created using the above seven explanatory variables: 1) all wetlands, 2) downstream wetlands, 3) upstream wetlands, 4) close-located wetlands, and 5) distant-located wetlands. Thus, the total of 20 logistic regression models was established, and the models with significant variables were selected.

Table 5.1. Summary of wetlands with local human activities (C – Close-located wetlands; M – Mid-located wetlands; D – Distant-located wetlands).

	Upstream				Downstream				TSL			INT	No-dam
	C	M	D	All	C	M	D	All	TSL1	TSL2	All		
Total Counts	14	14	7	35	17	23	57	97	48	8	56	2	159
HI	100% (14)	71% (10)	100% (7)	89% (35)	100% (17)	100% (23)	100% (57)	100% (97)	88% (42)	88% (8)	88% (56)	100% (2)	96% (153)
HIC	14% (2)	7% (1)	14% (1)	11% (4)	41% (7)	9% (2)	37% (21)	31% (30)	44% (21)	0% (0)	38% (21)	0% (0)	23% (37)
LCC	86% (12)	50% (7)	100% (7)	74% (26)	76% (13)	91% (21)	95% (54)	91% (88)	67% (32)	75% (6)	68% (38)	100% (2)	80% (127)
WU	93% (13)	57% (8)	100% (7)	80% (280	82% (14)	91% (21)	95 (54)	92% (89)	79% (38)	88% (7)	80% (45)	100% (2)	92% (147)

5.3. Results

5.3.1. Wetlands with human activities

Among the 362 wetlands studied, 203 were in the watersheds where hydro dams exist, meaning that these wetlands are hydrologically connected to dams. The remaining 159 wetlands are not related to the dams (hereafter no-dam; See Figure 5.1 and Table 5.1). There are 35 wetlands located in upstream of dams (hereafter upstream wetlands; specifically, close-located: 14, mid-located: 14, and distant-located: 7), 97 wetlands in downstream of dams (hereafter downstream wetlands; specifically close-located: 17, mid-located: 23, and distant-located: 57), 56 wetlands located in the Tonle Sap system (floodplain of Mekong Basin located downstream, hereafter TSL; TSL1 (located between TSL between the mainstream of Mekong river): 48, and TSL2 (located upstream of TSL): 8; See Figure 5.1), and 2 wetlands located between upstream and downstream of dams (hereafter INT).

Human intervention (HI) refers to the human activities impacting wetland systems, such as agriculture, aquaculture, plantation, human settlement, and urbanization (Figure 5.3; Table 5.1). 94% of all wetlands in Southeast Asia suffer from human intervention. All downstream and

INT wetlands experienced HI, and there is HI for no-dam (96%), upstream (89%), and TSL wetlands (88%). The human intervention changes (HIC) refer to changes in HI, and land cover changes (LCC) refer to the changes in land coverage excluding HIC. In other words, HIC is based on the areas with human activities already (e.g., agricultural lands to settlement), but LCC is based on the areas with no human activity (e.g., forest to agricultural lands) (see the details in Method). 21% of all wetlands in Southeast Asia have human intervention changes. There are HIC for TSL (38%), downstream (31%), no-dam (23%), upstream (11%), and INT wetlands (0%) (Figure 5.3; Table 5.1). 83% of wetlands in the region suffer from land cover changes (LCC), including INT (100%), downstream (91%), no-dam (80%), upstream (74%), and TSL (68%) (Figure 5.3; Table 5.1). Water use (WU) refers to the evidence of direct water withdrawal from the wetlands like canals and damming (see the details in Method). 89% of the wetlands have direct water use, following INT (100%), downstream (92%), no-dam (92%), upstream (80%), and TSL (80%) (Figure 5.3; Table 5.1).

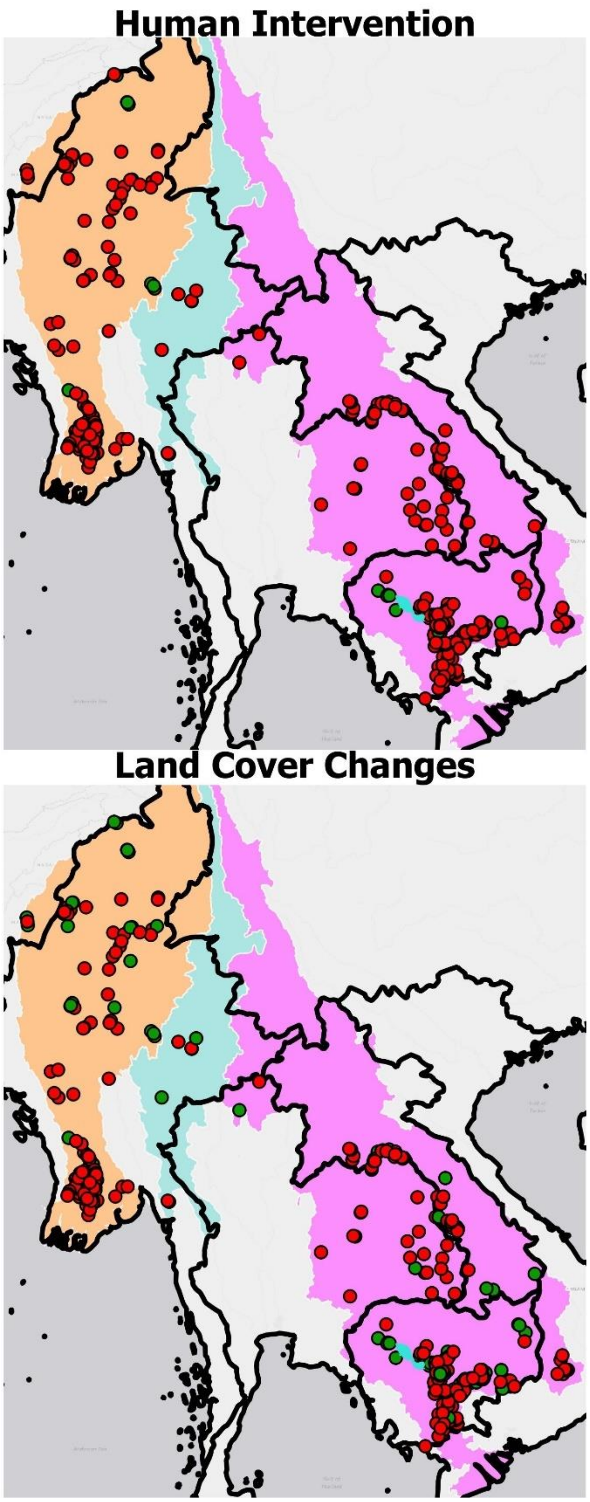

Figure 5.3. Local human activities in wetlands. The map shows HI, HIC, LCC, and WU. The red circle indicates the presence of local human activities, and the green circle indicates the absence of local human activities.

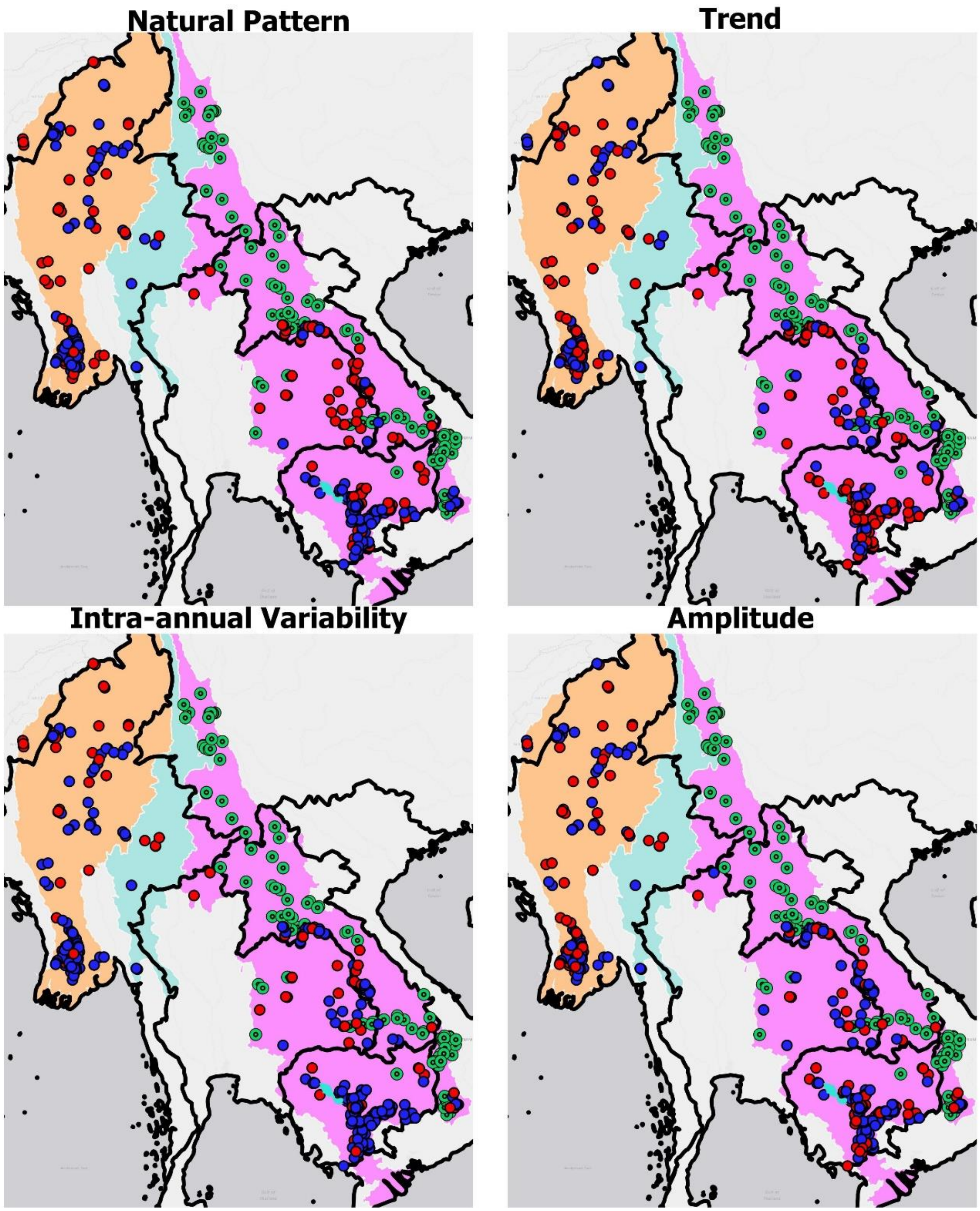

Figure 5.4. Hydrological alteration of wetlands. For the natural pattern of the inundation, red circles are wetlands which destroyed the natural pattern, and blue circles are wetlands with keeping the natural pattern. For the trend, intra-annual variability, and amplitude of the inundation, red circles indicate the decrease, and blue circles indicate the increase. For four maps, green circles are showing the commissioned dams.

Table 5.2. Summary of hydrological alterations in terms of human activities and locations of dams. The natural pattern, trend, intra-annual variability (V), and amplitude (A) of inundation were four hydrological alterations, and summarized by minimum, mean, and maximum values. For human activities, the existence of dams, HI, HIC, LCC, and WU were considered. For the locations of dams, 10 groups of wetlands in regard to the dam placement were considered.

			Minimum				Mean				Maximum			
			Trend	V	A	Pattern	Trend	V	A	Pattern	Trend	V	A	Pattern
Human activities	Presence of dams	0	-0.085	-0.077	-1.277	0.000	0.002	0.025	-0.009	0.002	0.096	0.414	0.606	0.065
		1	-0.093	-0.385	-0.970	0.000	-0.000	0.020	0.042	0.010	0.142	0.308	1.247	0.470
	HI	0	-0.028	-0.007	-0.007	0.000	-0.000	0.066	0.047	0.002	0.018	0.308	0.276	0.037
		1	-0.093	-0.385	-1.277	0.000	0.001	0.020	0.018	0.007	0.142	0.414	1.247	0.470
	HIC	0	-0.093	-0.385	-1.277	0.000	0.000	0.021	0.007	0.004	0.113	0.308	1.247	0.381
		1	-0.049	-0.381	-0.970	0.000	0.002	0.026	0.054	0.013	0.142	0.414	1.107	0.470
	LCC	0	-0.023	-0.024	-0.970	0.000	0.002	0.035	0.003	0.002	0.096	0.308	0.408	0.039
		1	-0.093	-0.385	-1.277	0.000	0.000	0.019	0.024	0.008	0.142	0.414	1.247	0.470
	WU	0	-0.028	-0.007	-0.970	0.000	-0.000	0.045	0.004	0.001	0.018	0.308	0.276	0.037
		1	-0.093	-0.385	-1.277	0.000	0.001	0.020	0.021	0.007	0.142	0.414	1.247	0.470
Locations of wetlands in regard to dam placement	Down-stream	Close	-0.090	-0.024	-0.090	0.000	0.002	0.013	0.035	0.002	0.142	0.078	0.432	0.040
		Mid	-0.018	-0.020	-0.208	0.000	0.005	0.017	0.044	0.009	0.113	0.097	0.509	0.162
		Distant	-0.093	-0.007	-0.580	0.000	-0.006	0.020	0.119	0.019	0.045	0.073	1.247	0.381
	TSL	TSL1	-0.049	-0.381	-0.970	0.000	-0.004	0.028	0.006	0.013	0.055	0.126	1.018	0.470
		TSL2	0.000	-0.015	-0.346	0.000	0.017	0.017	-0.018	0.007	0.043	0.055	0.296	0.019
	Upstream	Close	-0.006	-0.385	-0.027	0.000	0.003	-0.017	0.005	0.000	0.017	0.081	0.060	0.001
		Mid	0.000	-0.019	-0.043	0.000	0.010	0.062	0.014	0.001	0.099	0.308	0.113	0.007
		Distant	-0.080	-0.013	-0.799	0.000	-0.014	0.001	-0.109	0.004	0.002	0.009	0.229	0.021
	INT		0.000	0.001	0.005	0.000	0.006	0.015	0.018	0.000	0.012	0.028	0.032	0.000
	No-dam		-0.085	-0.077	-1.277	0.000	0.002	0.025	-0.009	0.002	0.096	0.414	0.606	0.065

5.3.2. Hydrological alteration of wetlands

The four hydrological alterations of wetlands were calculated based on Figure 5.2 (Figure 5.4 and Table 5.2). They can be summarized by human activities (Figure 5.5) and locations of wetlands in regard to dam placement (Figure 5.6). For the existence of dams, the wetlands with the linkage with the dam-watershed have more disturbance on cyclical patterns, decreased trend, decreased intra-annual variability and increased amplitude of inundation, compared to those without the dam watershed (Figure 5.5 and Table 5.2). For human intervention (HI), the wetlands with HI have more disturbance on cyclical patterns, increased trend, decreased intra-annual variability and larger amplitude of inundation, compared to those without HI (Figure 5.5 and Table 5.2). For human intervention changes (HIC), the wetlands with HIC have more disturbance on cyclical patterns, increased trend, decreased intra-annual variability and increased amplitude of inundation, compared to those without HIC (Figure 5.5 and Table 5.2). For the land cover changes (LCC), the wetlands with LCC have more disturbance on cyclical patterns, decreased trend, decreased intra-annual variability and increased amplitude of inundation, compared to those without LCC (Figure 5.5 and Table 5.2). For water use (WU), the wetlands with WU have more disturbance on cyclical patterns, increased trend, decreased intra-annual variability and increased amplitude of inundation, compared to those without WU (Figure 5.5 and Table 5.2).

In consideration of the locations, downstream-close wetlands (i.e., wetlands are downstream from dams and closely located to dams; see the labels in Method) have means of deviations of 0.04 for cyclical patterns, 0.002 for trend, 0.013 for intra-annual variability, and 0.035 for amplitude (Figure 5.6 and Table 5.2). In terms of downstream, the rests of four sub-categories-- downstream-mid, downstream-distant, TSL, and TSL2--had means of deviations from the cyclical patterns of 0.009, 0.019, 0.005, -0.018, trend of 0.005, -0.006, -0.004, 0.017, intra-annual variability of 0.017, 0.02, 0.03, 0.017, and amplitude of 0.044, 0.119, 0.028, 0.017 respectively (Figure 5.6 and Table 5.2). In terms of upstream and INT, the four sub-categories--upstream-close, upstream-mid, upstream-distant, and INT--had means of deviations from the cyclical patterns of 0.0002, 0.0008, 0.004, 0.00009, trend of 0.003, 0.01, -0.014, 0.006, intra-annual variability of -0.017, 0.06, 0.0007, 0.015, and amplitude of 0.005, 0.014, -0.109, 0.018 for (Figure 5.6 and Table 5.2).

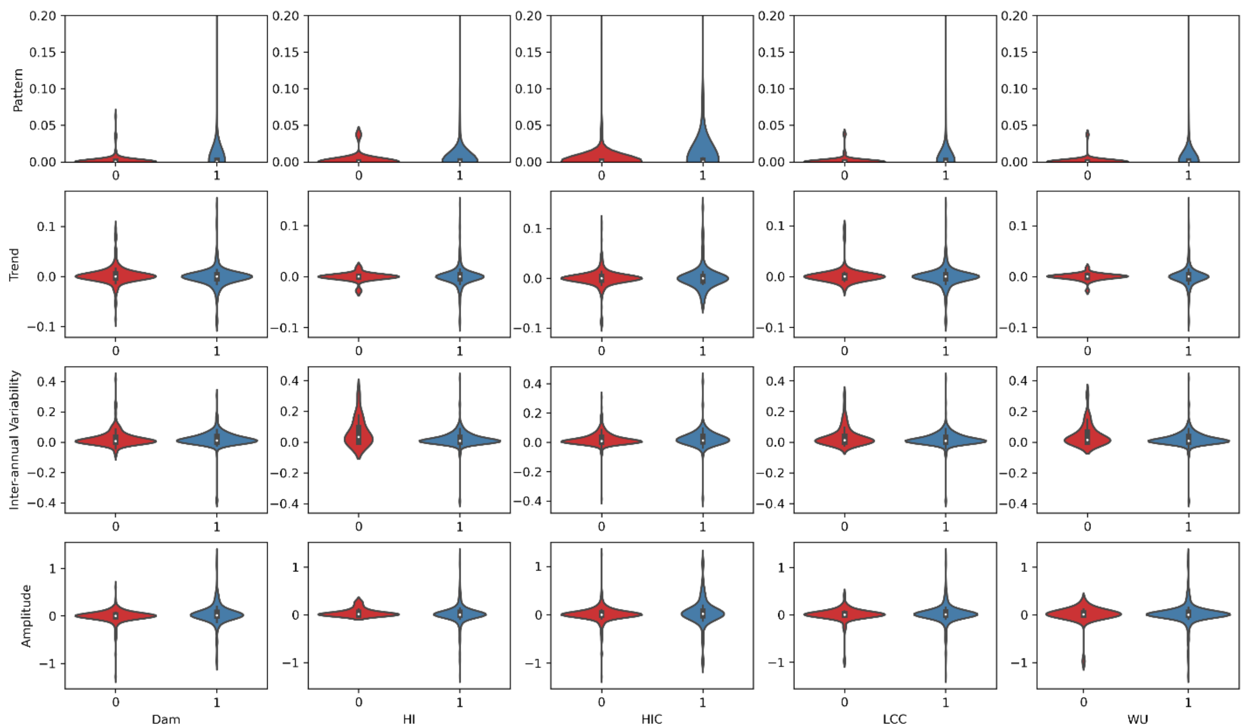

Figure 5.5. Summary of hydrological alteration and human activities. The presence of human activities which are the presence of dams, HI (human intervention), HIC (human intervention changes), LCC (land cover changes), WU (water use), and their relationship with four hydrological characteristics of wetlands.

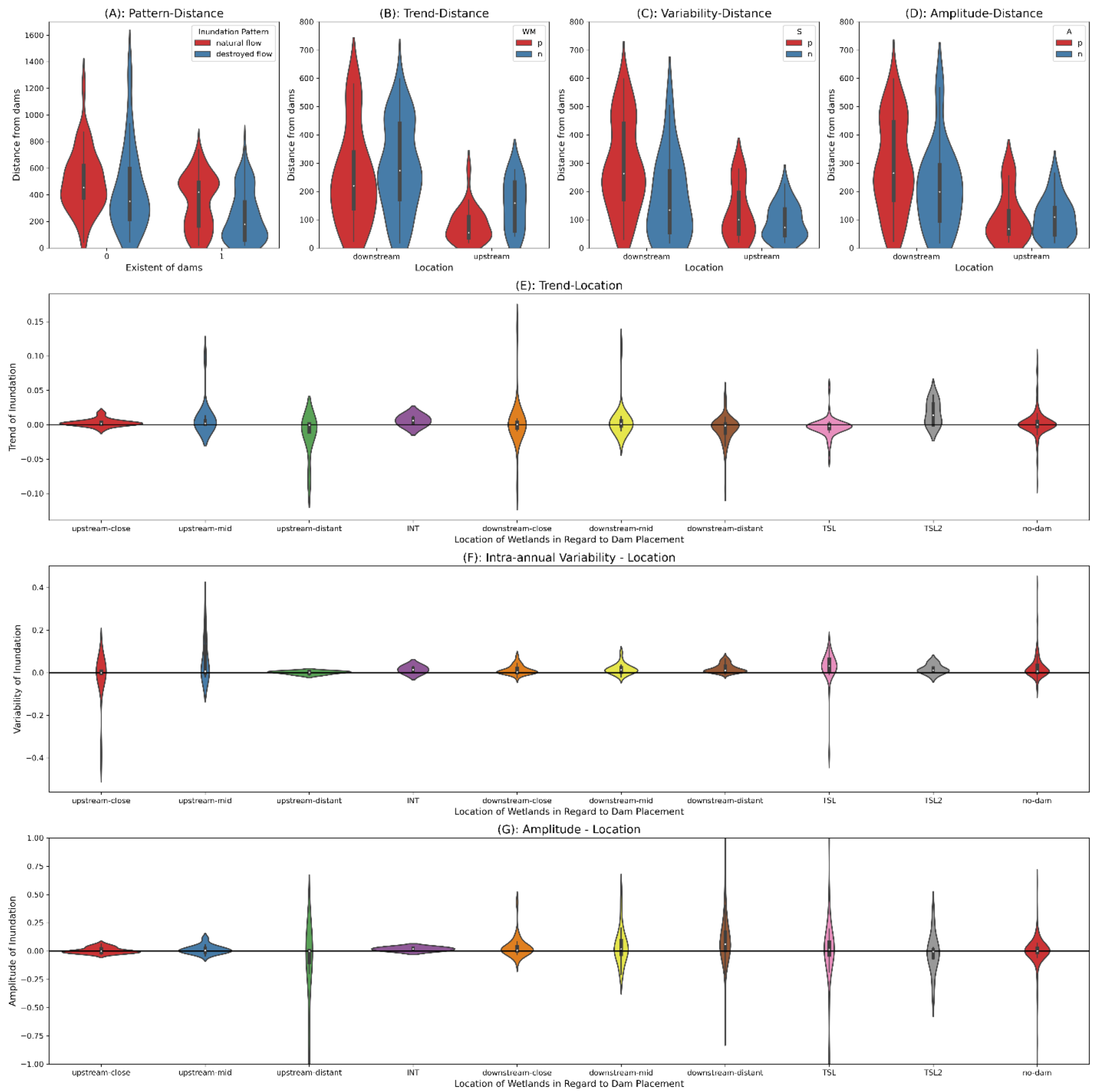

Figure 5.6. Summary of hydrological alteration in terms of dam location. (A) shows the distance of wetlands in regard to dam placement by considering the existence of dams and inundation pattern (red: cyclical patterns, blue: disturbed cyclical patterns). (B) - (D) shows the distance of wetlands in regard to dam placement and its relationship with trend (B), intra-annual variability (C), and amplitude (D) of inundation. Each hydrological characteristic is grouped by downstream versus upstream location. Also, the positive (red) and negative (blue) are separated in violin plots. (E) – (G) shows the location of wetlands in regard to dam placement and its relationship with trend (E), intra-annual variability (F), and amplitude (G) of inundation.

5.3.3. *Impacts of climate variability on the hydrology of wetlands*

Climate variability affected the hydrology of wetlands differently as the location of wetlands in regard to dam placement (Table 5.3). For regional climate regime, Niño 3.4 was considered for the effects of ENSO, and for the local climate regime, Palmer Drought Severity Index (PDSI) were considered. ENSO did not significantly affect the hydrological alteration of wetlands, but PDSI did. The hydrology of wetlands in the location of downstream-distant, upstream-distant, and TSL showed the significantly positive correlation with PDSI. However, wetlands in the other locations showed the insignificance.

Table 5.3. Results of correlation analysis between the climate variability and the hydrology of wetlands during 1987-2020. Spearman correlation analysis between standardized PDSI and standardized inundation areas (C – Close-located wetlands; M – Mid-located wetlands; D – Distant-located wetlands). * shows the significant correlation ($p<0.1$).

	Upstream			Downstream			TSL		INT	No-dam
	C	M	D	C	M	D	TSL1	TSL2		
Coef.	0.157	0.205	0.22	0.149	-0.008	0.273	0.298	0.137	-0.1	0.071
p.	0.226	0.111	0.091*	0.231	0.247	0.066*	0.034*	0.222	0.765	0.229

5.3.4. *Driving forces on the hydrological alteration*

The distance of wetlands from dams played a significant role in the impairment of the cyclical hydrologic regime with a 0.05 significance level (Table 5.4; See the details in Method). For downstream wetlands, the distance mattered for the cyclical patterns ($p<0.1$) but did not matter for upstream wetlands.

The existence of dams positively, and the distance ($p<0.005$) and WU ($p<0.1$) negatively affected the decreasing trend of inundation areas of wetlands (Table 5.4). For close-located wetlands, upstream location of wetlands ($p<0.005$) and LCC ($p<0.1$) significantly increased the trend. HI tended to increase the trend of mid-located wetlands ($p<0.05$), and the downstream location of wetlands were likely to decrease the trend of distantly located wetlands ($p<0.05$). For both downstream and upstream wetlands, the existence of dams seemed to increase the trend ($p<0.1$ and $p<0.005$, respectively), and distance from dams decreased the trend ($p<0.005$ and $p<0.05$, respectively). Also, the WU tended to decrease the trend in downstream wetlands ($p<0.1$).

Table 5.4. Results of logistic regression model for four hydrological characteristics. The logistic regression models were conducted using natural cyclical pattern (Pattern), trend, intra-annual variability (Var.), and amplitude of inundation (Amp.) as dependent variables (Dep.). Independent variables are the existence of dams (Ex.), distance of wetlands in regard to dams (Dis.), upstream located wetlands (Up.), downstream located wetlands (Down.), human intervention (HI), human intervention changes (HIC), land cover changes (LCC), and direct water use (WU). For each hydrological characteristics (Hy.), six logistic regression models using dependent variables, which are all, close-located, mid-located, distant-located, downstream, and upstream wetlands, were conducted, and only significant models were represented in the table. For significance level, †,*,** indicates 0.1, 0.05, 0.01, respectively.

Hy.	**Dep.**	**Ex.**	**Dis.**	**Up.**	**Down.**	**HI**	**HIC**	**LCC**	**WU**
Pattern	**All**	0.4	-0.37*	-	-	0.3	0.09	-0.73	0.38
	Downstream	0.23	-0.38†	-	-	0.18	0.2	-0.61	0.7
Trend	**All**	1.34*	-0.57**	0.69	-0.33	0.37	0.35	0.04	-1†
	Close	17	-	3.22**	1.42	0.16	2.2	3.03†	-19
	Distant	0.72	-	-1.51	-1.83*	0.1	0.5	0.22	-0.34
	Downstream	1†	-0.58**	-	-	0.17	0.33	0.15	-0.96†
	Upstream	3**	-1.08*	-	-	0.14	0.13	0.09	-0.45
Var.	**All**	-0.9	0.74**	-1.3*	0.09	-0.22	0.54	0.58	-0.07
	Downstream	-1	0.83**	-	-	0.06	0.45	0.33	-0.09
	Upstream	-1.67†	0.46	-	-	-0.01	1.01*	0.51	-0.44
Amp.	**All**	-0.18	0.11	-0.18	0.49	-0.31	0.44†	0.69	0.00
	Close	2.16	-	-2.06*	-1.07	-0.77	0.06	0.29	-0.07
	Downstream	0.19†	0.16	-	-	-0.33	0.42	0.81†	-0.16
	Upstream	-0.72	0.31	-	-	-0.37	0.78*	0.88	0.46

For the intra-annual variability of wetland inundation patterns, dams were likely to decrease the variability as close to wetlands ($p<0.005$) (Table 5.4). The intra-annual variability seemed to decrease closer to dams for downstream wetlands ($p<0.005$) but increase closer to dams for upstream wetlands ($p<0.05$). Also, HIC tended to increase the variability of upstream wetlands. ($p<0.05$)

The amplitude of wetlands tended to be increased by the HIC ($p<0.1$) (Table 5.4). For upstream wetlands, the close-located wetlands were likely to be negatively affected by dams ($p<0.05$) and positively affected by HIC ($p<0.05$). For downstream wetlands, the existence of dams ($p<0.1$) and LCC were related to increasing the amplitude ($p<0.1$).

5.4. Discussion

5.4.1. Hydrological control of climate variability on distantly located wetlands

Influences of climate variability was investigated to clarify the influences of dams on wetlands. The correlation analysis between the climate variability and the hydrology of wetlands shows that local climate variability affected the hydrological alteration of wetlands which are distantly located from the dams (Table 5.3). Specifically, distantly located wetlands were significantly correlated with local climate variability, closely located wetlands was not. This finding shows that the hydrology of closely located wetlands were controlled by other factors. Since this study considered the wetlands as the location in regard to dam placement (Table 5.3), this research infer that the water control by dams is likely to have larger impacts on the hydrology of closely located wetlands. The correlation analysis was not a precise method to quantify the effects of climate variability on the hydrology, but it can help us understand how dams have larger contributions to the hydrological alteration of the wetlands. Given that our research is focusing on the influence of human activity on the wetland hydrology, the correlation analysis is enough to support our findings on the relationship between the human activity and the hydrological alteration beyond the influence of climate variability.

5.4.2. Anthropogenic alteration of the cyclical inundation patterns of wetlands

These analyses figured out that the inundation pattern of wetlands is disturbed as close to dams (Table 5.4). This finding can be supported by Figure 5.6, which shows that wetlands with dams lose the cyclical pattern as close to dams, compared to wetlands without dams. Also, the result of correlation analysis between the climate variability and inundations (Table 5.3) and the contribution of local human activity according to the logistic regression model (Table 5.4) clarify that the alteration in cyclical patterns is mainly due to the dams. Given that there are very few studies about the relationship between wetlands and dams based on a data-driven approach (Vanderhoof et al., 2016), it can be supported by studies about the altered streamflow regime after dams. Many studies quantified that the hydrological patterns in dam-dominated river alter the magnitude, frequency, duration, timing, and rate of change (Fan et al., 2015; Poff et al., 1997). Given that hydro-dams irregularly release water to meet over daily, weekly, monthly, and yearly demands, dams increase the flow fluctuation (Hecht et al., 2019; Wang et al., 2014). For reducing the drought vulnerability in the dry season and flooding risk in the wet season, Southeast Asian dams release more water during the dry season but less water during the wet season (Mezger et al., 2021; Räsänen et al., 2012). Also, the range of the flow is increasing (Poff et al., 1997), and there are frequent sudden drops in the water level (Poff and Schmidt, 2016). These hydrological alterations of river flow (i.e., increases in variabilities, and decreases in seasonal pattern) make the dam-dominated flow regime be distinct from the natural flow regime. These findings can be inferred that the hydrological alteration of the river flow disturbs the cyclical inundation pattern of wetlands (Leibowitz et al., 2018; Vannote et al., 1980; Wohl, 2017).

5.4.3. Hydrological impacts of dams on upstream wetlands

This chapter found that dams increase inundation areas of upstream wetlands, but decrease intra-annual variability, and amplitude (Table 5.4, Figure 5.6, and Figure 5.7). The increases in inundation areas can be supported by the increases in lateral hydrologic connectivity (Leibowitz et al., 2018) and groundwater (Feiner and Lowry, 2015). Leibowitz et al. (2018) pointed out that dams lead to increases in inundated areas in upstream riparian areas and it increases the connectivity. It may increase the water flow to wetlands, so the inundation areas would be increased. Additionally, the increased groundwater by dams will lead to an increase in the surface water (Feiner and Lowry, 2015), so there would be increases in the inundated areas of upstream wetlands. Increasing hydrologic connectivity leads to the decreases in intra-annual variability and amplitude of inundation patterns of upstream wetlands. Dams store large amounts of water and control the water release, and it decreases the seasonal variation of streamflow (Dang et al., 2016; Mezger et al., 2021). The connectivity may transfer loss of the seasonal variation to upstream wetlands. Huge amount of water impoundment in the dams already increased the inundation of water level and attenuate the seasonal variation, the amplitude is decreased.

5.4.4. Hydrological impacts of dams on downstream wetlands

This chapter showed that dams increase amplitude and inundation areas and decrease intra-annual variability of the closely located downstream wetlands (Table 5.4 and Figure 5.6). For distantly located downstream wetlands, dams decrease the inundation areas. Flow alteration usually reduces the variability, but enhances the amplitude of downstream (Poff et al., 1997), and its effect is stronger closer to the dams. The flow alteration by dams increases the amplitude of flow fluctuation (Cochrane et al., 2014; Hecht et al., 2019; Poff et al., 1997), and it consequently increases the amplitude of the closely located downstream wetlands. For water extents, Southeast Asian dams release more water in the dry season (Mezger et al., 2021; Räsänen et al., 2012), and the closely located wetlands would have a significant influence on them. Given that small rises in the dry season wetland water would increase inundation areas and permanently inundate the wetlands (Kummu and Sarkkula, 2008), the closely located downstream wetlands increased the inundation areas. For intra-annual variability, dams attenuate downstream variability by reducing the streamflow in the wet season and increasing the streamflow in the dry season (Leibowitz et al., 2018; Mezger et al., 2021; Piman et al., 2013). For instance, Piman et al. (2013) simulated the hydrological effects of the potential development of new dams in tributaries of the Mekong River and found that the dams will increase 63% of dry season flows and decrease 22% of wet season flows in the outlet of the tributaries, where dams are closely located (50-300 km).

Compared to the closely located downstream wetlands, distantly located downstream wetlands do not show decreases in intra-annual variability but have increasing amplitude and decreasing inundated areas (Table 5.3,4, Figure 5.6, and Figure 5.7). This can be explained by the larger influence from local climate variability and weaker influence from the distantly located dams. As distant from dams, the reduced flow variability seems to have insignificant effects on distantly located wetlands, but the local climate variability affects the variability. Findings from Table 5.3 shows that the local climate variability increased the variability of the hydrology and dam impacts reduced the variability for closely located wetlands. Conversely, the distantly located wetlands are less impacted from dams, but more impacted from climate variability, so they can keep the intra-annual variability. However, increasing the amplitude of flow is still significant to distantly located wetlands. I speculated that maximum and minimum inundation areas of wetlands are controlled by the mainstream (Kummu and Sarkkula, 2008). The decreased inundation areas of distantly located wetlands can be supported by the finding that local climate variability reduced the inundation areas (Table 5.3). Also, it can be supported by previous studies on the dam impacts using wetland modeling (Nielsen et al., 2020), hydrological modeling (Piman et al., 2013), streamflow discharge (Lu et al., 2014), and earth observations (Wang et al., 2014). Dams reduce the flows downstream so they result in decreasing inundation extent, inundation duration, and connectivity for distantly downstream wetlands, especially floodplain wetlands (Hecht et al., 2019; Nielsen et al., 2020; Wang et al., 2014). Lower water discharge downstream in both dry and wet seasons can also elaborate the decreased water extents (Lu et al., 2014). Additionally, dams cause incision and erratic channel flow so water flows into the floodplain tend to be lowered (Middleton and Souter, 2016).

5.4.5. Hydrological alteration of wetlands from surrounding local human activities

Even though the selected wetlands in this study are naturally occurring wetlands, most show local human activities (Figure 5.3; Table 5.1). In fact, local human activity and wetland changes can be inter-related. For example, dams decrease the water availability in dry season, so this causes the local community to use water from the wetlands. However, given that our main purpose is to distinguish the influence of dams from local human activity on wetlands, this chapter assumed that local human activity causes the wetland changes. In this context upstream wetlands and TSL wetlands are showing relatively smaller disturbances from local human activities (Figure 5.5, Table 5.2, and Table 5.3). Given that most Southeast Asian dams have been built in steep and mountainous sites (Kuenzer et al., 2013), many upstream wetlands are isolated wetlands, so they are far from human settlement. Also, TSL is one of the undisturbed floodplain systems (Arias et al., 2012; Kummu and Sarkkula, 2008), so wetlands here have fewer local human activities. However, downstream and INT wetlands are types of floodplains and riverine wetlands, which have active human activities, so almost all of wetlands there have disturbance.

Additional to the hydrological effects of dams on wetlands, this study found that direct water use (WU) decreases the inundation areas and increased human intervention (HIC) mainly induced the enlarged amplitudes of wetlands (Figure 5.5, Table 5.2, and Table 5.3). First, the direct water uses only impacts the inundation areas, but does not significantly affect the amplitude and intra-annual variability (Table 5.4). In many catchments, direct water use is the primary reason for wetland loss (Nielsen et al., 2020), and 311 wetlands (86%) in Southeast Asia showed evidence of direct water use (Table 5.1), such as canals and pumps. Also, the region with the high temporal variability and uneven agricultural areas like Southeast Asia shows water scarcity issues during the dry season caused by water uses in agriculture, cities, and industry (Middleton and Souter, 2016; Nesbitt et al., 2004; Pokhrel et al., 2018). In addition to water use in the dry season, Hecht et al. (2019) pointed out that irrigation withdraws also contribute to a decline in streamflow in the wet season.

As discussed in water withdrawal, agricultural activity usually extracts more water in the dry season. However, in the wet season, the precipitation sufficiently provides enough water, so the water extraction is decreased. This cycle will increase the amplitude of inundation patterns of wetlands (Nesbitt et al., 2004; Pokhrel et al., 2018). Also, increased variability and decreased amount of river flow caused by dams may make local livelihoods rely on water resources from wetlands, and it consequently increases the amplitude of the inundation of wetlands. For upstream wetlands, dams decrease the intra-annual variability. However, given that agricultural activities require water infrequently due to the irregular demands, local human activities may increase the intra-annual variability of upstream wetlands (Hecht et al., 2019; Middleton and Souter, 2016; Millar et al., 2019; Nesbitt et al., 2004). Only downstream showed increased amplitude of wetlands related to the land cover changes (LCC). The conversion of natural vegetation is correlated to flood duration (Arias et al., 2013; Palacios-Cabrera et al., 2022), and deforestation reduces the ability to hold water (Zhao et al., 2022). Thus, land cover changes would increase the amplitude of downstream wetlands by decreasing water in the dry season and increasing water in the wet season.

5.5. Conclusions

This chapter advances our current understanding of the influence of human activities on wetlands. Specifically, findings in this research stress the importance of the geographical relationship of wetlands with dams in characterizing the hydrological alteration. The distance and location of wetlands in regard to dam placement causes different patterns of hydrological alteration. Also, this study considers both dams and local human activities. This chapter discussed how each activity altered the hydrology, so this can reduce biased understanding of hydrological alteration. Additionally, a novel method in measuring the cyclical pattern can provide baseline information about the degree of hydrological alteration.

These advanced understandings can be extended to understanding of ecosystem disturbances from the hydrological alteration caused by human activities. Given that hydrological characteristics are the most important factors for wetland ecosystems (Brock et al., 1999; Middleton and Souter, 2016), hydrological alteration damages the ecosystems. A further study on the ecological effects of the hydrological alteration of the wetlands may establish future links about how dams affect the distant ecosystems and local livelihoods.

This chapter has some limitations. First, this study only considered inundation areas in hydrology, but the water level should be included. Even though inundation areas and water level have the linear relationship (Khandelwal et al., 2017), the water level measurement can explain different perspectives (Arias et al., 2012; Loiselle et al., 2021). ICESat-2 launched in 2018, and SMAP, which will be launched in late 2022, can be used. Second, only the quantity of water was discussed, but the quality was not discussed. Given that human activities alter temperature, turbidity, and nutrients (Richter et al., 1996), the changes of quality can be a good indicator of the hydrological alteration from human activities. Third, this study covered a relatively short monitoring period due to the availability of the data. Since this chapter's method is based on a data-driven approach, a longer period could strengthen our findings. Fourth, this study only considered human activities which are visible from Earth observations. However, soil mining is a major threat to the wetlands (NG and Park, 2021), so including other invisible activities can provide a comprehensive understanding of wetland changes. Last, this research should consider the climate variability in more detail. In order to focus on various human activities, this chapter conducted the simple analysis to examine the impacts of climate variability. Given that climate factor is another driving force on hydrology along with human activities (Middleton and Souter, 2016), the advanced analysis on quantifying the contribution of climate variability to the wetland hydrology will improve our understanding of the impacts of human activity on the hydrological alteration.

APPENDIX

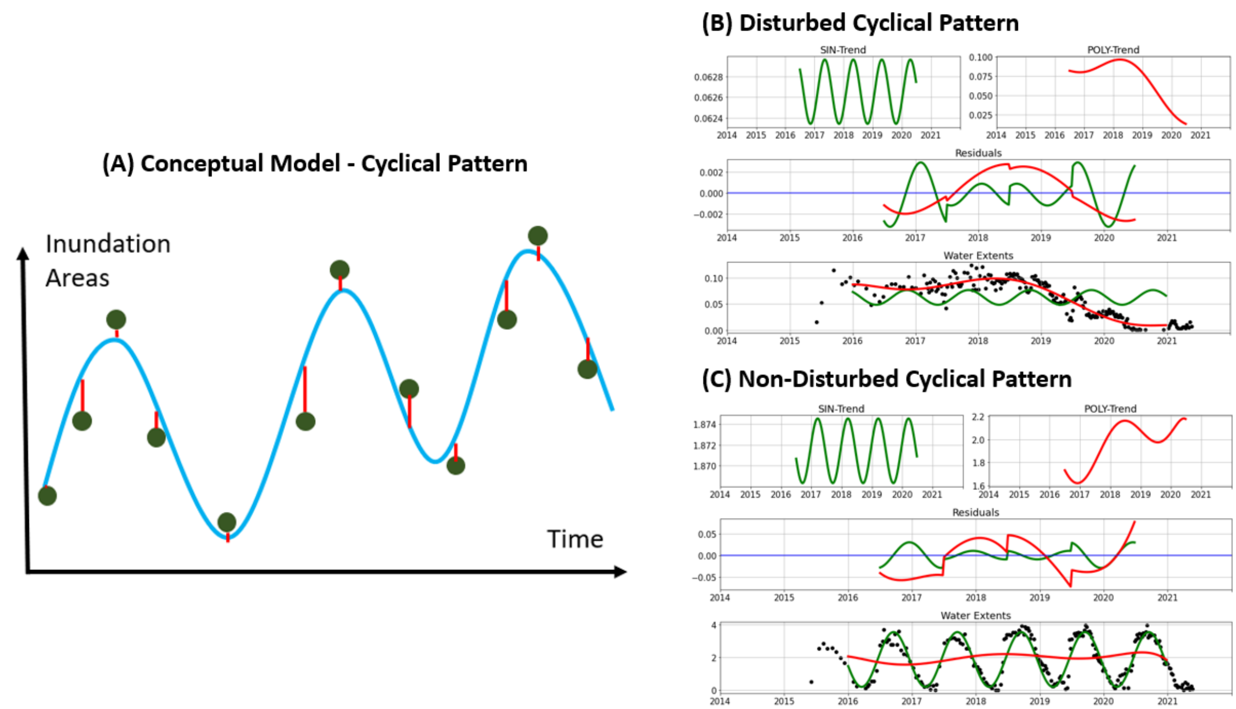

Figure 5.7. Examples of measuring the cyclical pattern. Due to lose of the cyclical pattern, (B) showed a wetland with the disturbed cyclical pattern. The polynomial model (red line) outperformed the sinusoidal model (green line). On the contrary, (C) has the cyclical pattern, so the sinusoidal model outperformed.

Chapter 6. Distant Spatial Impacts of Dams on Watersheds

6.1. Introduction

Hydro-dams critically affect ecosystems and society even if they are distantly located from the dams (Looy et al., 2014; Winemiller et al., 2016). Dams fragment the river flow and control the hydrological regime by irregularly storing and releasing the water (Barbarossa et al., 2020). The hydrological alteration caused by dams influences both upstream and downstream ecosystems and local livelihoods (Arias et al., 2013; Palmer and Ruhi, 2019; Rosenberg et al., 2000). In order to a better estimate of the dam impacts on ecosystems and society, the spatial boundaries of the dam consequences should be quantified (Rufin et al., 2019).

However, there is a less understanding of the spatial patterns and distance of dam impacts on watersheds. The spatial pattern and distance of the impacts near the dam sites were studied, but their boundaries beyond the dam sites were rarely quantified (Chen et al., 2015). Given that dams disrupt the river flow in the watersheds, the distant effects, which refers to the dam consequences beyond the dam sites, on hydrology can be measured at the watershed scale (Baird et al., 2021; Winemiller et al., 2016). For quantifying the distant effects on hydrology in a watershed, streamflow discharges from the gauging stations have been widely used by comparing before and after dams (Han et al., 2019; Lu et al., 2014), isolating the dam impacts from climate variability (Poff et al., 2007), and modeling the contribution of dams to the downstream (Chaudhari and Pokhrel, 2022). However, most studies qualitatively estimated how far dams affect streamflow, for example, by selecting a few distantly located stations (Bussi et al., 2021; Zheng et al., 2019). This approach is problematic for quantifying the dam impacts especially in developing regions like Southeast Asia, because they do not have sufficient stations to characterize the hydrological alteration caused by dams (Bonnema and Hossain, 2019; Salmivaara et al., 2013). In this context, delineating the spatial boundaries of the dam consequences is required to characterize the distant effects of dams in watersheds.

Natural wetlands can represent how far dams affect the watershed due to their hydrological linkage with dams at the watershed level. Wetlands are sensitive to external pressure, such as hydrological changes (Dang et al., 2016), climate variability (Erwin, 2009), and land use/land cover changes (Ekumah et al., 2020). A significant hydrological alteration caused by dams results in changes of the inundation characteristics and water level fluctuations of wetlands (Arias et al., 2012; Wang et al., 2014). These characteristics of wetlands can be used to determine the spatial pattern and spatial boundaries of the distant effects of dams on watersheds. Furthermore, the hydrological changes of wetlands affect their ecosystems and local livelihoods (Piman et al., 2013), so characterizing the distant effects using the location of wetlands (in regard to dam placement) can show the dam impacts on watersheds. Additionally, different dam impacts on upstream and downstream watersheds less studied (Kirchherr et al., 2016; Middleton and Souter, 2016). Thus, delineating the spatial boundaries for upstream and downstream can quantify how dams affect upstream and downstream watersheds differently.

The objective of this chapter is to develop a methodology to quantify the spatial boundaries of the distant effects of dams in watersheds and characterize their spatial pattern. Using characteristics of watersheds about the upstream, downstream, or non-linkage, the spatial relationship between dams and wetlands was considered to quantify the spatial boundaries of distant effects of dams. Hydrological characteristics of monthly wetland inundation were used to determine the influence of dams. To achieve the objective, this paper would like to answer the following two research questions: 1) how far do dams affect the hydrological characteristics of wetlands at the watershed scale? and 2) How do dams affect upstream- and downstream-located watersheds differently? For the study area, three major basins in Southeast Asia were selected to characterize the spatially distant effect of dams.

6.2. Methods and Materials

6.2.1. Study area

The Mekong, Salween, and Irrawaddy Basins in the mainland of Southeast Asia were selected as study areas because many dams have been constructed recently that impose strong impacts on the local communities and ecosystems (Figure 6.1). By 2017, 186 hydro-dams were already commissioned, 45 were under construction, and 110 were proposed and planned (WLE, 2017). Additionally, the basins share a similar climate, topography, and society characteristics, so it is good to characterize the spatial impacts of dams on watersheds. The region is controlled by Southwest Asian monsoon and East Asian monsoon with wet and dry seasons (Räsänen and Kummu, 2013). Also, El Niño Southern Oscillation (ENSO) causes interannual climatic variabilities. El Niño events are responsible for a decrease in rainfall, while LaNiña increases rainfall (Frappart et al., 2018). The climate system in the region is a major factor affecting hydrology, which plays significant roles in ecosystems and society (Bridgestock et al., 2022; Dang et al., 2016; Shamsudduha and Panda, 2019). For topography, the rivers of the three basins originate from high mountainous areas, which are Himalayan Mountains and Tibetan Plateau, with steep narrow valleys, and snowmelts as the major water sources (Bridgestock et al., 2022; Pokhrel et al., 2018). For downstream, They are flowing out to river mouth with tributaries, and precipitation and groundwater are the major water sources (Pokhrel et al., 2018; Shamsudduha and Panda, 2019). For the Mekong Basin, tributaries contribute to 84% of river flow (MRC, 2005). Population in the region highly relies on foods from rainfed and irrigation rice, and population growth requires more water for irrigation (Arias et al., 2012; Yoshida et al., 2020). Also, the population is consuming 47-82% of their protein from wetlands and river fisheries (Dugan et al., 2010; Intralawan et al., 2018).

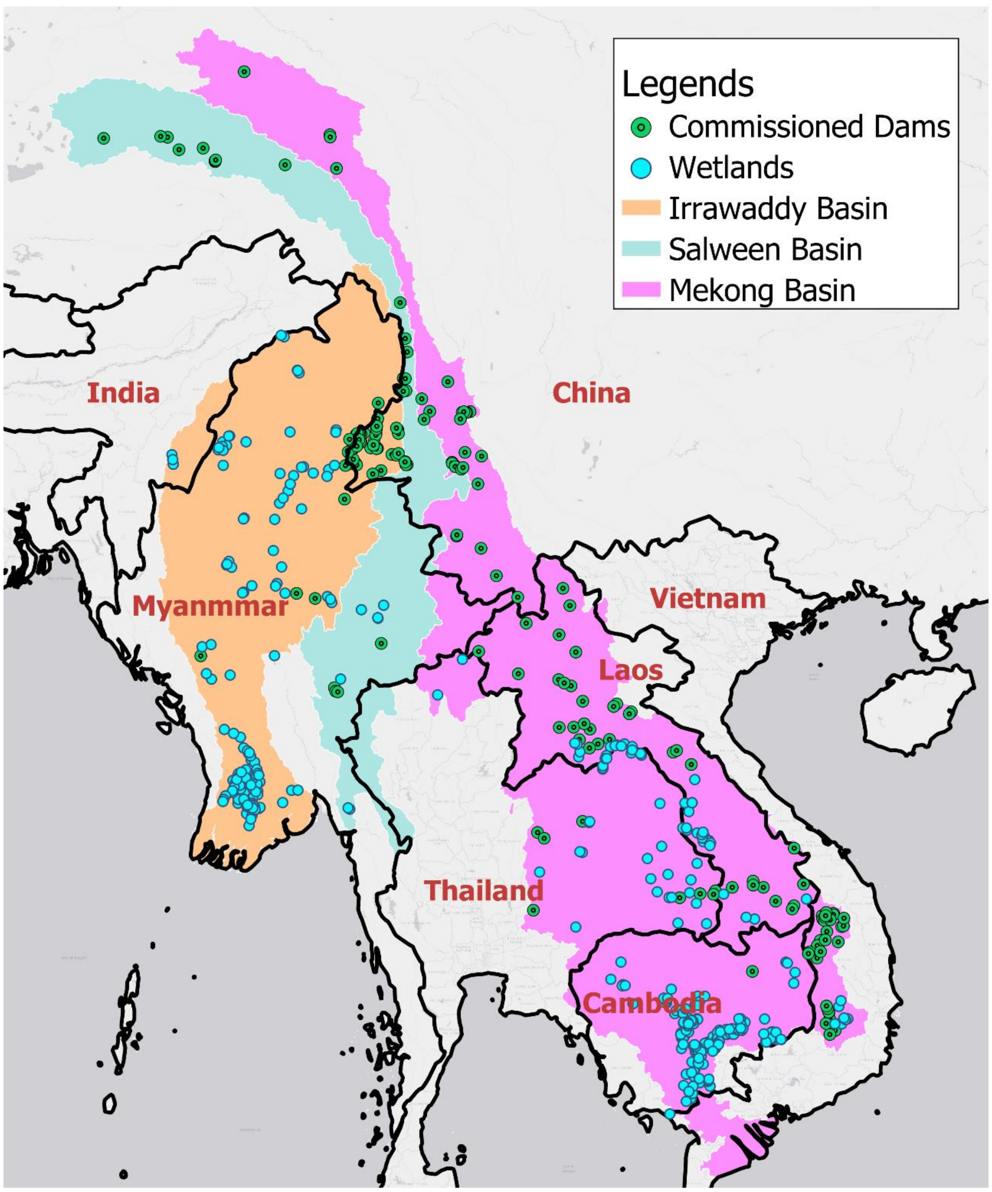

Figure 6.1. Study area for Chapter 6. three basins (Mekong, Salween, and Irrawaddy Basins) in mainland Southeast Asia, and their commissioned dams, planned dams, and wetlands.

6.2.2. Materials

6.2.2.1. Watershed

The HydroBASINS dataset was used to obtain watershed boundaries. HydroBASINS was derived from the World Wildlife Fund's HydroSHEDS (Hydrological data and maps based on SHuttle Elevation Derivatives at multiple Scales) which provides hydrographic information based on Shuttle Radar Topography Mission (SRTM) (Lehner and Grill, 2013). Watersheds were delineated in a hierarchical sub-basin breakdown using Pfafstetter coding system by considering upstream, downstream, or non-linkage (Verdin and Verdin, 1999). HydroBASINS has 12 hierarchical levels of basins, where level 1 is the largest basin and level 12 is the smallest basin. In other words, level 1 is divided into sub-basins of level 2, level 2 is divided into sub-basins of level 3, and so on Also the Pfafstetter coding system is useful to examine the upstream and downstream. Here, we considered the basin level from 7 to 11 because levels higher than level 7 are too coarse and level 12 is too small to have enough sample sizes.

6.2.2.2. Dams

Dam data were from the '2017 Dataset on the Dams of the Irrawaddy Mekong, Red, and Salween River Basins' provided by the Greater Mekong Consultative Group on International Agricultural Research (CGIAR) Research Program on Water, Land, and Ecosystems (WLE, 2017). This dataset was created from official reports, and visual check on earth observations. Earth imageries. Commissioned hydropower dams were selected for the study (Figure 6.1). 173 hydro-dams that began operation from 1966 to 2017.

6.2.2.3. Selection of natural wetlands

HydroLAKES was used to select natural wetlands. The HydroLAKES dataset was derived from the eight water products, including MOD44W and the Global Lakes and Wetlands Database (GLWD). The dataset has 1,427,688 water bodies over 10 ha, so it is widely used for various studies (Cooley et al., 2021; Messager et al., 2016). I manually selected the natural wetlands through visual inspections of a variety of images (i.e., Google Earth, Sentinel 2 A/B, and Landsat 5-8), because HydroLAKES provided insufficient information determining the natural wetlands. Here, natural wetlands refer to naturally occurring water bodies, so we found the evidence of dammed or artificially created structures in visual inspection to determine whether natural wetlands or artificial water bodies. As a result, 439 natural wetlands were selected from 2651 HydroLAKES water masks in the study area (Figure 6.1).

6.2.2.4. Water inundation data

The European Commission's Global Water Surface Layer (GWSL) was used for monitoring the inundation dynamics of wetlands. The GWSL was derived from the three million Landsat images using expert systems based on a procedural sequential decision tree classification (Pekel et al., 2016). This product provides annual and monthly inundation data globally at 30m spatial resolution from 1984 to 2020. This chapter used monthly data to examine the inundation patterns of wetlands. Given that this is the only available and widely used dataset, this study used the GWSL, although the Producer’s Accuracy (i.e., 1 - Omission Error) for monthly data is not good (74 - 77%).

6.2.2.5. Precipitation data

Monthly precipitation data from TerraClimate was used to determine the contribution of precipitation variability to inundation patterns. TerraClimate is a gridded climate product that was derived from climate observations and climate reanalysis datasets (Abatzoglou et al., 2018). Monthly precipitation data from 1987 to 2020 in 4638.3 m was extracted for the pixels of the wetland water masks.

6.2.3. Methods

6.2.3.1. Hydrological characteristics of wetlands from monthly inundation areas

Since HydroLAKES provides a static water mask, the water mask should be updated to capture seasonal dynamics (Khandelwal et al., 2017). Thus, the water masks were updated by the maximum inundation area from GWSL. Some wetlands sharing the same water inundation areas were grouped as same wetlands during the wet season. Also, I thought that some wetlands combined with rivers during the wet season are largely influenced by the streamflow; thus, this chapter used the different inundation frequencies from GWSL showing the separation of wetlands from the river. As a result, 362 water masks for wetlands were updated from the 493 selected water bodies.

Based on 362 water masks, monthly inundation areas from 1984 to 2020 were delineated from GWSL. GWSL labels pixels for water, land, and cloud, so each label was extracted within the updated water mask. Due to the effects of cloud cover, this chapter selected the observations with a cloud cover of less than 10% for the 362 wetlands.

Alterations of three hydrological characteristics - trend, intra-annual variability, and amplitude of inundation areas - were derived from monthly inundation areas for examining the dam impacts on wetlands. First, the trend of inundation refers to the tendency of monthly water inundation areas. It was calculated by the seasonal Kendall Trend test, which is a nonparametric test analyzing whether seasonal data are changed in monotonic trends (Hirsch et al., 1982) (1-4):

$$S_i = \sum_{k=1}^{n_i-1} \sum_{j=k+1}^{n_i} sgn(x_{ij} - x_{ik}) \quad (1)$$

$$sgn\,(x_{ij} - x_{ik}) = \begin{cases} 1, & x_{ij} - x_{ik} > 0 \\ 0, & x_{ij} - x_{ik} = 0 \\ -1, & x_{ij} - x_{ik} < 0 \end{cases} \quad (2)$$

where x_{ij} is an observation (an inundated area) of year *j* in month *i*, and n_i is the observation of year *n* in month *i*. $sgn(x_{ij} - x_{ik})$ decides the value 1, 0, and -1 according to its sign. For example, x_{ij} is larger than the x_{ik}, then the value 1 is assigned. S_i shows whether positive value (negative value) shows inundated areas in month *i* in the later years tend to be larger (smaller) than those in month *i* in earlier years.

$$Var\,(S_i) = n_i(n_i - 1)(2n_i + 5) - \sum_{p=1}^{g_i} t_{ip}(t_{ip} - 1)(2t_{ip} + 5) \quad (3)$$

where g_i is the number of tied groups for the month *i*, and t_{ip} is the number of data in the group *p* for month *i*. Then, S' and $VAR(S')$ are calculated by summing all values of S_i and $Var\,(S_i)$, respectively, from month 1 to 12 (*i*).

$$Tr = \begin{cases} \dfrac{S' - 1}{(Var\,(S'))^{1/2}}, & S' > 0 \\ 0, & S' = 0 \\ \dfrac{S' + 1}{(Var\,(S'))^{1/2}}, & S' < 0 \end{cases} \quad (4)$$

where *Tr* is the result of the seasonal Kendall Trend test for a wetland over the observations, and a positive (negative) value indicates that the inundation areas trend to increase (decrease) over time. The trend of the inundated areas of wetlands (*Tr*) was used for the study, but the significance of level was not considered. The slope was converted to binary variables for the logistic regression model; 1 (positive) and 0 (negative).

Second, the intra-annual variability refers to the degree of fluctuations in monthly inundation areas. The measure was based on the method suggested by Feng et al. (2013) that comparing distribution of monthly inundated areas for a year by the uniform distribution, which has same inundated areas for a year (5-8):

$$\bar{I}_k = \sum_{m=1}^{12} i_{k,m} \quad (5)$$

which is total inundated areas at the monthly scale for a year *k*, and $i_{k,m}$ is an inundated area for a month *m* in year *k*.

$$\bar{P}_{m,k} = \frac{i_{k,m}}{\bar{I}_k} \quad (6)$$

which is probability distribution of the total inundated areas for a month *k* in year *y*.

$$\bar{D}_k = \sum_{w=1}^{52} \bar{P}_{m,k} \cdot \log_2(12 \cdot \bar{P}_{m,k}) \quad (7)$$

which measures the distance between the distribution of an observed monthly inundated area in for a year *k* and the uniform distribution of monthly inundated areas (i.e., 1/12).

$$IV_k = \bar{D}_k \cdot \frac{\bar{I}_k}{\bar{I}_{max}} \quad (8)$$

where $\bar{I}_{max}$ is the maximum inundated areas for the entire observations. IV_k measures the intra-annual variability for a year *k* by comparing the observed distribution with the uniform distribution. IV_k is 0 when the inundated areas are same for a year *k* and IV_k is maximized (at $\log_2 12$ = 3.585) when a wetland is inundated only for one month.

The intra-annual variability was calculated for each year, and the trend of the variability was calculated using Sen's Slope Estimator for the robustness, which takes the median value of the slopes by all pairs of sample points (Hirsch et al., 1982).

Third, the amplitude refers to differences between the maximum and minimum peaks of inundated areas in a year. The measure was based on (9):

$$Amp = I_{k,max} - I_{k,min} \quad (9)$$

where the difference between a maximum inundated area ($I_{k,max}$) and a minimum inundation area ($I_{k,min}$) for a year *k*. The amplitude was calculated for each year, and the trend of the amplitude was calculated using Sen's Slope Estimator for robustness.

6.2.3.2. Pfafstetter: determining upstream and downstream wetlands

This chapter determined the location of wetlands in regard to the dam placement - whether wetlands are located upstream or downstream of dams, or no linkage with dams - using the Pfafstetter coding system in HydroBASINS. HydroBASINS generated watershed boundaries using Pfafstetter coding system, which was developed by Verdin and Verdin (1999), and it provides Pfafstetter codes (i.e., basin identification numbers) for each watershed. Using the Pfafstetter codes, the topographical relationship between watersheds (i.e., upstream and downstream) can be derived (Figure 6.2). Thus, we would like to determine whether each wetland is located upstream or downstream of each dam, or whether it has no linkage with dams for examining the distant effects of dams on wetlands using the rule of Pfafstetter coding system.

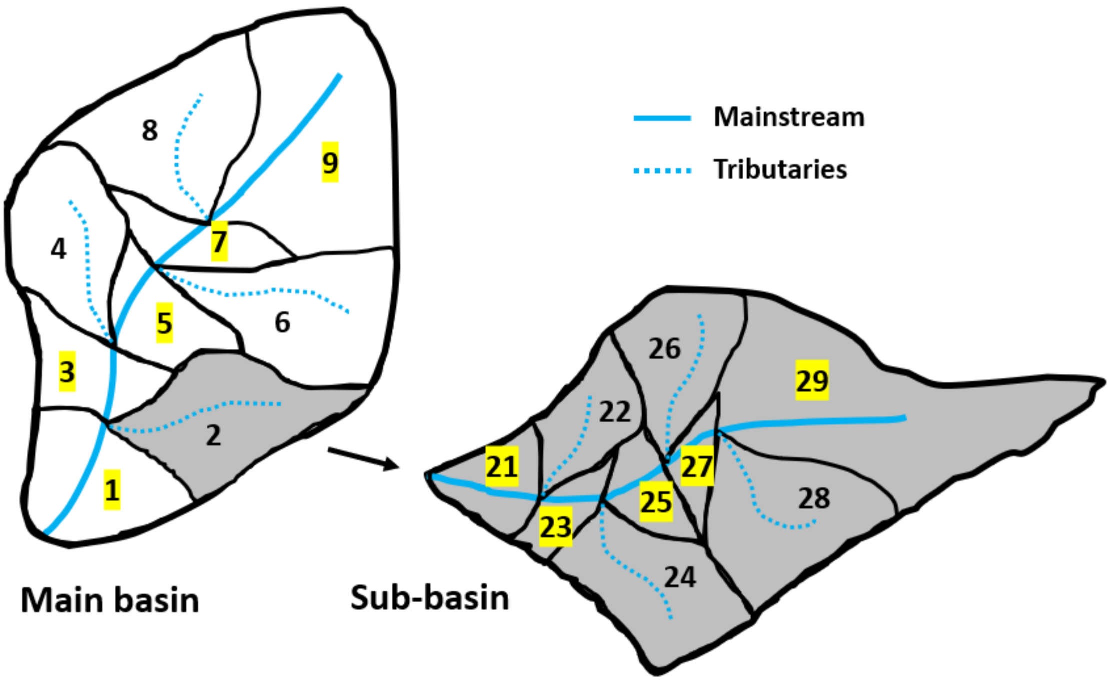

Figure 6.2. Pfafstetter codes for identifying topographical relationships of watersheds with examples of main basin (left) and sub-basin (right). Lower numbers are closer to river mouth. From number 1, each basin was labeled by the number from 1 to 9. Even numbers were for tributaries and odd numbers were inter-basin, which is a mainstream located between two tributaries (highlighted numbers). Each basin hierarchically has its own sub-basins. For example, basin 2 (left) has sub-basins (right).

HydroBASINS gave digits to represent a level of watershed, for example, level 7 has seven digits. The Pfafstetter coding system labels a number from 1 to 9 for a digit, and labels 0 if current watershed boundaries were the same with the higher-level ones (Figure 6.2). The Pfafstetter coding system distinguishes two types of watersheds which are tributary and inter-basin. The tributary is a watershed separated from the confluence to the upstream of the tributary, which is flowing to mainstream. The inter-basin is the area of the mainstream located between two tributaries. Even numbers were used for tributaries, and odd numbers were labelled for inter-basin. Tracing a river from the mouth to source, number from 1 to 9 was labelled. Even though there are more tributaries upstream, if the number is reached to 9, then stop labelling them. The watershed is then broken into sub-basins, and are re-labelled again from 1 to 9.

For determining whether each wetland is located upstream or downstream of hydro-dams, or if there is no linkage with the dams, we examine Pfafstetter codes focusing on a selected digit number from the last digit by the following:

1. A selected digit number is odd
    a. Upstream: the watershed whose digit number is larger
    b. Downstream: the watershed whose digit number is odd and smaller
2. A selected digit number is even
    a. Upstream: All sub-basins will be upstream
    b. Downstream: the watershed whose digit number is odd and smaller
3. A selected digit number is 0: It is the same with the main-basin (i.e., higher level watershed), so skip for this.

For the odd number of the last digit of Pfafstetter codes, it is inter-basin, so upstream would be all watersheds located upstream from a selected watershed. Given that the tributary does not have an inter-basin as upstream, the downstream would be inter-basin watersheds located downstream from the selected watershed. Let's say there is a watershed with the code number, 54865. Its upstream would be 54866, 54867, 54868, and 54869, and its downstream would be 54861 and 54863. For the even number of the last digit, it is a tributary, so it does not have upstream in the selected digit. Instead, its sub-basins would be its upstream. Like the odd number, the downstream would be inter-basin watersheds located downstream from the selected watershed. For example, if the code number is 5486, then its downstream would be 5487, 5488, and 5489, and its upstream would be sub-basins of 5486, which are 54861, 54862, 54863, 54864, 54865, 54866, 54867, 54868, and 54869.

Using this rule, this study focused on the Pfafstetter codes for hydro-dams and link their locations with Pfafstetter codes for wetlands to decide whether wetlands are located upstream or downstream of dams, or non-linkage with dams. For the last digit, we examined the relationship of linkage between dams and wetlands, and moved to the main-basin (i.e., higher level watershed) and did the same thing. This procedure was repetitively done until reaching the first three digits as these give information about continent and region. For instance, a dam has 4885235 as Pfafstetter codes in level 7 of HydroBASINS. This chapter examined the relationship of upstream and downstream of watersheds for the last digit 5, then moved to 488523X, 48852XX, and 4885XXX sequentially, and stopped examining for 488XXXX. Based on Pfafstetter codes for hydro-dams, this research determined whether wetlands are located upstream or downstream of dams, or no linkage with dams.

6.2.3.3. Quantification of dam impacts on wetlands

Mann-Whitney U test was used to quantify the dam impacts on wetlands (Figure 6.3). The Mann-Whitney U test is a nonparametric test of the null hypothesis whether two groups are from same population (Mann and Whitney, 1947). Here, this chapter would like to compare wetlands with dam linkage and without dam linkage based on three hydrological characteristics of wetlands using Mann-Whitney U test. In this context, the null hypothesis is that wetlands with dam linkage and without dam linkage have similar characteristics of inundation changes. Thus, we would like to focus on the rejection of the null hypothesis that indicates differences in hydrological alteration between wetlands with dam linkage and without dam linkage.

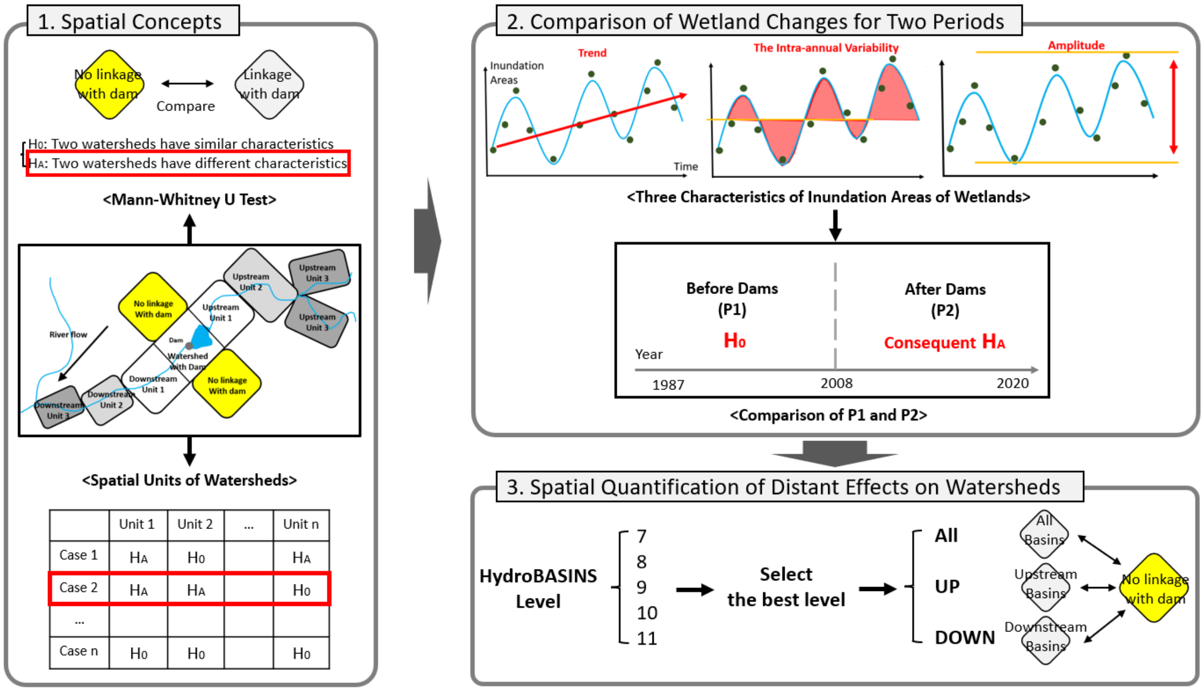

	Unit 1	Unit 2	...	Unit n
Case 1	HA	H0		HA
Case 2	HA	HA		H0
...				
Case n	H0	H0		H0

Figure 6.3. Workflow for Chapter 6. Step 1. spatial units were determined using the topographical information of HydroBASINS. Each spatial unit, the Mann-Whitney U test was conducted to find the rejection of the null hypothesis (HA). Step 2. Three characteristics of inundation areas of wetlands (trend, intra-annual variability, and amplitude) were calculated for P1 and P2. The P1 with failed to reject the null hypothesis and the P2 with the rejection to the null hypothesis consequently is showing the significant impact of dams on watersheds. Step 3. Using step 1 and 2, the best HydroBASINS level was selected. For the selected level, three cases (i.e., All, Up, and DOWN) were tested to quantify the best spatial units showing the significant distant impacts of dams on watersheds. Different spatial units for cases are showing the different spatial patterns of the distant impacts on watersheds.

In order to examine the dam impacts, this chapter divided the entire period (i.e., 1987-2020) into two, 1) before dam period (P1) and 2) after dam period (P2) (Figure 6.3). The failure to reject to the null hypothesis in before dam periods, but the rejection to the null hypothesis in after dam periods would show that there must be hydrological alteration on wetlands with dam linkage. In other words, we can confirm that there are dam impacts on wetlands. The year 2008 was selected for breaking into two periods: before dam period (P1; 1987-2007) and after dam period (P2: 2008-2020). Given that hydro-dams have been built since 1966, it is difficult to have the period without any dam. Instead, we selected a year that did not have many dams and did have enough samples for the test. Based on year 2008, the P1 (before dam period; 1987-2007) has 46 hydro-dams, and the P2 (after dam period; 2008-2020) has 75 dams. 52 of the dams with unknown commissioned years were excluded in the analysis.

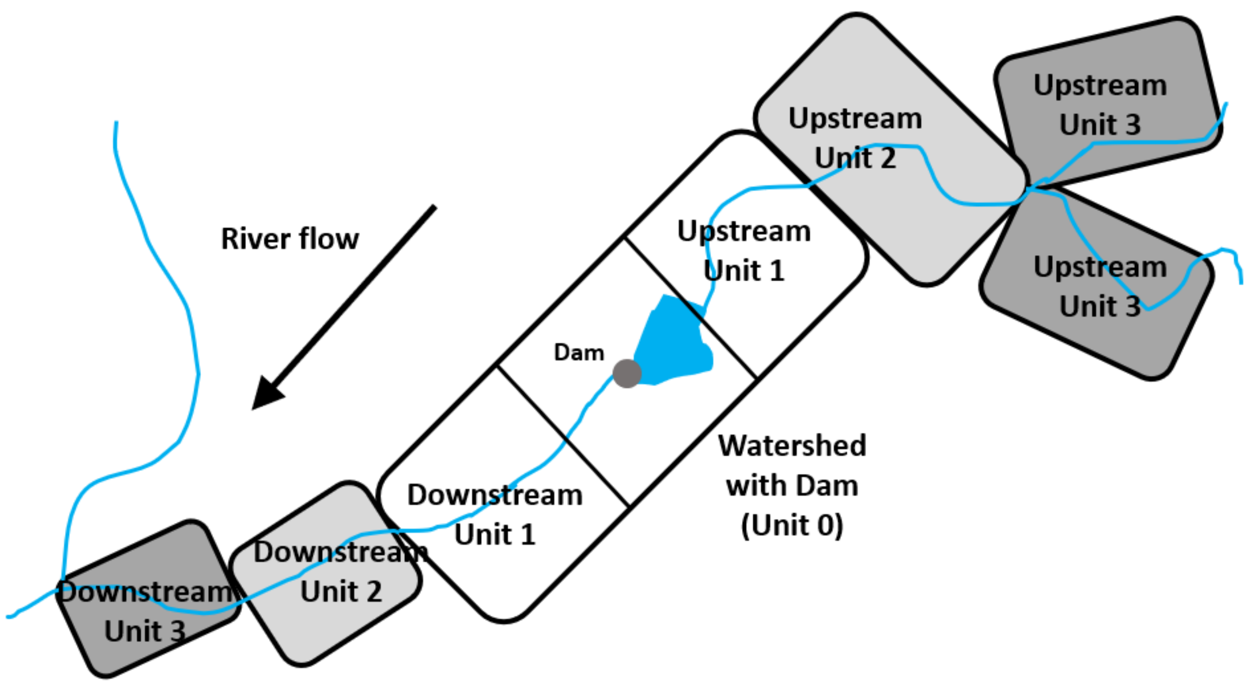

Figure 6.4. A conceptual graph for spatial units. From the watershed with dam (unit 0), units were sequentially labeled from unit 1. This concept was applied to HydroSHEDS level from 7-11 to quantify the distant effects of dams on watersheds.

Spatial units were devised to quantify the spatial boundary of the distant effects of dams (Figure 6.4). Here, spatial units refer to how distantly a watershed is away from the watershed with a dam. For example, a watershed having a selected dam is spatial unit 0 because this watershed is not away from the dam. Direct upstream and downstream watersheds of a dam watershed would be spatial unit 1 because only one watershed unit is away from the dam watershed. Then, direct upstream and downstream watersheds of spatial unit 1's watersheds would be spatial unit 2 because two watershed unit is away from the dam watershed. Based on this rule, spatial units of watersheds were labelled for each dam.

The Mann-Whitney U test was applied for every spatial unit for HydroBASIN level 7-11 to find a watershed level and unit describing the dam impacts (Figure 6.3). Then, the spatial unit with rejecting to the null hypothesis ($p<0.1$) was selected. The watershed levels having the rejection with consecutive spatial units starting from 1 were considered significant dam impacts because dams have more effects on closely located watersheds (Dang et al., 2016; Zhang et al., 2022). For instance, the unit 2 and 3 reject the null hypothesis, but the unit 1 fails to reject, then this watershed level is not considered as significant dam impacts. Lastly, the watershed level which has failed the rejection to the null hypothesis for the P1 (before dam period) but showed rejection of the null hypothesis for the P2 (after dam period) was selected, then its significant spatial units were considered as the spatial boundaries of the dam impacts.

A set of three Mann-Whitney U tests were conducted (Figure 6.3), following 1) watersheds with dam linkage against the watersheds without dam linkage (ALL), 2) watersheds located upstream of dams against the watersheds without dam linkage (UP), and 3) watersheds located downstream of dams against the watersheds without dam linkage (DOWN). These can characterize the spatial boundaries and spatial patterns of the distant effects of dams.

6.2.3.4. Determination of influence of climate variability on the inundation

Given that precipitation is a major factor of wetland inundation, the correlation analysis between precipitation and inundation areas was conducted to examine the influences of precipitation on the inundation changes. By clarifying that the precipitation did not affect the inundation changes of wetlands, we can confirm that the wetland changes were caused by dams. The correlation analysis was conducted for both P1 (before dams) and P2 (after dams). If the result of the correlation analysis was not different between the P1 and P2, then the impacts of climate variability on the wetland inundation are not different between for two period. This can isolate the climate variability in quantifying the dam impacts on wetlands (Poff et al., 2007; Xue et al., 2011). The Pearson correlation was conducted to measure the linear correlation. The standardization was conducted for precipitation and inundation areas, respectively, because their units are different.

6.3. Results

6.3.1. Mann-Whitney U tests for various levels and spatial units

HydroBASIN level 7 showed the significance in the distant effects of dams on wetlands (Table 6.1). Compared to the P1, the trend, intra-annual variability, and amplitude of inundation during the P2 showed the significance for unit 1 (0.036, 0.004, 0.012) and 2 (0.048, 0.008, 0.011). For unit 3's P2, the trend failed to reject the null hypothesis (0.172) despite the rejection for intra-annual variability (0.011) and amplitude (0.014), so unit 3 was not considered due to no dam impacts on wetlands. For level 8, the trend and amplitude for unit 2 was not significant (0.136, 0.103), so it was difficult to show the remarkable dam impacts. For level 9, any hydrological characteristics have the significance (0.358, 0.163, 0.183), so it was not having significant dam impacts. For level 10, the trend of unit 2 has significance (0.054), but all characteristics of unit 4 has insignificance (0.041, 0.173, 0.125). For level 11, unit 2 has failed to reject the null hypothesis (0.215, 0.117, 0.252).

Table 6.1. Results of Mann-Whitney tests for the selected level, HydroBASIN level 7. Per. Indicates period (P1 – before dams; P2 – after dams), # indicates number of wetlands which have linkage with dams within watersheds, Tr. indicates the trend of inundation, Var. indicates the intra-annual variability of inundation, and Amp. Indicates the amplitude of inundation. The values of Tr., Var., and Amp. Are significance level of the Mann-Whitney tests, and * indicates the rejection to the null hypothesis ($p<0.1$). Spatial units 4 and 5 for downstream and 1 and 2 for upstream have same results due to same samples for the test because the spatial units' boundaries are beyond the study area (Southeast Asia).

Unit	Per.	ALL				DOWN				UP			
		#	Tr.	Var.	Amp.	#	Tr.	Var.	Amp.	#	Tr.	Var.	Amp.
1	P1	12	0.176	0.571	0.564	4	0.146	0.993	0.729	10	0.565	0.459	0.379
	P2		0.036*	0.004*	0.012*		0.807	0.003*	0.017*		0.094*	0.023*	0.067*
2	P1	14	0.216	0.883	0.958	6	0.243	0.293	0.223	10	0.565	0.459	0.379
	P2		0.048*	0.008*	0.011*		0.773	0.015*	0.020*		0.094*	0.023*	0.067*
3	P1	19	0.110	0.623	0.687	12	0.049*	0.269	0.218				
	P2		0.172	0.011*	0.014*		0.880	0.011*	0.014*				
4	P1					39	0.074*	0.819	0.554				
	P2						0.121	0.177	0.007*				
5	P1					39	0.074*	0.819	0.554				
	P2						0.121	0.177	0.007*				

In consideration of the upstream and downstream located wetlands, the level 7's unit 2 was the boundary of the distant effects, but the boundary for upstream and downstream was different (Table 6.1). For downstream impacts, the unit 1-3 showed the significant dam impacts on the intra-annual variability (0.003, 0.015, 0.011) and amplitude (0.017, 0.02, 0.014). On the other hand, the upstream unit 1 had the significant impacts on trend (0.093), intra-annual variability (0.023), and amplitude (0.067).

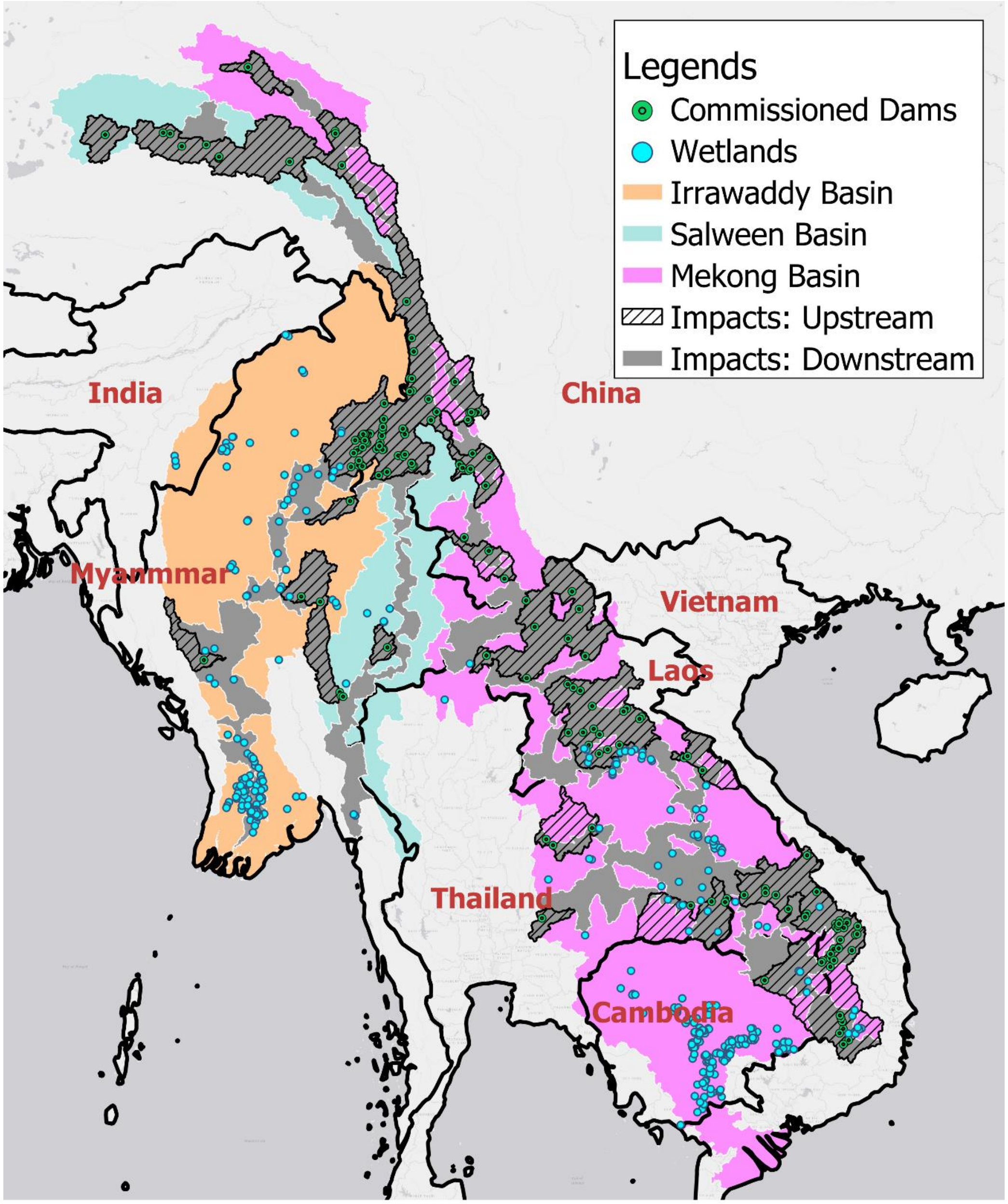

Figure 6.5. Spatial boundaries of the distant impacts of dams on upstream watersheds (inclined lines) and downstream watersheds (grey filled color).

Spatially, an averaged size of watersheds is 2,342km^2 (Figure 6.5 and 6.6). For the distant impacts of dams on upstream watersheds, the distances are from 1.1km to 655.2km with averaged distance 133.4km and median distance 55.8km. The areas are from 1,251km^2 to 39,026km^2 with averaged areas 12,356km^2 and median areas 11,695km^2. For the distant impacts of dams on downstream watersheds, the distances are from 33.7km to 1,577.5km with averaged distance 641km and median distance 441.4km. The areas are from 22,588km^2 to 463,544km^2 with averaged areas 165,361km^2 and median areas 153,452km^2.

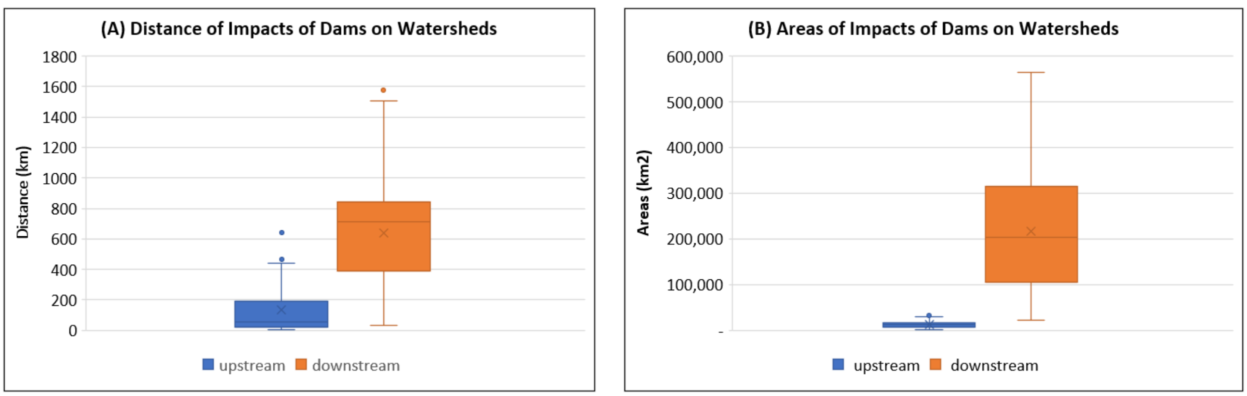

Figure 6.6. Distance and Areas of Impact of Dams on Watersheds.

6.3.2. Correlation analysis between precipitation and inundation areas

The correlation analysis showed that climate variability did not differently affect the wetland inundation areas. Of 19 wetlands with dam linkage, there were 3 wetlands that had a significant correlation with precipitation variability for the P1. The median correlation coefficient was 0.284. Also, the P2 has 3 wetlands that had a correlation with the precipitation variability with 0.229 of the median correlation coefficients. That the correlation results for the P1 and P2 were not changed indicated that the climate variability did not differently affect the wetland inundation areas. In other words, the changed results of the Mann-Whitney U test from the insignificance for the P1 to the significance for the P2 meant that the dams made different hydrological characteristics of wetlands compared to those of wetlands without dam linkage.

6.4. Discussion

The quantification of the distance and areas of distant impacts of dams on watersheds improves our understanding of the consequences of dams. This can support the qualitative definition of the spatial impacts of dams (Table 6.1 & Figure 6.5). For downstream impacts on watersheds, previous studies addressed that the impacts of dams on hydrology are significant for the distance from 5 km to approximately 1,000km (Feng et al., 2016; Graf, 2006; Han et al., 2018; Maingi and Marsh, 2002; Mei et al., 2015; Pal and Saha, 2018; Wang et al., 2014; Zhang et al., 2022; Zheng et al., 2019). The 1,000km of spatial distance was derived from studies about the impacts of Three Gorges Dam (TGD), which is the largest dam in the world, on Poyang Lake, which is one of the largest Chinese lakes with 3,500km^2 of surface area (Feng et al., 2016; Han et al., 2018; Mei et al., 2015; Wang et al., 2014; Zhang et al., 2022). Given the consideration that this spatial relationship is unique, the spatial distance was determined within approximately 700km excluding the studies about the TGD (Graf, 2006; Maingi and Marsh, 2002; Pal and Saha, 2018; Zheng et al., 2019). This qualitatively determined spatial distance (700km) is close to our quantitative distance (averaged distance - 641km). Also, Xue et al. (2011) addressed that upstream dams did not have significant impacts on downstream discharge in 1,600 km. This study can confirm our findings. Since little is known about the spatial impacts of dams on upstream watersheds so far, our quantitative distance (averaged distance - 133km) can shed light on the spatial distance of dam consequences on upstream watersheds.

The different spatial boundaries of dam impacts on downstream and upstream watershed units showed the anisotropy pattern of the distant effects of dams (Table 6.1 & Figure 6.5). Far-reaching distance of dam impacts downstream is consistent with the different dam impacts on upstream and downstream. Even though the distance was not considered, the downstream stations showed twice larger hydrological alteration values than the upstream ones (Timpe and Kaplan, 2017). The main impacts of dams on upstream are impounding water, elevating water table.(Leibowitz et al., 2018), and increasing groundwater level (Feiner and Lowry, 2015). On the other hand, the major impacts of dams on downstream are increasing fluctuations (Poff et al., 2007). Also, given that dams control the water release downstream (Schmitt et al., 2019), their impacts on streamflow are more critical for downstream streamflow than upstream streamflow. Previous studies had qualitatively decided different distance and intensity of the dam impacts as their purposes, but this chapter's result showed that dams have more distant effects on downstream. In this context, our research quantitatively characterized how different dam impacts on upstream and downstream result in the spatial boundaries differently.

Lastly, the characterization on spatial boundaries of the dam impacts will improve our understanding of the cumulative effects and enhance dam-relevant policies. Many negative effects of individual dams on individual systems (e.g., ecosystems, hydrology, and society) are well studied, but the cumulative effects were unanswered yet (Poff et al., 2007). This was mainly due to unclear spatial boundaries of the dam impacts on watershed (Baird et al., 2021; Winemiller et al., 2016). In this context, our determination of the spatial boundaries of the impacts can provide the spatial base information to quantify the cumulative effects from multiple dams on various systems. Furthermore, this can be utilized in establishing policies in estimating and reducing the dam impacts, since the spatial boundaries were less considered in them (Tullos, 2009; Vaidyanathan, 2011). Also, it can fill the gaps in considering the transboundary effects of dams on other nations in dam practices (López-Moreno et al., 2009). This will be helpful in reducing the unintended consequences from the dams.

6.5. Conclusions

This paper quantified the spatial boundaries and patterns of the distant effects of dams on watersheds using the topography of watersheds and the spatial relationship between hydro-dams and natural wetlands. The HydroBASINS level 7 – unit was the spatial boundary in considering all directions (i.e., upstream and downstream). The unit 1 was the spatial boundary for the dam impacts on the upstream, and the unit 3 was that on the downstream. The spatial impacts of dams reach 614 km downstream and 133 km upstream in averaged distance. The dams affect the watershed coverage of 217,132 km^2 downstream and 13,303 km^2 upstream in average. This different spatial boundary showed the anisotropy of the spatial pattern of the dams in the watersheds. Our results provide the spatial baseline information in estimating the effects of dams on watershed.

This chapter will fill the gaps in spatial boundaries and spatial patterns of the distant effects of dams, but this has some limitations. First, study areas should be extended to global scale for a more straightforward application. The study area was the (sub-) tropical areas with monsoon climate system, so it may be difficult to apply to other regions, such as arid areas. Also, we need to have more sample sizes in statistical analysis. Even though we examined 362 wetlands over three large basins, only 19 wetlands were applicable in considering the linkage with dams. Larger sample sizes through expanding the study areas to a global scale will strengthen our findings. Second, the monthly inundation data that we used in our analysis (i.e., GWSL) had gaps in observations due to cloud cover issues. The GWSL detected water bodies by only using Landsat series which are optical sensors, so it failed to detect the water bodies under the cloud. Given the 4-month wet season over Southeast Asia, the gaps can be problematic. The SAR can fill the gaps by penetrating the cloud covers, but the high-resolution SAR, Sentinel 1 began its mission from 2014 and prior SARs have insufficient spatial resolution to detect the small-sized wetlands. By developing a new remote sensing approach to fit the water inundation data from multiple sensors to a statistical model, this chapter may fill these gaps and strengthen our findings.

Chapter 7. Conclusions and Future Envisions

7.1. Summary

Hydro-dams bring many benefits and losses to Southeast Asia, but the lack of spatial information about the consequences of dams causes inaccurate estimation of the dam impacts on ecosystems and society. Due to the large-scaled impacts of dams, the spatial impacts of dams occur in distantly areas, a long time after the dam operation, cumulative with other dams, and indirectly. The complicated consequences of dams result in different spatial patterns of dam impacts in locations and scales. To address the spatial heterogeneity of the dam impacts, this dissertation achieved three main objectives by developing novel remote sensing and geospatial methods. The findings of this dissertation can be summarized according to each research objective.

Objective 1: to quantify the site-based spatial impacts of dams on land systems. In Chapter 4, I developed a method to quantify the spatiotemporal impacts of dams using remote sensing and statistical analyses. The spatial boundaries of the dam impacts were derived from changes in human activity and ecosystems, and different spatial boundaries were proved according to dam stages. Using the derived spatial boundaries, the spatial impacts of dams in site-based scale were quantified from the land use/land cover changes. The different spatial impacts of dams characterize the spatial heterogeneity of the impacts on different time.

Objective 2: to characterize the watershed scaled spatial impacts of dams on wetlands. In Chapter 5, I quantified the hydrological alteration of dams on wetland inundation in watersheds, along with characterizing local human activities and climate variability. A multi-sensor approach was devised to delineate water inundation areas in weekly scale of 362 natural wetlands. The pattern, trend, intra-annual variability, and amplitude of inundation were facilitated to quantify the impacts of dams on wetlands in terms of the location and distance of wetlands from hydro-dams. This chapter implies the importance of the location and distance of wetlands in regard to hydro-dams in determining the impacts of dams on watersheds.

Objective 3: to address the distant impacts of dams on watersheds. In Chapter 6, I developed a method to characterize the distance and areas of dam impacts on watersheds to address the distant impacts on upstream and downstream watersheds. Since Chapter 5 proved the distance and location of wetlands matter in understanding the consequences of dams, the spatial boundaries of the distant effects were quantified based on inundation characteristics of wetlands in long-term and relationship of watersheds with upstream and downstream. This chapter suggested the distance and coverage of the distant impacts of dams on watersheds and showed the anisotropy of the spatial pattern of the impacts on upstream and downstream watersheds.

7.2. Contributions and Implications

This dissertation addresses dam issues, which are subject to environmental sciences, in geographical perspectives using remote sensing. Thus, I would like to define the contributions and implications of this dissertation in three points following: 1) environmental sciences, 2) geography, and 3) remote sensing.

An approach for understanding of impacts of dams on ecosystems and society. Environmental Sciences have studied the impacts of dams on ecosystems and society with the cooperation of various disciplines, and they require spatial approaches for a better estimate of these effects. This dissertation provides spatial boundaries of the dam impacts and spatial approaches for quantifying the spatial impacts in multiple scales. This can provide the spatial baseline information so that disciplines can quantify the dam impacts over the spatial information, and they can be merged in the defined spatial information. This can suggest comprehensive understanding of the impacts of dams on ecosystems and society.

A characterization of the influence of large-scaled human activity geographically. Linking the human activities and their legacy effects on environmental changes spatially is a major concern of Geography. Especially, large-scaled human activity (in this dissertation, dams) have complicated consequences over space, so the quantification of this linkage spatially is an important contribution of geography to the world. This dissertation links the hydro-dams with their consequences over space and quantifies how dams affect environment differently in location and scale. This can help understand the influence of large-scaled human activities in geographical perspectives.

A development of remote sensing method to quantify the human-environmental interactions. This dissertation unravels the complicated linkage between human activity and the environment using remote sensing. Remote sensing can detect most of the events on the surface, but characterizing the meaningful patterns is challenging. In this context, this dissertation develops various remote sensing approaches to quantify the human-environmental interactions, focusing on the impacts of dams on ecosystems and society. This can allow remote sensing to play a significant role in understanding of how human activity alters the Earth systems and how the systems respond to the alteration.

7.3. Limitations and Future Directions

Even though this dissertation successfully addresses the multi-scaled spatial impacts of dams, there are still limitations which will be improved in my future directions. Given that the hydrological alteration significantly affects the relevant ecosystems and society (Han et al., 2018; Junk, 2002), this dissertation qualitatively linked the inundation dynamics caused by hydro-dams with the ecosystems and society. For a better estimate of the impacts of dams on wetlands in a watershed scale, systematic and quantitative research on the linkage of dams with ecosystems and society is necessary. Still, changes in ecosystems and society surrounding wetlands (especially, small sized wetlands) caused by dams have been addressed by a single or a several case study quantitatively or qualitatively from previous studies (Arias et al., 2012; Winemiller et al., 2016). In the future, changes in structure, composition, and diversity of wetland ecosystems should be quantified and linked with the hydrological alteration of dams. The landscape ecology based on field data, remote sensing, and geographical analysis will help to characterize the linkage of wetland ecosystems with dams (Roy and Tomar, 2000; Turner and Gardner, 2015; Zhao et al., 2012). Also, changes in social characteristics of local livelihoods, such as economy activity, food reliance, and perception, should be included in understanding the impacts of dams on distantly located societies in watershed level (Baird et al., 2021). Along with earth observations on social aspects (land use changes and nighttime lights) and official reports, Participatory GIS (PGIS) will quantify the qualitative social information in spatial format (Bernard et al., 2011; Karimi et al., 2015). The combination of this multi-source dataset will shed the lights on the influence of dams on society in watershed scale.

BIBLIOGRAPHY

BIBLIOGRAPHY

Abatzoglou, J.T., Dobrowski, S.Z., Parks, S.A., Hegewisch, K.C., 2018. TerraClimate, a high-resolution global dataset of monthly climate and climatic water balance from 1958–2015. Sci. data 5.

Ablat, X., Liu, G., Liu, Q., Huang, C., 2019. Application of Landsat derived indices and hydrological alteration matrices to quantify the response of floodplain wetlands to river hydrology in arid regions based on different dam operation strategies. Sci. Total Environ. 688, 1389–1404.

Amaral, S., Câmara, G., Monteiro, A.M.V., Quintanilha, J.A., Elvidge, C.D., 2005. Estimating population and energy consumption in Brazilian Amazonia using DMSP night-time satellite data. Comput. Environ. Urban Syst. 29, 179–195.

Anderson, E.P., Jenkins, C.N., Heilpern, S., Maldonado-Ocampo, J.A., Carvajal-Vallejos, F.M., Encalada, A.C., Rivadeneira, J.F., Hidalgo, M., Cañas, C.M., Ortega, H., Salcedo, N., Maldonado, M., Tedesco, P.A., 2018. Fragmentation of Andes-to-Amazon connectivity by hydropower dams. Sci. Adv. 4, 1–8.

Ansar, A., Flyvbjerg, B., Budzier, A., Lunn, D., 2014. Should we build more large dams? The actual costs of hydropower megaproject development. Energy Policy 69, 43–56.

Arias, M.E., Cochrane, T.A., Norton, D., Killeen, T.J., Khon, P., 2013. The flood pulse as the underlying driver of vegetation in the largest wetland and fishery of the mekong basin. Ambio 42, 864–876.

Arias, M.E., Cochrane, T.A., Piman, T., Kummu, M., Caruso, B.S., Killeen, T.J., 2012. Quantifying changes in flooding and habitats in the Tonle Sap Lake (Cambodia) caused by water infrastructure development and climate change in the Mekong Basin. J. Environ. Manage. 112, 53–66.

Arias, M.E., Farinosi, F., Lee, E., Livino, A., Briscoe, J., Moorcroft, P.R., 2020. Impacts of climate change and deforestation on hydropower planning in the Brazilian Amazon. Nat. Sustain. 3, 430–436.

Arias, M.E., Holtgrieve, G.W., Ngor, P.B., Dang, T.D., Piman, T., 2019. Maintaining perspective of ongoing environmental change in the Mekong floodplains. Curr. Opin. Environ. Sustain. 37, 1–7.

Ashraf, S., Brabyn, L., Hicks, B.J., 2012. Image data fusion for the remote sensing of freshwater environments. Appl. Geogr. 32, 619–628.

Baird, I.G., Silvano, R.A.M., Parlee, B., Poesch, M., Maclean, B., Napoleon, A., Lepine, M., Hallwass, G., 2021. The Downstream Impacts of Hydropower Dams and Indigenous and Local Knowledge: Examples from the Peace–Athabasca, Mekong, and Amazon. Environ. Manage. 67, 682–696.

Barbarossa, V., Schmitt, R.J.P., Huijbregts, M.A.J., Zarfl, C., King, H., Schipper, A.M., 2020. Impacts of current and future large dams on the geographic range connectivity of freshwater fish worldwide. Proc. Natl. Acad. Sci. U. S. A. 117.

Bernard, E., Barbosa, L., Carvalho, R., 2011. Participatory GIS in a sustainable use reserve in Brazilian Amazonia: Implications for management and conservation. Appl. Geogr. 31, 564–572.

Bonnema, M., Hossain, F., 2019. Assessing the Potential of the Surface Water and Ocean Topography Mission for Reservoir Monitoring in the Mekong River Basin. Water Resour. Res. 55, 444–461.

Bonnema, M., Hossain, F., 2017. Inferring reservoir operating patterns across the Mekong Basin using only space observations. Water Resour. Res. 53, 3791–3810.

Brasil, M.C.O., Magalhães Filho, R. de, Espírito-Santo, M.M. do, Leite, M.E., Veloso, M. das D.M., Falcão, L.A.D., 2021. Land-cover changes and drivers of palm swamp degradation in southeastern Brazil from 1984 to 2018. Appl. Geogr. 137, 102604.

Bridgestock, L., Henderson, G.M., Holdship, P., Khant, W., Thu, W.M., Aung, M., Chi, N., Jotautas, J., Tipper, E., Chapman, H., Bickle, M., 2022. Dissolved trace element concentrations and fluxes in the Irrawaddy, Salween, Sittaung and Kaladan Rivers. Sci. Total Environ. 156756.

Brock, M.A., Smith, R.G.B., Jarman, P.J., 1999. Drain it, dam it: Alteration of water regime in shallow wetlands on the New England Tableland of New South Wales, Australia. Wetl. Ecol. Manag. 7, 37–46.

Bussi, G., Darby, S.E., Whitehead, P.G., Jin, L., Dadson, S.J., Voepel, H.E., Vasilopoulos, G., Hackney, C.R., Hutton, C., Berchoux, T., Parsons, D.R., Nicholas, A., 2021. Impact of dams and climate change on suspended sediment flux to the Mekong delta. Sci. Total Environ. 755, 142468.

Castro, M.C., Krieger, G.R., Balge, M.Z., Tanner, M., Utzinger, J., Whittaker, M., Singer, B.H., 2016. Examples of coupled human and environmental systems from the extractive industry and hydropower sector interfaces. Proc. Natl. Acad. Sci. 113, 14528–14535.

Chang, C.H., Lee, H., Kim, D., Hwang, E., Hossain, F., Chishtie, F., Jayasinghe, S., Basnayake, S., 2020. Hindcast and forecast of daily inundation extents using satellite SAR and altimetry data with rotated empirical orthogonal function analysis: Case study in Tonle Sap Lake Floodplain. Remote Sens. Environ. 241, 111732.

Chapman, H., Bickle, M., Thaw, S.H., Thiam, H.N., 2015. Chemical fluxes from time series sampling of the Irrawaddy and Salween Rivers , Myanmar. Chem. Geol. 401, 15–27.

Chaudhari, S., Pokhrel, Y., 2022. Alteration of River Flow and Flood Dynamics by Existing and Planned Hydropower Dams in the Amazon River Basin. Water Resour. Res. 58.

Chen, G., Powers, R.P., Carvalho, L.M.T. de, Mora, B., 2015. Spatiotemporal patterns of tropical deforestation and forest degradation in response to the operation of the Tucuruí hydroelectricdam in the Amazon basin. Appl. Geogr. 63, 1–8.

Cochrane, S.M.V., Matricardi, E.A.T., Numata, I., Lefebvre, P.A., 2017. Landsat-based analysis of mega dam flooding impacts in the Amazon compared to associated environmental impact assessments: Upper Madeira River example 2006–2015. Remote Sens. Appl. Soc. Environ. 7, 1–8.

Cochrane, T.A., Arias, M.E., Piman, T., 2014. Historical impact of water infrastructure on water levels of the Mekong River and the Tonle Sap system. Hydrol. Earth Syst. Sci. 18, 4529–4541.

Connors, J.P., Lei, S., Kelly, M., 2012. Citizen Science in the Age of Neogeography Utilizing Volunteered Geographic Information for Environmental Monitoring. Ann. Assoc. Am. Geogr. 102, 6, 1267–1289.

Cooley, S.W., Ryan, J.C., Smith, L.C., 2021. Human alteration of global surface water storage variability. Nature 591, 78–81.

Dahlin, K.M., Asner, G.P., Field, C.B., 2014. Linking vegetation patterns to environmental gradients and human impacts in a mediterranean-type island ecosystem. Landsc. Ecol. 29, 1571–1585.

Dang, A.N., Jackson, B.M., Benavidez, R., Tomscha, S.A., 2021. Review of ecosystem service assessments: Pathways for policy integration in Southeast Asia. Ecosyst. Serv. 49, 101266.

Dang, T.D., Cochrane, T.A., Arias, M.E., Van, P.D.T., de Vries, T.T., 2016. Hydrological alterations from water infrastructure development in the Mekong floodplains. Hydrol. Process. 30, 3824–3838.

Delgado, J.M., Apel, H., Merz, B., 2010. Flood trends and variability in the Mekong river. Hydrol. Earth Syst. Sci. 14, 407–418.

Delgado, J.M., Merz, B., Apel, H., 2012. A climate-flood link for the lower Mekong River. Hydrol. Earth Syst. Sci. 16, 1533–1541.

Dugan, P.J., Barlow, C., Agostinho, A.A., Baran, E., Cada, G.F., Chen, D., Cowx, I.G., Ferguson, J.W., Jutagate, T., Mallen-cooper, M., Marmulla, G., Nestler, J., Petrere, M., Welcomme, R.L., Winemiller, K.O., 2010. Fish Migration, Dams, and Loss of Ecosystem Services in the Mekong Basin. Ambio 39, 344–348.

Ekumah, B., Armah, F.A., Afrifa, E.K.A., Aheto, D.W., Odoi, J.O., Afitiri, A.-R., 2020. Assessing land use and land cover change in coastal urban wetlands of international importance in Ghana using Intensity Analysis. Wetl. Ecol. Manag. 28, 271–284.

Ellis, L.E., Jones, N.E., 2013. Longitudinal trends in regulated rivers: A review and synthesis within the context of the serial discontinuity concept. Environ. Rev. 21, 136–148.

Elvidge, C.D., Baugh, K.E., Dietz, J.B., Bland, T., Sutton, P.C., Kroehl, H.W., 1999. Radiance Calibration of DMSP-OLS Low-Light Imaging Data of Human Settlements. Remote Sens. Environ. 68, 77–88.

Elvidge, C.D., Hsu, F.C., Baugh, K.E., Ghosh, T., 2014. National trends in satellite-observed lighting 1992-2012, in: Global Urban Monitoring and Assessment: Through Earth Observation. pp. 97–120.

Erwin, K.L., 2009. Wetlands and global climate change: The role of wetland restoration in a changing world. Wetl. Ecol. Manag. 17, 71–84.

Ezcurra, E., Barrios, E., Ezcurra, P., Ezcurra, A., Vanderplank, S., Vidal, O., Villanueva-Almanza, L., Aburto-Oropeza, O., 2019. A natural experiment reveals the impact of hydroelectric dams on the estuaries of tropical rivers. Sci. Adv. 5.

Fan, H., He, D., Wang, H., 2015. Environmental consequences of damming the mainstream lancang-mekong river: A review. Earth-Science Rev.

Faria, F.A.M. de, Davis, A., Severnini, E., Jaramillo, P., 2017. The local socio-economic impacts of large hydropower plant development in a developing country. Energy Econ. 67, 533–544.

Fearnside, P.M., 2016. Environmental and Social Impacts of Hydroelectric Dams in Brazilian Amazonia: Implications for the Aluminum Industry. World Dev. 77, 48–65.

Feiner, K., Lowry, C.S., 2015. Simulating the effects of a beaver dam on regional groundwater flow through a wetland. J. Hydrol. Reg. Stud. 4, 675–685.

Feng, L., Han, X., Hu, C., Chen, X., 2016. Four decades of wetland changes of the largest freshwater lake in China: Possible linkage to the Three Gorges Dam? Remote Sens. Environ. 176, 43–55.

Feng, X., Porporato, A., Rodriguez-Iturbe, I., 2013. Changes in rainfall seasonality in the tropics. Nat. Clim. Chang. 3, 811–815.

Fernanda, L., Olaya-rodríguez, M.H., Cepeda-valencia, J., Lara, D., Arroyave-suárez, J., Finlayson, C.M., Palomo, I., 2017. Future impacts of drivers of change on wetland ecosystem services in Colombia. Glob. Environ. Chang. 44, 158–169.

Feyisa, G.L., Meilby, H., Fensholt, R., Proud, S.R., 2014. Automated Water Extraction Index: A new technique for surface water mapping using Landsat imagery. Remote Sens. Environ. 140, 23–35.

Fok, H.S., He, Q., Chun, K.P., Zhou, Z., Chu, T., 2018. Application of ENSO and drought indices for water level reconstruction and prediction: A case study in the lower Mekong River estuary. Water 10.

Frappart, F., Biancamaria, S., Normandin, C., Blarel, F., Bourrel, L., Aumont, M., Azemar, P., Vu, P.L., Le Toan, T., Lubac, B., Darrozes, J., 2018. Influence of recent climatic events on the surface water storage of the Tonle Sap Lake. Sci. Total Environ. 636, 1520–1533.

Frey, C.M., Kuenzer, C., 2014. Land-surface temperature dynamics in the Upper Mekong Basin derived from MODIS time series. Int. J. Remote Sens. 35, 2780–2798.

Furfey, P.H., 1927. A note on Lefever's" standard deviational ellipse". Am. J. Sociol. 33, 94–98.

Gauthier, C., Lin, Z., Peter, B.G., Moran, E.F., 2019. Hydroelectric Infrastructure and Potential Groundwater Contamination in the Brazilian Amazon: Altamira and the Belo Monte Dam. Prof. Geogr. 71, 292–300.

Gong, J., 2002. Clarifying the standard deviational ellipse. Geogr. Anal. 34, 155–167.

Gorelick, N., Hancher, M., Dixon, M., Ilyushchenko, S., Thau, D., Moore, R., 2017. Google Earth Engine: Planetary-scale geospatial analysis for everyone. Remote Sens. Environ. 202, 18–27.

Graf, W.L., 2006. Downstream hydrologic and geomorphic effects of large dams on American rivers. Geomorphology 79, 336–360.

Grill, G., Ouellet Dallaire, C., Fluet Chouinard, E., Sindorf, N., Lehner, B., 2014. Development of new indicators to evaluate river fragmentation and flow regulation at large scales: A case study for the Mekong River Basin. Ecol. Indic. 45, 148–159.

Grumbine, R.E., Xu, J., 2011. Mekong hydropower development. Science. 332, 6026, 178–179.

Guo, H., Bao, A., Liu, T., Ndayisaba, F., He, D., Kurban, A., De Maeyer, P., 2017. Meteorological drought analysis in the Lower Mekong Basin using satellite-based long-term CHIRPS product. Sustainability 9.

Han, X., Feng, L., Hu, C., Chen, X., 2018. Wetland changes of China's largest freshwater lake and their linkage with the Three Gorges Dam. Remote Sens. Environ. 204, 799–811.

Han, Z., Long, D., Fang, Y., Hou, A., Hong, Y., 2019. Impacts of climate change and human activities on the flow regime of the dammed Lancang River in Southwest China. J. Hydrol. 570, 96–105.

Hecht, J.S., Lacombe, G., Arias, M.E., Dang, T.D., Piman, T., 2019. Hydropower dams of the Mekong River basin: A review of their hydrological impacts. J. Hydrol. 568, 285–300.

Hennig, T., Wang, W., Feng, Y., Ou, X., He, D., 2013. Review of Yunnan's hydropower development. Comparing small and large hydropower projects regarding their environmental implications and socio-economic consequences. Renew. Sustain. Energy Rev. 27, 585–595.

Hilker, T., Wulder, M.A., Coops, N.C., Seitz, N., White, J.C., Gao, F., Masek, J.G., Stenhouse, G., 2009. Generation of dense time series synthetic Landsat data through data blending with MODIS using a spatial and temporal adaptive reflectance fusion model. Remote Sens. Environ. 113, 1988–1999.

Hirsch, P., 2016. The shifting regional geopolitics of Mekong dams. Polit. Geogr. 51, 63–74.

Hirsch, R.M., Slack, J.R., Smith, R.A., 1982. Techniques of trend analysis for monthly water quality data. Water Resour. Res. 18, 107–121.

Holdman, J., 2011. Spokanes seek new Grand Coulee deal. The Spokesman-Review.

Hortle, K.G., 2009. Fisheries of the Mekong River Basin, in: The Mekong. Biophysical Environment of a Transboundary River. New York: Elsevier, pp. 199–352.

Huang, B., Zhang, L., Wu, B., 2009. Spatiotemporal analysis of rural-urban land conversion. Int. J. Geogr. Inf. Sci. 23, 379–398.

Humbord, C., Ittekkot, V., Cociasu, A., Bodungen, B. v., 1997. Effect of Danube River dam on Black Sea biogeochemistry and ecosystem structure. Nature 386, 385–388.

IAIA, 1999. Principles of Environmental Impact Assessment, IAIA International Headquarters.

Intralawan, A., Wood, D., Frankel, R., Costanza, R., Kubiszewski, I., 2018. Tradeoff analysis between electricity generation and ecosystem services in the Lower Mekong Basin. Ecosyst. Serv. 30, 27–35.

Ji, X., Li, Y., Luo, X., He, D., 2018. Changes in the lake area of Tonle Sap: Possible linkage to runoff alterations in the Lancang River? Remote Sens. 10.

Jiang, X., Lu, D., Moran, E., Calvi, M.F., Dutra, L.V., Li, G., 2018. Examining impacts of the Belo Monte hydroelectric dam construction on land-cover changes using multitemporal Landsat imagery. Appl. Geogr. 97, 35–47.

Junk, W.J., 2002. Long-term environmental trends and the future of tropical wetlands. Environ. Conserv. 29, 414–435.

Kang, J.Y., Aldstadt, J., Vandewalle, R., Yin, D., Wang, S., 2020. A CyberGIS Approach to Spatiotemporally Explicit Uncertainty and Global Sensitivity Analysis for Agent-Based Modeling of Vector-Borne Disease Transmission. Ann. Am. Assoc. Geogr. 110, 1855–1873.

Kashaigili, J.J., Mbilinyi, B.P., Mccartney, M., Mwanuzi, F.L., 2006. Dynamics of Usangu plains wetlands: Use of remote sensing and GIS as management decision tools. Phys. Chem. Earth 31, 967–975.

Karimi, A., Brown, G., Hockings, M., 2015. Methods and participatory approaches for identifying social-ecological hotspots. Appl. Geogr. 63, 9–20.

Kent, J., Leitner, M., 2007. Efficacy of Standard Deviational Ellipses in the Application of Criminal Geographic Profiling. J. Investig. Psychol. Offender Profi ling 4, 147–165.

Khandelwal, A., Karpatne, A., Marlier, M.E., Kim, J., Lettenmaier, D.P., Kumar, V., 2017. An approach for global monitoring of surface water extent variations in reservoirs using MODIS data. Remote Sens. Environ. 202, 113–128.

Kim, M., Choi, J., 2015. Spatiotemporal patterns of outdoor artificial nighttime lights exposure in the Republic of Korea between 1995 and 2010. Cartogr. Geogr. Inf. Sci. 42, 69–78.

Kingsford, R.T., 2000. Review Ecological impacts of dams , water diversions and river management on floodplain wetlands in Australia. Austral Ecol. 25, 109–127.

Kirchherr, J., Pohlner, H., Charles, K.J., 2016. Cleaning up the big muddy: A meta-synthesis of the research on the social impact of dams. Environ. Impact Assess. Rev. 60, 115–125.

Kominoski, J.S., Ruhí, A., Hagler, M.M., Petersen, K., Sabo, J.L., Sinha, T., Sankarasubramanian, A., Olden, J.D., 2018. Patterns and drivers of fish extirpations in rivers of the American Southwest and Southeast. Glob. Chang. Biol. 24, 1175–1185.

Kornijów, R., 2009. Controversies around dam reservoirs: Benefits, costs and future. Ecohydrol. Hydrobiol. 9, 141–148.

Kuenzer, C., 2014. Remote sensing the Mekong. Int. J. Remote Sens. 35, 2747–2751.

Kuenzer, C., Campbell, I., Roch, M., Leinenkugel, P., Tuan, V.Q., Dech, S., 2013. Understanding the impact of hydropower developments in the context of upstream-downstream relations in the Mekong river basin. Sustain. Sci. 8, 565–584.

Kuenzer, C., Leinenkugel, P., Vollmuth, M., Dech, S., 2014. Comparing global land-cover products – implications for geoscience applications: an investigation for the trans-boundary Mekong Basin. Int. J. Remote Sens. 35, 2752–2779.

Kummu, M., Keskinen, M., Varis, O., 2008. Modern Myths of The Mekong: A critical review of water and development concepts, principles and policies, Water & Development Publications -Helsinki University of Technology.

Kummu, M., Sarkkula, J., 2008. Impact of the Mekong River flow alteration on the Tonle Sap flood pulse. Ambio 37, 185–192.

Kura, Y., Joffre, O., Laplante, B., Sengvilaykham, B., 2017. Coping with resettlement: A livelihood adaptation analysis in the Mekong River basin. Land use policy 60, 139–149.

Latrubesse, E.M., Arima, E.Y., Dunne, T., Park, E., Baker, V.R., D'Horta, F.M., Wight, C., Wittmann, F., Zuanon, J., Baker, P.A., Ribas, C.C., Norgaard, R.B., Filizola, N., Ansar, A., Flyvbjerg, B., Stevaux, J.C., 2017. Damming the rivers of the Amazon basin. Nature 546, 363–369.

Lauri, H., De Moel, H., Ward, P.J., Räsänen, T.A., Keskinen, M., Kummu, M., 2012. Future changes in Mekong River hydrology: Impact of climate change and reservoir operation on discharge. Hydrol. Earth Syst. Sci. 16, 4603–4619.

Lee, D.R., Sallee, G.T., 1970. A Method of Measuring Shape. Geogr. Rev. 60, 555–563.

Lefever, D.W., 1926. Measuring Geographic Concentration by Means of the Standard Deviational Ellipse. Am. J. Sociol. 32, 88–94.

Lehner, B., Döll, P., 2004. Development and validation of a global database of lakes, reservoirs and wetlands. J. Hydrol. 296, 1–22.

Lehner, B., Grill, G., 2013. Global river hydrography and network routing: Baseline data and new approaches to study the world's large river systems. Hydrol. Process. 27, 2171–2186.

Leibowitz, S.G., Wigington, P.J., Schofield, K.A., Laurie, C., Vanderhoof, M.K., Golden, H.E., Scott, G., Wigington, P.J., Schofield, K.A., Alexander, L.C., Vanderhoof, M.K., Golden, H.E., 2018. Connectivity of streams and wetlands to downstream waters: an integrated systems framework. J. Am. Water Resour. Assos. 54.

Li, Y., Qin, T., Tun, Y.Y., Chen, X., 2021. Fishes of the Irrawaddy River: Diversity and conservation. Aquat. Conserv. Mar. Freshw. Ecosyst. 31, 1945–1955.

Lin, Z., Qi, J., 2019. A New Remote Sensing Approach to Enrich Hydropower Dams ' Information and Assess Their Impact Distances : A Case Study in the Mekong River Basin. Remote Sens. 11.

Lin, Z., Qi, J., 2017. Hydro-dam–A nature-based solution or an ecological problem: The fate of the Tonlé Sap Lake. Environ. Res. 158, 24–32.

Liu, J., Dietz, T., Carpenter, S.R., Alberti, M., Folks, C., Moran, E.F., Pell, A.N., Deadman, P., Kratz, T., Lubchenco, J., Ostrom, E., Ouyang, Z., Provencher, W., Redman, C.L., Schneider, S.H., Taylor, W.W., 2007. Complexity of Coupled Human and Natural Systems. Science (80-.). 317, 1513–1516.

Liu, Q., Yang, Y., Tian, H., Zhang, B., Gu, L., 2014. Assessment of human impacts on vegetation in built-up areas in China based on AVHRR, MODIS and DMSPOLS nighttime light data, 1992-2010. Chinese Geogr. Sci. 24, 231–244.

Liu, Z., He, C., Zhang, Q., Huang, Q., Yang, Y., 2012. Extracting the dynamics of urban expansion in China using DMSP-OLS nighttime light data from 1992 to 2008. Landsc. Urban Plan. 106, 62–72.

Loiselle, A., Proulx, R., Larocque, M., Pellerin, S., 2021. Resilience of lake-edge wetlands to water level changes in a southern boreal lake. Wetl. Ecol. Manag. 7, 867–881.

Looy, K. Van, Tormos, T., Souchon, Y., 2014. Disentangling dam impacts in river networks. Ecol. Indic. 37, 10–20.

López-Moreno, J.I., Vicente-Serrano, S.M., Begueria, S., Garcia-Ruiz, J.M., Portela, M.M., Almeida, A.B., 2009. Dam effects on droughts magnitude and duration in a transboundary basin: The lower river tagus, pain and Portugal. Water Resour. Res. 45, 1–13.

Lu, X.X., Li, S., Kummu, M., Padawangi, R., Wang, J.J., 2014. Observed changes in the water flow at Chiang Saen in the lower Mekong: Impacts of Chinese dams? Quat. Int. 336, 145–157.

MacAlister, C., Mahaxay, M., 2009. Mapping wetlands in the Lower Mekong Basin for wetland resource and conservation management using Landsat ETM images and field survey data. J. Environ. Manage. 90, 2130–2137.

Maceachren, A.M., 1985. Compactness of geographic shape: comparison and evaluation of measures. Geogr. Ann. Ser. B 67, 53–67.

Maingi, J.K., Marsh, S.E., 2002. Quantifying hydrologic impacts following dam construction along the Tana River, Kenya. J. Arid Environ. 50, 53–79.

Mann, H.B., Whitney, D.R., 1947. On a Test of Whether one of Two Random Variables is Stochastically Larger than the Other. Ann. Math. Stat. 18, 50–60.

Markert, K.N., Markert, A.M., Mayer, T., Nauman, C., Haag, A., Poortinga, A., Bhandari, B., Thwal, N.S., Kunlamai, T., Chishtie, F., Kwant, M., Phongsapan, K., Clinton, N., Towashiraporn, P., Saah, D., 2020. Comparing Sentinel-1 surface water mapping algorithms and radiometric terrain correction processing in southeast Asia utilizing Google Earth Engine. Remote Sens. 12, 1–20.

Matthews, N., McCartney, M., 2018. Opportunities for building resilience and lessons for navigating risks: Dams and the water energy food nexus. Environ. Prog. Sustain. Energy 37, 56–61.

Mei, X., Dai, Z., Du, J., Chen, J., 2015. Linkage between Three Gorges Dam impacts and the dramatic recessions in China's largest freshwater lake, Poyang Lake. Sci. Rep. 5, 1–9.

Messager, M.L., Lehner, B., Grill, G., Nedeva, I., Schmitt, O., 2016. Estimating the volume and age of water stored in global lakes using a geo-statistical approach. Nat. Commun. 7, 1–11.

Mezger, G., González del Tánago, M., De Stefano, L., 2021. Environmental flows and the mitigation of hydrological alteration downstream from dams: The Spanish case. J. Hydrol. 598, 0–2.

Middleton, B.A., Souter, N.J., 2016. Functional integrity of freshwater forested wetlands, hydrologic alteration, and climate change. Ecosyst. Heal. Sustain. 2.

Millar, J., Robinson, W., Baumgartner, L., Homsombath, K., 2019. Local perceptions of changes in the use and management of floodplain fisheries commons : the case of Pak Peung wetland in Lao PDR. Environ. Dev. Sustain. 21, 1835–1852.

Miller, H.J., Wentz, E.A., 2003. Representation and spatial analysis in geographic information systems. Ann. Assoc. Am. Geogr. 93, 574–594.

Modaresi Rad, A., Kreitler, J., Abatzoglou, J.T., Fallon, K., Roche, K.R., Sadegh, M., 2022. Anthropogenic stressors compound climate impacts on inland lake dynamics: The case of Hamun Lakes. Sci. Total Environ. 829, 154419.

Mohammed-Ali, W., Mendoza, C., Holmes, R.R., 2020. Influence of hydropower outflow characteristics on riverbank stability: case of the lower Osage River (Missouri, USA). Hydrol. Sci. J. 65, 1784–1793.

Moran, E.F., Lopez, M.C., Moore, N., Müller, N., Hyndman, D.W., 2018. Sustainable hydropower in the 21st century. Proc. Natl. Acad. Sci. 201809426.

MRC, 2005. Overview of the Hydrology of the Mekong Basin, Mekong River Commission, Vientiane.

Myers, N., Mittermeler, R.A., Mittermeler, C.G., Da Fonseca, G.A.B., Kent, J., 2000. Biodiversity hotspots for conservation priorities. Nature 403, 853–858.

Nesbitt, H., Johnston, R., Solieng, M., 2004. Mekong River water: will river flows meet future agriculture needs in the Lower Mekong Basin? Water Agric. 116.

Newsome, T.H., Walcott, W.A., Smith, P.D., 1998. Urban activity spaces: Illustrations and application of a conceptual model for integrating the time and space dimensions. Transportation (Amst). 25, 357–377.

NG, W.X., Park, E., 2021. Shrinking Tonlé Sap and the recent intensification of sand mining in the Cambodian Mekong River. Sci. Total Environ. 777.

Nguyen, T.H., Jones, S.D., Soto-Berelov, M., Haywood, A., Hislop, S., 2018. A spatial and temporal analysis of forest dynamics using Landsat time-series. Remote Sens. Environ. 217, 461–475.

Nielsen, D.L., Merrin, L.E., Pollino, C.A., Karim, F., Stratford, D., O'Sullivan, J., 2020. Climate change and dam development: Effects on wetland connectivity and ecological habitat in tropical wetlands. Ecohydrology 13, 1–13.

Nystuen, J.D., Marble, D.F., 1963. An approach to the direct measurement of community mean information fields. Papers in Regional Science 11, 1, 99-109

Ouyang, W., Shan, Y., Hao, F., Shi, X., Wang, X., 2013. Accumulated impact assessment of river buffer zone after 30 years of dam disturbance in the Yellow River Basin. Stoch. Environ. Res. Risk Assess. 27, 1069–1079.

Pal, S., Saha, T.K., 2018. Identifying dam-induced wetland changes using an inundation frequency approach: The case of the Atreyee River basin of Indo-Bangladesh. Ecohydrol. Hydrobiol. 18, 66–81.

Palacios-Cabrera, T., Valdes-Abellan, J., Jodar-Abellan, A., Rodrigo-Comino, J., 2022. Land-use changes and precipitation cycles to understand hydrodynamic responses in semiarid Mediterranean karstic watersheds. Sci. Total Environ. 819.

Palmer, M., Ruhi, A., 2019. Linkages between flow regime, biota, and ecosystem processes: Implications for river restoration. Science. 365.

Pearse-Smith, S.W.D., 2012. The Impact of Continued Mekong Basin Hydropower Development on Local Livelihoods. Cons. J. Sustain. Dev. 7, 62–75.

Pekel, J.-F., Cottam, A., Gorelick, N., Belward, A.S., 2016. High-resolution mapping of global surface water and its long-term changes. Nature 540, 418–422.

Perdinan, Winkler, J.A., 2015. Selection of climate information for regional climate change assessments using regionalization techniques : an example for the Upper Great Lakes Region , USA. Int. J. Climatol. 35, 1027–1040.

Piman, T., Cochrane, T.A., Arias, M.E., Green, A., Dat, N.D., 2013. Assessment of Flow Changes from Hydropower Development and Operations in Sekong, Sesan, and Srepok Rivers of the Mekong Basin. J. Water Resour. Plan. Manag. 139, 723–732.

Poff, N.L.R., Allan, J.D., Bain, M.B., Karr, J.R., Prestegaard, K.L., Richter, B.D., Sparks, R.E., Stromberg, J.C., 1997. The natural flow regime: A paradigm for river conservation and restoration. Bioscience 47, 769–784.

Poff, N.L.R., Olden, J.D., Merritt, D.M., Pepin, D.M., 2007. Homogenization of regional river dynamics by dams and global biodiversity implications. Proc. Natl. Acad. Sci. U. S. A. 104, 5732–5737.

Poff, N.L.R., Schmidt, J.C., 2016. How dams can go with the flow. Science (80-.). 353, 1099–1100.

Pokhrel, Y., Burbano, M., Roush, J., Kang, H., Sridhar, V., Hyndman, D.W., 2018. A Review of the Integrated Effects of Changing Climate, Land Use, and Dams on Mekong River Hydrology. Water 10, 266.

Pueppke, S.G., Nurtazin, S.T., Graham, N.A., Qi, J., 2018. Central Asia’s Ili River ecosystem as a wicked problem: Unraveling complex interrelationships at the interface of water, energy, and food. Water 10, 1–21.

Qi, J., Bobushev, T.S., Kulmatov, R., Groisman, P., Gutman, G., 2012. Addressing global change challenges for Central Asian socio-ecosystems. Front. Earth Sci. 6, 115–121.

Räsänen, T.A., Koponen, J., Lauri, H., Kummu, M., 2012. Downstream Hydrological Impacts of Hydropower Development in the Upper Mekong Basin. Water Resour. Manag. 26, 3495–3513.

Räsänen, T.A., Kummu, M., 2013. Spatiotemporal influences of ENSO on precipitation and flood pulse in the Mekong River Basin. J. Hydrol. 476, 154–168.

Reis, V., Hermoso, V., Hamilton, S.K., Bunn, S.E., Fluet-Chouinard, E., Venables, B., Linke, S., 2019. Characterizing seasonal dynamics of Amazonian wetlands for conservation and decision making. Aquat. Conserv. Mar. Freshw. Ecosyst. 29, 1073–1082. *

Richter, B.D., Baumgartner, J. V., Powell, J., Braun, D.P., 1996. A Method for Assessing Hydrologic Alteration within Ecosystems. Conserv. Biol. 10, 1163–1174.

Robinson, R.A.J., Bird, M.I., Nay, W.O., Hoey, T.B., Maung, M.A., Higgitt, D.L., Lu, X.X., Aung, S., Tin, T., Swe, L.W., 2007. The irrawaddy river sediment flux to the Indian ocean: The original nineteenth-century data revisited. J. Geol. 115, 629–640. *

Rosenberg, D.M., McCully, P., Pringle, C.M., 2000. Global-scale environmental effects of hydrological alterations: Introduction. Bioscience 50, 746–751. *

Roy, P.S., Tomar, S., 2000. Biodiversity characterization at landscape level using geospatial modelling technique. Biol. Conserv. 95, 95–109.

Rufin, P., Gollnow, F., Müller, D., Hostert, P., 2019. Synthesizing dam-induced land system change. Ambio 48, 1183–1194.

Sabo, J.L., Ruhi, A., Holtgrieve, G.W., Elliott, V., Arias, M.E., Ngor, P.B., Räsänen, T.A., Nam, S., 2017. Designing river flows to improve food security futures in the Lower Mekong Basin. Science (80-.). 358.

Salmivaara, A., Kummu, M., Keskinen, M., 2013. Using Global Datasets to Create Environmental Profiles for Data-Poor Regions : A Case from the Irrawaddy and Salween River Basins. Environ. Manage. 51, 897–911.

Schmitt, R.J.P., Bizzi, S., Castelletti, A., Opperman, J.J., Kondolf, G.M., 2019. Planning dam portfolios for low sediment trapping shows limits for sustainable hydropower in the Mekong. Sci. Adv. 5.

Scudder, T., 2005. The future of large dams: Dealing with social, environmental, institutional and political costs. Routledge.

Sen, P.K., 1968. Estimates of the regression coefficient based on Kendall's tau. J. Am. Stat. Assoc. 63, 1379–1389.

Shamsudduha, M., Panda, D.K., 2019. Spatio-temporal changes in terrestrial water storage in the Himalayan river basins and risks to water security in the region : A review. Int. J. Disaster Risk Reduct. 35, 101068.

Shao, X., Cao, C., Zhang, B., Qiu, S., Elvidge, C.D., Von Hendy, M., 2014. Radiometric calibration of DMSP-OLS sensor using VIIRS day/night band, in: Earth Observing Missions and Sensors: Development, Implementation, and Characterization III. p. 92640A.

Sirisena, T.A.J.G., Maskey, S., Bamunawala, J., Ranasinghe, R., 2021. Climate Change and Reservoir Impacts on 21st-Century Stream flow and Fluvial Sediment Loads in the Irrawaddy River, Myanmar. Front. Earth Sci. 9, 644527.

Sivongxay, A., Greiner, R., Garnett, S.T., 2017. Livelihood impacts of hydropower projects on downstream communities in central laos and mitigation measures. Water Resour. Rural Dev. 9, 46–55.

Soukhaphon, A., Baird, I.G., Hogan, Z.S., 2021. The impacts of hydropower dams in the mekong river basin: A review. Water 13, 1–18.

Suepa, T., Qi, J., Lawawirojwong, S., Messina, J.P., 2016. Understanding spatio-temporal variation of vegetation phenology and rainfall seasonality in the monsoon Southeast Asia. Environ. Res. 147, 621–629.

Timpe, K., Kaplan, D., 2017. The changing hydrology of a dammed Amazon. Sci. Adv. 3.

Tobón-Marín, A., Cañón Barriga, J., 2020. Analysis of changes in rivers planforms using google earth engine. Int. J. Remote Sens. 41, 8654–8681.

Townsend, P.A., Foster, J.R., 2002. A synthetic aperture radar-based model to assess historical changes in lowland floodplain hydroperiod. Water Resour. Res. 38, 20-1-20–10.

Tran, T. V, Tran, D.X., Myint, S.W., Latorre-carmona, P., Ho, D.D., 2019. Assessing Spatiotemporal Drought Dynamics and Its Related Environmental Issues in the Mekong River Delta. Remote Sens. 11, 2742.

Tullos, D., 2009. Assessing the influence of environmental impact assessments on science and policy: An analysis of the Three Gorges Project. J. Environ. Manage. 90, S208–S223.

Turner, K.G., Anderson, S., Gonzales-Chang, M., Costanza, R., Courville, S., Dalgaard, T., Dominati, E., Kubiszewski, I., Ogilvy, S., Porfirio, L., Ratna, N., Sandhu, H., Sutton, P.C., Svenning, J.C., Turner, G.M., Varennes, Y.D., Voinov, A., Wratten, S., 2016. A review of methods, data, and models to assess changes in the value of ecosystem services from land degradation and restoration. Ecol. Modell. 319, 190–207.

Turner, M.G., Gardner, R.H., 2015. Landscape Ecology in Theory and Practice: Pattern an Process (Second Edition), Springer.

Ustin, S., 2004. Manual of remote sensing, remote sensing for natural resource management and environmental monitoring. John Wiley & Sons.

Vaidyanathan, G., 2011. Dam controversy: Remaking the Mekong. Nature 478, 305–307.

Vanderhoof, M.K., Alexander, L.C., Todd, M.J., 2016. Temporal and spatial patterns of wetland extent influence variability of surface water connectivity in the Prairie Pothole Region, United States. Landsc. Ecol. 31, 805–824.

Vannote, R.L., Minshall, G.W., Cummnins, K.W., Sedell, J.R., Cushing, C.E., 1980. The River Continuum Concept. Can. J. Fish. Aquat. Sci. 37, 130–137.

Verdin, K.L., Verdin, J.P., 1999. A topological system for delineation and codification of the Earth's river basins. J. Hydrol. 218, 1–12.

Wang, H., Asefa, T., Erkyihun, S., 2021. Interannual variabilities of the summer and winter extreme daily precipitation in the Southeastern United States. J. Hydrol. 603, 127013.

Wang, J., Sheng, Y., Tong, T.S.D., 2014. Monitoring decadal lake dynamics across the Yangtze Basin downstream of Three Gorges Dam. Remote Sens. Environ. 152, 251–269.

Wang, P., Lassoie, J.P., Dong, S., Morreale, S.J., 2013. A framework for social impact analysis of large dams: A case study of cascading dams on the Upper-Mekong River, China. J. Environ. Manage. 117, 131–140.

Wang, W., Lu, H., Ruby Leung, L., Li, H.Y., Zhao, J., Tian, F., Yang, K., Sothea, K., 2017. Dam Construction in Lancang-Mekong River Basin Could Mitigate Future Flood Risk From Warming-Induced Intensified Rainfall. Geophys. Res. Lett. 44, 10,378-10,386.

Ward, P.J., Beets, W., Bouwer, L.M., Aerts, J.C.J.H., Renssen, H., 2010. Sensitivity of river discharge to ENSO. Geophys. Res. Lett. 37, 1–6.

Wentz, E.A., 2000. A Shape Definition for Geographic Applications Based on Edge, Elongation, and Perforation. Geogr. Anal. 32, 95–112.

Wild, T.B., Reed, P.M., Loucks, D.P., Mallen-Cooper, M., Jensen, E.D., 2019. Balancing Hydropower Development and Ecological Impacts in the Mekong: Tradeoffs for Sambor Mega Dam. J. Water Resour. Plan. Manag. 145, 05018019.

Wilson, T.S., Matchett, E., Byrd, K.B., Conlisk, E., Reiter, M.E., Wallace, C., Flint, L.E., Flint, A.L., Joyce, B., Moritsch, M.M., 2022. Climate and land change impacts on future managed wetland habitat: a case study from California's Central Valley. Landsc. Ecol. 37, 861–881.

Winemiller, K.O., McIntyre, P.B., Castello, L., Fluet-Chouinard, E., Giarrizzo, T., Nam, S., Baird, I.G., Darwall, W., Lujan, N.K., Harrison, I., Stiassny, M.L.J., Silvano, R.A.M., Fitzgerald, D.B., Pelicice, F.M., Agostinho, A.A., Gomes, L.C., Albert, J.S., Baran, E., Petrere, M., Zarfl, C., Mulligan, M., Sullivan, J.P., Arantes, C.C., Sousa, L.M., Koning, A.A., Hoeinghaus, D.J., Sabaj, M., Lundberg, J.G., Armbruster, J., Thieme, M.L., Petry, P., Zuanon, J., Torrente Vilara, G., Snoeks, J., Ou, C., Rainboth, W., Pavanelli, C.S., Akama, A., Van Soesbergen, A., Sáenz, L., 2016. Balancing hydropower and biodiversity in the Amazon, Congo, and Mekong. Science (80-.). 351, 128–129.

WLE, 2017. Dataset on the Dams of the Irrawaddy, Mekong, Red and Salween River Basins. Vientiane, Lao PDR: CGIAR Research Program on Water, Land and Ecosystems - Greater Mekong.

Wohl, E., 2017. Connectivity in rivers. Prog. Phys. Geogr. 41, 345–362.

Wu, H., Zeng, G., Liang, J., Zhang, J., Cai, Q., Huang, L., Li, X., Zhu, H., Hu, C., Shen, S., 2013. Changes of soil microbial biomass and bacterial community structure in Dongting Lake: Impacts of 50,000 dams of Yangtze River. Ecol. Eng. 57, 72–78.

Wyatt, A.B., Baird, I.G., 2007. Transboundary impact assessment in the Sesan River Basin: The case of the Yali Falls Dam. Int. J. Water Resour. Dev. 23, 427–442.

Xue, Z., Liu, J.P., Ge, Q., 2011. Changes in hydrology and sediment delivery of the Mekong River in the last 50 years: Connection to damming, monsoon, and ENSO. Earth Surf. Process. Landforms 36, 296–308.

Yang, J. jie, Liu, S. liang, Wang, C., Deng, L., Dong, S. kui, 2014. Forest pattern dynamics and landscape connectivity changes in the Manwan Basin after dam construction in the Lancang River, China. Landsc. Ecol. Eng. 10, 77–83.

Yang, J., Yang, Y.C.E., Chang, J., Zhang, J., Yao, J., 2019. Impact of dam development and climate change on hydroecological conditions and natural hazard risk in the Mekong River Basin. J. Hydrol. 579, 124177.

Yoshida, Y., Lee, H.S., Trung, B.H., Tran, H.D., Lall, M.K., Kakar, K., Xuan, T.D., 2020. Impacts of mainstream hydropower dams on fisheries and agriculture in lower mekong basin. Sustainability 12, 1–21.

Yue, H., Li, Y., Qian, J., Liu, Y., 2020. A new accuracy evaluation method for water body extraction. Int. J. Remote Sens. 41, 1–32.

Yuill, R.S., 1971. The Standard Deviational Ellipse; An Updated Tool for Spatial Description. Geogr. Ann. Ser. B, Hum. Geogr. 53, 28–39.

Zeitoun, M., Warner, J., 2006. Hydro-hegemony–a framework for analysis of trans-boundary water conflicts. Water policy 8, 435–460.

Zhang, Q., Li, L., Wang, Y.G., Werner, A.D., Xin, P., Jiang, T., Barry, D.A., 2012. Has the Three-Gorges Dam made the Poyang Lake wetlands wetter and drier? Geophys. Res. Lett. 39.

Zhang, Z., Jin, G., Tang, H., Zhang, S., Zhu, D., Xu, J., 2022. How does the three gorges dam affect the spatial and temporal variation of water levels in the poyang lake? J. Hydrol. 605, 127356.

Zhao, B., Lei, H., Yang, D., Yang, S., Santisirisomboon, J., 2022. Runoff and sediment response to deforestation in a large Southeast Asian monsoon watershed. J. Hydrol. 606, 127432.

Zhao, Q., Liu, S., Deng, L., Dong, S., Cong, Wang, Yang, Z., Yang, J., 2012. Landscape change and hydrologic alteration associated with dam construction. Int. J. Appl. Earth Obs. Geoinf. 16, 17–26.

Zhao, Q., Liu, S., Dong, S., 2010. Effect of dam construction on spatial-temporal change of land use: A case study of Manwan, Lancang River, Yunnan, China. Procedia Environ. Sci. 2, 852–858.

Zheng, Y., Zhang, G., Wu, Y., Xu, Y.J., Dai, C., 2019. Dam effects on downstream riparian wetlands: The Nenjiang River, Northeast China. Water 11.

Zick, S.E., Matyas, C.J., 2016. A Shape Metric Methodology for Studying the Evolving Geometries of Synoptic-Scale Precipitation Patterns in Tropical Cyclones. Ann. Am. Assoc. Geogr. 106, 1217–1235.

Ziv, G., Baran, E., Nam, S., Rodriguez-Iturbe, I., Levin, S.A., 2012. Trading-off fish biodiversity, food security, and hydropower in the Mekong River Basin. Proc. Natl. Acad. Sci. 109, 5609–5614.